ÇUKUROVA UNIVERSITY
INSTITUTE OF NATURAL AND APPLIED SCIENCES

MSc THESIS

Emre KOCA

DESIGN, ANALYSIS AND OPTIMIZATION OF CHASSIS FOR AN ELECTRIC VEHICLE

DEPARTMENT OF AUTOMOTIVE ENGINEERING

ADANA, 2015

ÇUKUROVA UNIVERSITY
INSTITUTE OF NATURAL AND APPLIED SCIENCES

DESIGN, ANALYSIS AND OPTIMIZATION OF CHASSIS FOR AN ELECTRIC VEHICLE

Emre KOCA

MSc THESIS

DEPARTMENT OF AUTOMOTIVE ENGINEERING

We certify that the thesis titled above was reviewed and approved for the award of degree of the Master of Science by the board of jury on 28/07/2015

....	....	....
Assoc. Prof. Dr. Abdulkadir YAŞAR	Asst. Prof. Dr. Durmuş Ali BİRCAN	Prof. Dr. Kadir AYDIN
SUPERVISOR	Co-SUPERVISOR	MEMBER

…………………………………..	………………………………..
Assoc. Prof. Dr. Mustafa ÖZCANLI	Asst. Prof. Dr. Kerimcan ÇELEBİ
MEMBER	MEMBER

This MSc Thesis is written at the Department of Institute of Natural And Applied Sciences of Çukurova University.
Registration Number:

Prof. Dr. Mustafa Gök
Director
Institute of Natural and Applied Sciences

ABSTRACT

MSc THESIS

DESIGN, ANALYSIS AND OPTIMIZATION OF CHASSIS FOR AN ELECTRIC VEHICLE

Emre KOCA

ÇUKUROVA UNIVERSITY
INSTITUTE OF NATURAL AND APPLIED SCIENCES
DEPARTMENT OF AUTOMOTIVE ENGINEERING

Supervisor : Assoc. Prof. Dr. Abdulkadir YAŞAR
Co-Supervisor : Asst. Prof. Dr. Durmuş Ali Bircan
Year: 2015, Pages: 99
Jury : Assoc. Prof. Dr. Abdulkadir YAŞAR
: Asst. Prof. Dr. Durmuş Ali BİRCAN
: Prof. Dr. Kadir AYDIN
: Assoc. Prof. Dr. Mustafa ÖZCANLI
: Asst. Prof. Dr. Kerimcan ÇELEBİ

The purpose of this study is to design rigid and lightweight chassis for an electric vehicle. Design criteria and constraints are obtained from the TÜBİTAK electromobile racing rules. Various chassis types with different geometries are considered and 18 units of chassis are designed using computer aided design (CAD) software. Designs are analysed using finite element analysis (FEA) software and performance characteristics are parametrically and structurally optimized. Final design has aluminium 5042 H-19 space frame structure type and weighs 28.163 kg. Maximum von-Mises stress of the design is 15.465 MPa and the value is far below the material's yield strength of 345 MPa. Torsional stiffness value of the chassis is generated from the result of 2.495 mm maximum torsional deformation and calculated as 1828.289 Nm/deg.

Keywords: Electric Vehicle, Chassis, Computer Aided Design, Finite Element Method, Taguchi Method

ÖZ

YÜKSEK LİSANS TEZİ

ELEKTRİKLİ BİR ARAÇ ŞASİSİNİN TASARIM, ANALİZ VE OPTİMİZASYONU

Emre KOCA

ÇUKUROVA ÜNİVERSİTESİ
FEN BİLİMLERİ ENSTİTÜSÜ
OTOMOTİV MÜHENDİSLİĞİ ANABİLİM DALI

Danışman	: Doç. Dr. Abdulkadir YAŞAR
2. Danışman	: Yrd. Doç. Dr. Durmuş Ali Bircan
	Yıl: 2015, Sayfa: 99
Jüri	: Doç. Dr. Abdulkadir YAŞAR
	: Yrd. Doç. Dr. Durmuş Ali BİRCAN
	: Prof. Dr. Kadir AYDIN
	: Doç. Dr. Mustafa ÖZCANLI
	: Yrd. Doç. Dr. Kerimcan ÇELEBİ

Bu çalışmanın amacı elektrikli bir araç için sağlam ve hafif bir şasi tasarlamaktır. Tasarım ölçütleri ve sınırlamaları TÜBİTAK elektromobil yarış kurallarından edinilmiştir. Tasarım için birbirinden farklı şasi tipleri farklı geometrilerde oluşturulmuş ve 18 adet tasarım bilgisayar destekli tasarım yazılımıyla oluşturulmuştur. Tasarımlar sonlu elemanlar analizi yazılımıyla analiz edilmiş ve performans özellikleri parametrik ve yapısal olarak optimize edilmiştir. Elde edilen final tasarımı alüminyum 5042-H19 malzemeli uzay çatı şasi tipine sahiptir ve 28.163 kg ağırlığındadır. Tasarımın maksimum von-Mises gerilmesi 15.465 MPa'dır ve bu değer malzemenin 345 MPa olan akma dayanımının çok altındadır. Şasinin burulma direnci 2.495 mm maksimum burulma deformasyonundan elde edilmiş ve 1828.289 Nm/deg olarak hesaplanmıştır.

Anahtar Kelimeler: Elektrikli Araç, Şasi, Bilgisayar Destekli Tasarım, Sonlu Elemanlar Metodu, Taguchi Metodu

ACKNOWLEDGEMENTS

I would like to express special appreciation and thanks to my supervisors Assoc. Prof. Dr. Abdulkadir Yaşar and Asst. Prof. Dr. Durmuş Ali Bircan who has guided my research into this field.

I would also like to express my gratitude to my mother Tuluhan KOCA, my father Orhan KOCA and my sister Ela KOCA for their endless support and encouragement.

Last, but not least, I would like to thank my love Beril YAZICI for her understanding and patience during the past few years. Her support and encouragement was in the end what made this thesis possible.

CONTENTS **PAGE**

LIST OF TABLES **PAGE**

LIST OF FIGURES **PAGE**

1. INTRODUCTION

Renewable energy integration to the transportation increasing rapidly due to uncertainties in petroleum reserves and increasing environmental pollution caused by carbon dioxide emission. Petroleum reserve scenarios depend on the peak theory developed by M. King Hubbert, based on the extraction of the maximum amount of petroleum and after that peak point production of the petroleum will enter in a region of irreversible decrease (Chapman, 2014). There are three different scenarios depend on the peak theory, scenario one claims that reserves already reached the peak, scenario two claims that reserves will reach the peak in near future while scenario three claims there is no reliable data to discuss about peak point. Scenario one and scenario two are illustrated in Figures 1.1 and 1.2.

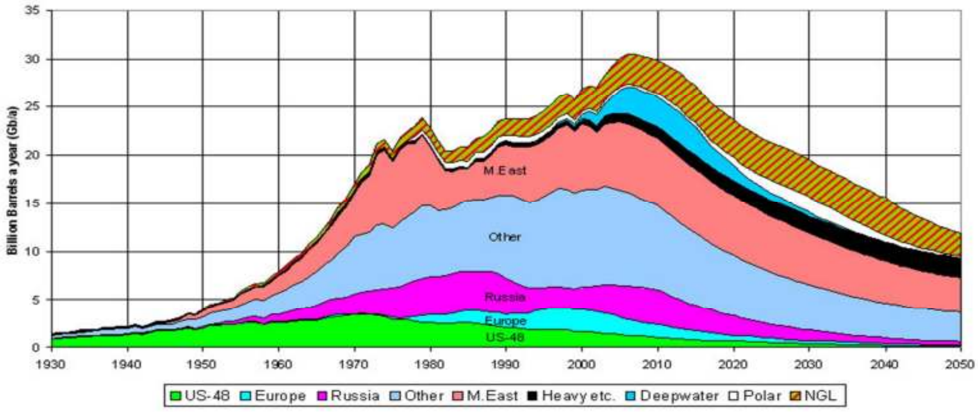

Figure 1.1. Reserves already reached the peak point (www.peakoil.net)

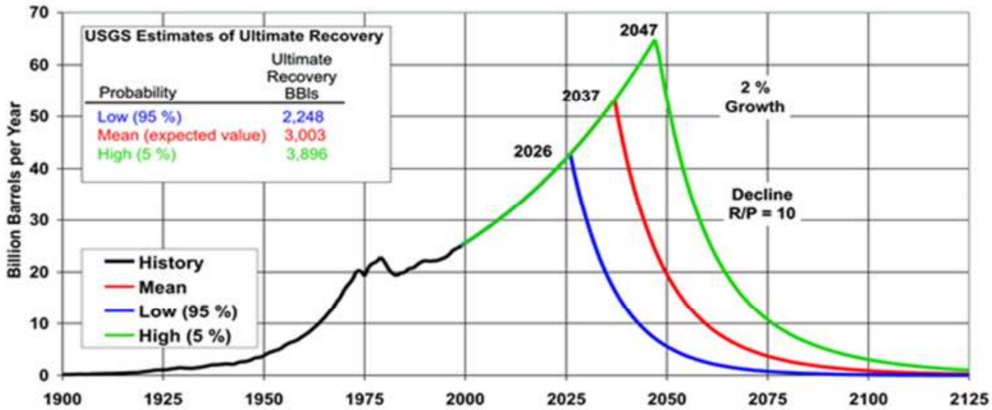

Figure 1.2. Reserves will reach the peak point in near future (Wood et al., 2004)

Electricity as a renewable energy is the major alternative to petroleum in transportation. Electric vehicle's environmentally friendly characteristic due to zero carbon dioxide emission makes it a good alternative to conventional internal combustion engine vehicles. Electric vehicle sales numbers shows that projection to 2020 there will be over 20 million electric vehicles in the streets; predicted numbers (in thousands) given in Figure 1.3.

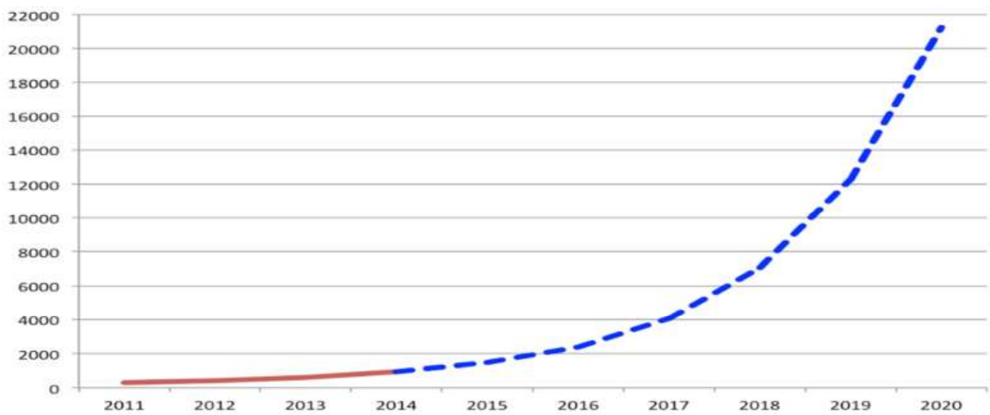

Figure 1.3. Electric vehicle sales numbers and projection to 2020 (www.raywills.net)

Generally, electric vehicles consist of a chassis that resists all the loadings, an electric motor that runs the wheels and battery that supplies energy to the electric motor. Controlling and monitoring of the vehicle overall performance are handled by battery management system and motor controller system. Battery technology has a huge impact on the development of electric vehicles (Boria and Pettinari, 2014). The range of an electric vehicle with one charge is directly dependent on the battery capacity. Battery specifications such as type, number and weight directly affect the range of an electric vehicle for one charge (Poullikkas, 2015). The battery pack of an electric vehicle has a considerable amount of weight compared to the total weight of the electric vehicle.

The weight of an electric vehicle becomes the major consideration because of the heavy battery packs. Weight increase of electric vehicles results in the decrease of the range without recharging. Vehicle manufacturers are striving to balance the heavy battery pack weight using lightweight chassis.

Chassis is the main structure of a vehicle that all other components like engine, powertrain, steering system and wheels assembled on it. The main function of the chassis is to carry all the loads on it and to resist all the forces. Forces on chassis could be an inner force in case of acceleration and braking or could be an outer force due to road condition or crash impact. Manufacturers aimed to have more rigid and more lightweight chassis for safety and energy consumption considerations.

The weight of the chassis related to its design and materials (Kopp et. al., 2012). Innovative design and material use could significantly reduce the weight of the chassis and increase the range of the vehicle. The lightening process of the chassis also related with the safety of the chassis and lightweight chassis design must be structurally rigid. Innovative material use for the chassis could meet the desired safety and weight values when combined with the robust design. Different design types are used in chassis manufacturing. Type of the chassis directly affects the weight, safety and handling of the vehicle. Mainly two major types of structures are used for the vehicle production depending on frame and body relations. Body and frame are integrated in most of the today's vehicles and this structure type called unibody or monocoque. The one-piece structure of chassis represents the structure of the entire vehicle. The other type of structure is body on frame. This structure type includes chassis and body separately. In body on frame structures, the body is mounted on the chassis and vehicle body shape is independent from the chassis shape. Pickups, trucks, racing cars and some electric vehicles use this type of structure. The body on frame structures include different chassis types such as ladder frame, backbone and space frame.

Ladder frame is one of the oldest chassis type and as the name implies has a shape of ladder and consists of two longitudinal members joint together with cross members. For both longitudinal and cross members, a large variety of section geometry choices exists for ladder frame manufacturing. Ladder frame chassis is widely used for trucks and pickups.

Backbone chassis has a closed box section that combines front axle and rear axle of a vehicle. Square and circular section geometries used for backbone chassis and generally, sports cars use this type of chassis.

Space frame chassis consists of lots of tubes that welded together. Tubes could be either square or circular. Space frame chassis has three-dimensional structure and racing cars use this type of frame.

The aim of the present study is to investigate chassis for an electric vehicle and motivated from the uncertainty of petroleum resources and heavy weight of the electric vehicle chassis due to heavy batteries. Design and analysis research topics of electric vehicle chassis can be found on the literature. Few studies include optimization part of this design and analysis parts, in addition, most of the studies include only one chassis type. In this study, different chassis types with different materials will be designed and analysed in terms of both weight and safety characteristics for an electric vehicle. The data gathered from the analysis results will be optimized. The optimization process will include both parametric and structural optimization. As a result of the optimization, lightweight, rigid and feasible electric vehicle chassis design aimed.

2. LITERATURE REVIEW

Interest on the electric vehicle research increased after developing technology and increasing market share. Various electric vehicle research areas can be found in the literature. One of the main research area related to electric vehicles is chassis. Chassis as a research area includes subtitles like material, design, structural analysis and optimization. Articles related to this study can be summarized as follows;

Mat and Ghani (2012) investigated the design and analysis of car chassis for Perodua eco-challenge race. Racing cars were single seated and built considering the fuel efficiency. Due to the race regulations chassis type was designed as space frame and mild steel is used as a material. Chassis is designed in the CATIA software as beam elements using circular and square hollow sections. Circular hollow section had 50 mm diameter and 2.5 mm thickness while square section had 50 mm side length and 2.3 mm thickness. For the analysis, Abaqus/CAE software used to create finite element model. Simulation was conducted using loading conditions as static loading, main hoop loading, acceleration, braking and torsional loading. Static loading analysis was considered for the whole weight of the car with a driver. Loads were applied to specific points and front and rear wheels were thought as simply supported constraints. Maximum stress 52.3 MPa occurred in the engine mounting points while maximum displacement of 1.68 mm was observed in the seat mounting points. Main hoop loading analysis was created by fixing the bottom part of the vehicle and applying 4g load on the main hoop. Maximum stress and displacement values were 85.6 MPa and 7.6 mm respectively. Acceleration and braking were simulated on the chassis and 86.8 MPa of maximum stress and 4.2 mm of maximum displacement values obtained from 1.5g acceleration while 73 MPa of maximum stress and 3.79 mm of maximum displacement obtained from 1.5g braking. Front end of the chassis was subjected to torsion to simulate the 2500 Nm/deg torsional loading and maximum stress of 199.6 MPa and maximum displacement of 5.2 mm were obtained as a result. Design was safe due to 300 MPa yield strength of the material.

Liu et. al. (2013) studied the crashworthiness and side impact analysis of an electric vehicle. Vehicle structure consists of three independent modules called driving, body and protection module. Driving module was made of aluminium chassis while body module was made of sandwich materials. Special attention was given to the protection module, which was made of high strength, lightweight composite material. Carbon fiber reinforced plastic (CFRP) was used as a composite material which includes T300 carbon twill weave fabric as reinforcement material and epoxy resin 618 as matrix material. Mechanical properties of composite calculated analytically and verified experimentally. Calculated properties assigned to the material and composite material was modelled using finite element analysis. After the load condition definition, deformation values generated for the roof crash analysis and analysis results were in the safe region of federal safety standards. The same method was used with a different material which is glass fiber reinforced plastic (GFRP) and results exceeded the safe region. Pole side impact crash analysis also conducted using CFRP and GFRP materials and CFRP was safer in terms of deformation values. Using CFRP rather than GFRP made the structure 28% lighter.

Taufik et. al. (2014) investigated design and analysis of an electric car chassis. Chassis was modelled and analysed in CATIA software using beam elements. Circular hollow section with a diameter of 32 mm and thickness of 1.5 mm used in the design. Mild steel AISI 1018 selected as a material of the chassis with yield strength of 386 MPa and with a safety factor of 1.5. Finite element analysis used for the static analysis of the chassis. Simply supported constraints applied to the front and rear wheelbase of the chassis and nine distributed forces were applied on the chassis starting from 700 N to 1500 N. Maximum deformation values and von-Mises stress values were considered. Maximum deformation values occurred in the driver seat mountings. Most of the maximum stresses were below the yield strength of the material of mild steel.

Hirsch (2011) presented the aluminium use in lightweight car design. Aluminium use in European cars was 62 kg in the year 1990 and increased to 132 kg in the year 2005 and estimated to increase in same grow rate. 132 kg aluminium use includes 69 kg in powertrain, 37 kg in chassis and suspension and 26 kg in car body. Body weight of the car consists 30% of the whole weight in conventional steel cars. Whole aluminium body reduced the car weight significantly for example Audi A8 aluminium body space frame concept was 40% lighter than the lightweight steel version. A new concept of multi material design was an alternative to whole aluminium design; concept includes application of variable materials for specific areas. BMW 5-E60 includes 20% deep drawing steels, 42% higher strength steels, 20% highest strength steels and 18% aluminium alloys. Two alloys of aluminium were highly used for automotive applications, which are 5000 series and 6000 series alloys. Application area affects the aluminium alloy type that used in the design. Aluminium use in chassis applications can reduce weight up to %40. Weight reduction increases the safety and handling characteristic of the car. Special 5000 series alloys (e.g. alloy AA5042-AlMg3.5Mn) used for the chassis applications in mass production for its static strength and intergranular corrosion resistance. Aluminium was a good alternative in lightweight car manufacturing with its reasonable cost and safety characteristics.

Nor et. al. (2012) presented stress analysis of a low loader chassis. Low loader aimed to work for heavyweight transportation and manufactured by a commercial company. Design of the chassis conducted in CATIA software and three-dimensional model was generated from the two-dimensional drawings of the chassis, which was supplied by the company. Analysis of the chassis was also performed using the same software by using finite element analysis. ASTM low alloy steel A 710 C (Class 3) used as chassis material that has yield strength of 550 MPa. The model was meshed using parabolic element type and 50 mm element size. Boundary conditions were applied by fixing the front of the chassis and axle mountings. 350 kN of uniformly distributed load was applied to chassis. Different sizes of I-beams were used for the analysis, maximum von-Mises stress and maximum displacement values occurred on different beams while the location of these stress and deformation points are the same. Numerical and analytical results compared to find the safety factor. Analytical results of maximum stress was 226.74 MPa while deformation was 7.79 mm. Numerical values were obtained and safety factor of 3.5 had the closest value of stress and deformation which are 200 MPa and 6.47 mm respectively. Future study will include the experimental results to find the actual deformation of the beam.

Yanhong and Feng (2011) examined the sub-frame of a dump truck. Sub-frame consists of edge beams that connected to main frame and used for increasing the strength and stiffness of the main frame. Dump truck was used for the transportation in field operations and after three to five month, cracking observed in the sub-frame due to poor working conditions. Material of the sub-frame was 16 MnL, which had 345 MPa yield strength, and due to poor working conditions, safety factor of 1.2 was used to determine 287.5 MPa allowable stress. Geometric model created in Pro/E software and imported to ANSYS software for finite element analysis. Simulating the working conditions lifting height of the frame was examined in dimensions of both 20 mm and 50 mm. Simulation results showed three large stress values occurred in final end of the frame, right side of the square beams and turning point of the left stringer. 20 mm rising of the tire results in maximum von-Mises stress values of 331 MPa, 184 MPa and 184 MPa respectively. Stress value 331 MPa of final end of the frame exceeded the allowable stress. 184 MPa stress values for right side of the square beams and turning point of the left stringer were below the allowable stress. 50 mm rising of the tire resulted in the 924 MPa stress at final end of frame, 424 MPa stress at right side of the square beams and 530 MPa stress at turning point of the left stringer. These values were exceeded the allowable stress and may cause to failure of the sub-frame. Structural improvements like extra beam addition were made in the frame to increase the torsional stiffness. Analysis of the new sub-frame design repeated using 50 mm rising condition of the tire and maximum Von-Mises stress was 200 MPa occurred at the front beams, which was below the allowable stress. Stresses at the right side of the square beams and turning point of the left stringer also reduced to 50% of allowable stress of 287.5 MPa.

Patel et. al. (2013) studied the parametric optimization of the chassis for weight reduction. Material of the chassis was chosen as ST 52, which had yield strength of 360 MPa. Main purpose of the study was weight reduction and to achieve this purpose, parameters that affect the weight are identified. These parameters were sizes of the C-channel cross member and defined as thickness of web, upper flange and lower flange. These three different factors had five different thickness levels which are 3 mm, 4 mm, 5 mm, 6 mm and 7 mm. Experiments were designed due to

Taguchi's L25 orthogonal array which described three factors with five levels. Response values were needed to find out the optimum thickness and these response values were weight, shear stress and deformation which were obtained from the finite element analysis software ANSYS. Parameters and response values were analysed in software Minitab, using one of the design of experiment method Taguchi. Analysis results were converted to signal to noise ratios and these ratios were compared for response values of weight, shear stress and deformation. Safety factor of three was chosen for the design and as a result of safety factor allowable stress calculated as 120 MPa. Optimum design parameters of 5 mm web thickness, 4 mm upper flange thickness and 4 mm lower flange thickness were selected due to highest signal to noise ratios considering smaller is better quality characteristic and as a result of these parameters shear stress was predicted as 119.46 MPa. The model using optimum parameter sets were designed in Solidworks software and analysed in ANSYS software. The analysis result of stress was 118.35 MPa with a variation of 0.928%. Actual chassis weight was 321.25 kg and chassis weight with optimum parameter sets was 279.44 kg. As a result of optimization 13.01% weight reduction was obtained.

3. MATERIAL AND METHOD

Electric vehicle chassis is investigated under the subtitles of design, analysis and optimization. Proposed flow chart of this work is illustrated in Figure 3.1.

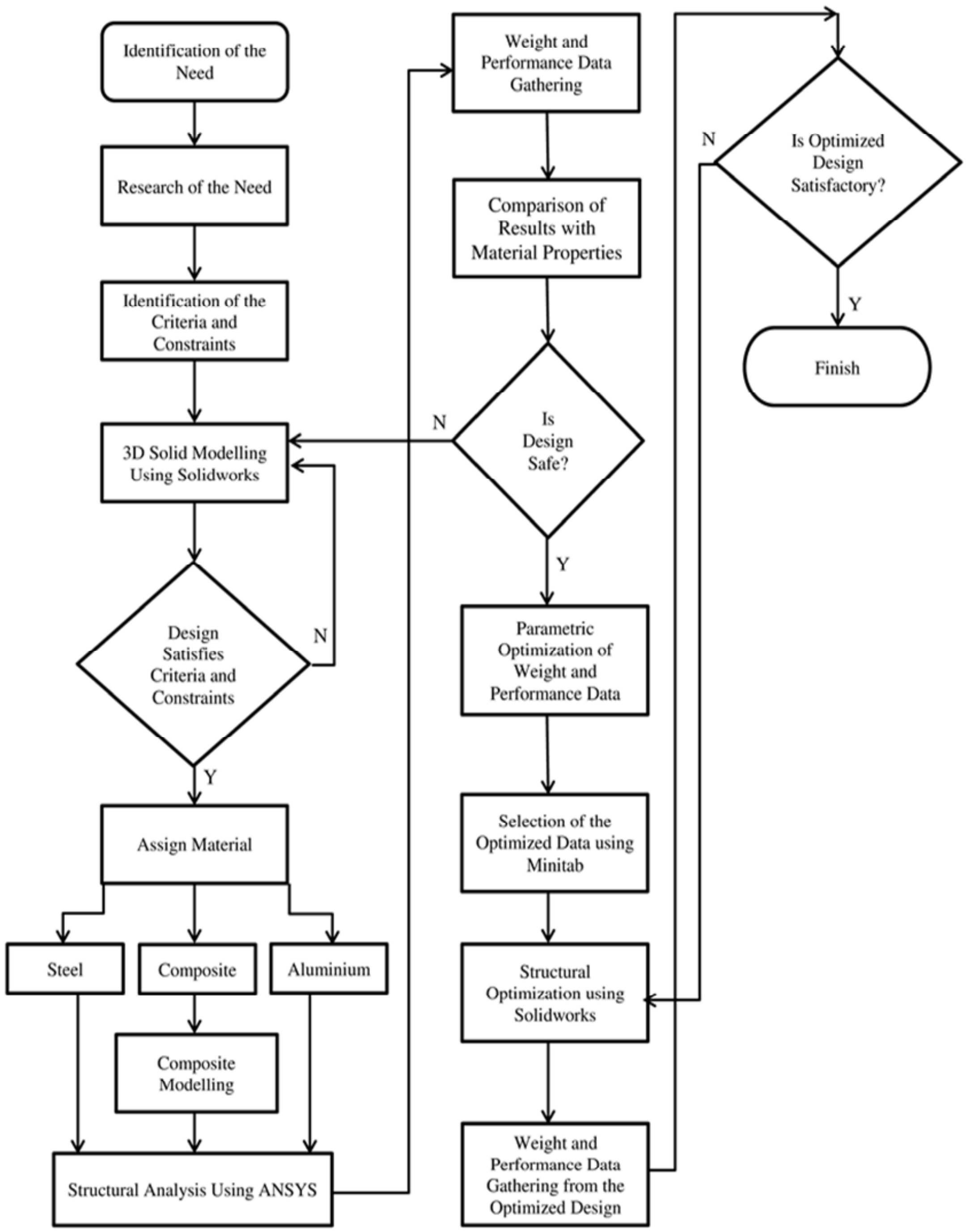

Figure 3.1. Proposed flow chart of the design, analysis and optimization phases

3.1. Chassis Design

3.1.1. Design Criteria of the Chassis

Chassis design process started with the selection of the structure type and determination of dimensions. Body on frame structure is considered for chassis type and three chassis types; ladder frame, backbone and space frame are selected for the design. Structural characteristics of these chassis types are different from each other.

Typical ladder frame consists of two side members and a number of cross members. Side members are generally made with channel sections while cross members are generally made with open or closed sections. Channel section provides easy mounting of the other components to side rails. Due to low torsion constant torsional stiffness of the ladder frame is low and if channel sections are used for the cross members it will be lower. Using closed sections for cross members rather than channel sections significantly increases the torsional stiffness. The ladder frame is one of the oldest chassis type and almost every vehicle that produced in the past used this type of chassis. Today, ladder frame chassis type is extensively used in pickups (Smith, 2002). A typical ladder frame of Chevrolet pickup is shown in Figure 3.2.

Figure 3.2. Ladder frame chassis of 2014 Chevrolet pickup (www.chevrolet.com)

Backbone chassis unlike the ladder frame has closed box section. Backbone structure firstly is seen on Tatra vehicles of the 1930s, but structure counted as a modern type of chassis. The structure of backbone chassis is located in the center of the vehicle and continues along the wheelbase so backbone structure has plenty of free space. Due to the closed box section torsional stiffness value of backbone structure is relatively higher than the ladder frame. Entire vehicle torsional stiffness is greater than the sum of the chassis and body stiffness's and this makes the structure statically indeterminate. Backbone structure can be produced by using triangulated tube sections. This structure type is used in sports cars of TVR Company (Crolla, 2009). Backbone chassis is illustrated in Figure 3.3.

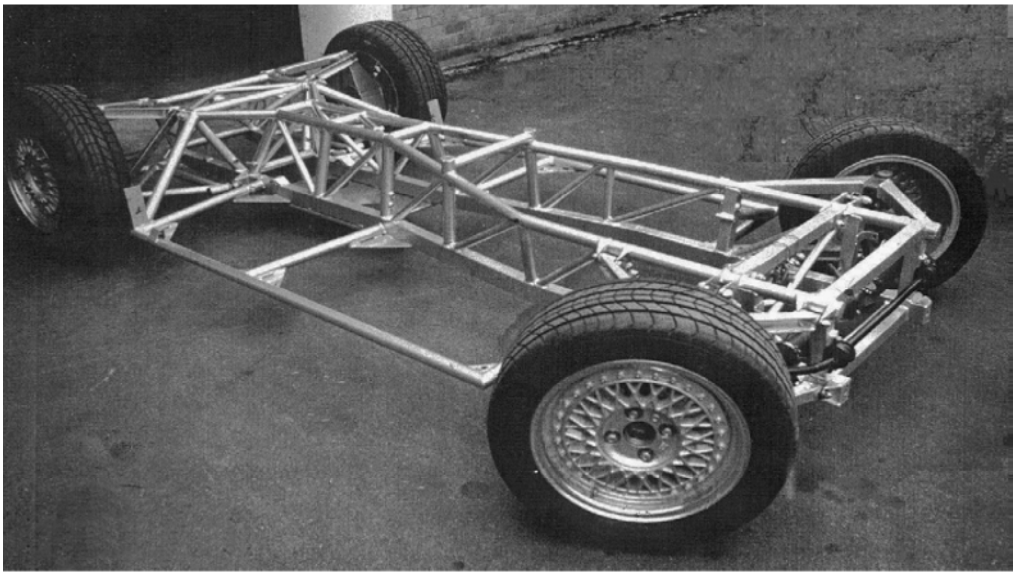

Figure 3.3. TVR backbone chassis (Crolla, 2009, p. 535)

Space frame chassis has a three-dimensional structure. Generally, square and circular profiles are used for the space frame chassis manufacturing. Manufacturing of the space frame chassis is time-consuming due to the welding of a large number of tubes. Triangulated tubes increase the torsional stiffness of the space frame chassis while decrease the accessibility of the components of the vehicles. Racing cars widely use this type of chassis because of its rigid structure.

The first space frame chassis is built by Mercedes Car Company and it is called 300 SL Gullwing. This car is named as Gullwing because its doors open towards up due having a large number of profiles and complex geometry of the space frame chassis. Space frame chassis is given in Figure 3.4.

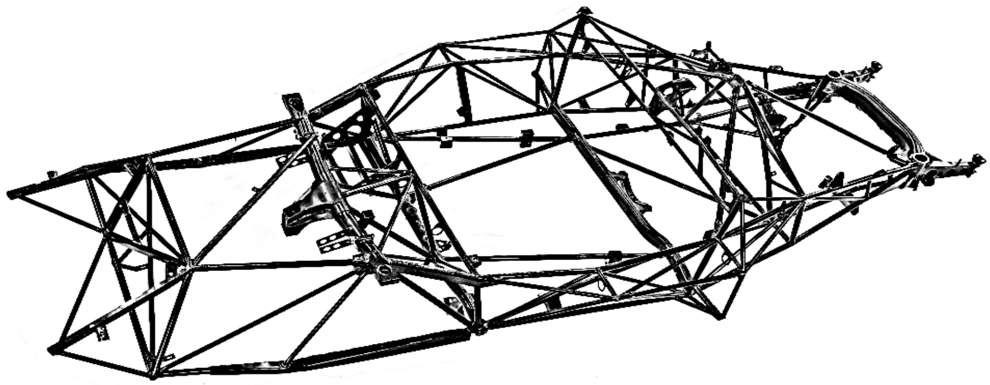

Figure 3.4. Mercedes 300 SL space frame chassis (300sl.org)

Dimensions of the chassis are determined by adopting the rules of electric vehicle races organised by the scientific and technological research council of Turkey (TÜBİTAK). These races are called TÜBİTAK electromobile races and main concept of the race is using the electrical energy efficiently. In this race, vehicles must have four wheels and minimum two seats. Dimensional constraints of the electromobile races that directly relevant to the chassis design are listed in Table 3.1.

Table 3.1. Dimensional constraints of the electromobile races

Dimension Type	**Min Dimension (cm)**	**Max Dimension (cm)**
Height	100	NS
Width	120	180
Length	200	450
Front Track Width	100	NS
Rear Track Width	80	NS
Wheelbase	130	NS
Ground Clearance	10	NS
Height of Driver Cabin	85	NS
Height of Passenger Cabin	85	NS
Width of Driver Cabin	65	NS
Width of Passenger Cabin	65	NS
NS: Not Specified		

3.1.2. Design Methodology of the Chassis

Chassis design is performed on the three-dimensional computer aided design (CAD) software. Solidworks 2014 CAD software of Dassault Systèmes Company is used for the design. Chassis is designed for an electric vehicle with entire vehicle's basic components because components are mounted to the chassis. Apart from the chassis, the entire vehicle consists of wheels, steering system, seats, electric motor, battery box and rear axle. The battery box is mounted on the front portion of the chassis while the electric motor is mounted on the rear portion of the chassis and seats are mounted on the middle portion of the chassis. All the chassis types are initially designed as wireframes and then converted to the solid models.

3.1.2.1. Design of the Chassis Types

Design process of the chassis types started with determining the main template for all of the chassis types. Main dimensions are selected as 1320 mm for front and rear track width and 2500 mm for chassis length. All designs are generated on this main template. All other vehicle component dimensions are considered and mounted as a sketch on the template. Design is generated as wireframe sketch.

Ladder frame design consists of side members and cross members. These members are designed as two-dimensional sketch due to the ladder frame's two-dimensional structure. Dimensions of the other vehicle components like wheels, battery box, seats and electric motor are also considered in the sketch. Wheels are also designed in true scale to observe the steering system and rear axle mounting locations. Mounting locations of the chassis is crucial for determining the ground clearance of the chassis and these points are used in the analysis part of this work. Sketch of the ladder frame is given in Figure 3.5.

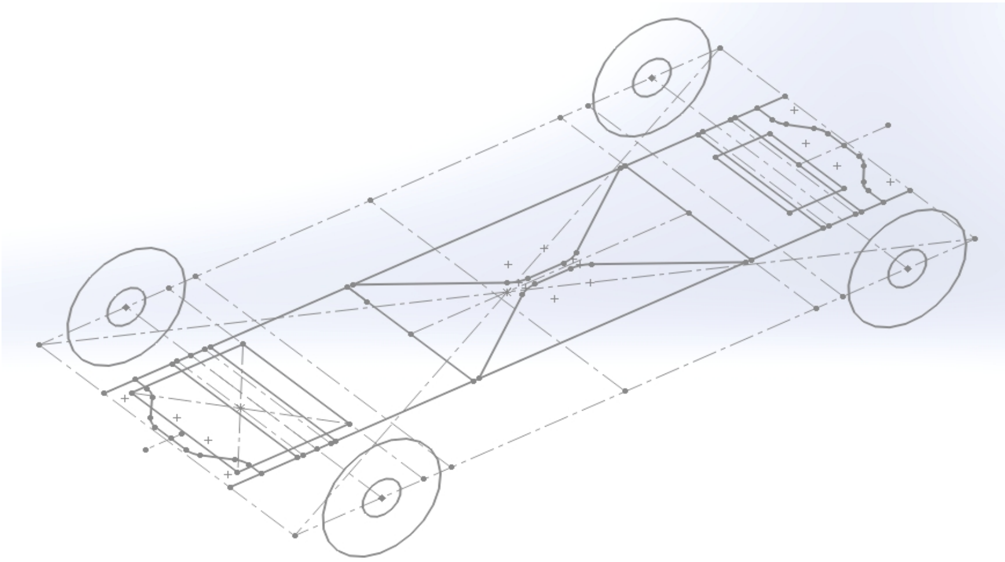

Figure 3.5. Wireframe design of the ladder frame chassis

Backbone chassis is designed using three-dimensional sketch command. Sketch is designed considering the dimensions of the other vehicle components like seats, battery box and electric motor. Sketch of the backbone chassis is illustrated in Figure 3.6.

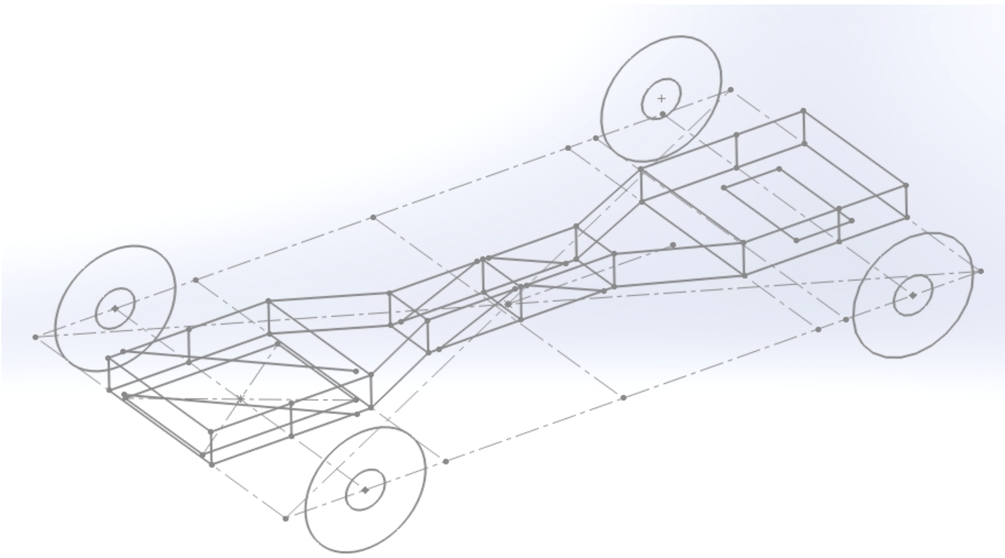

Figure 3.6. Wireframe design of the backbone chassis

Space frame chassis is designed as three-dimensional sketch considering the other vehicle component dimensions like seats, battery box and electric motor. Sketch of the space frame chassis is shown in Figure 3.7.

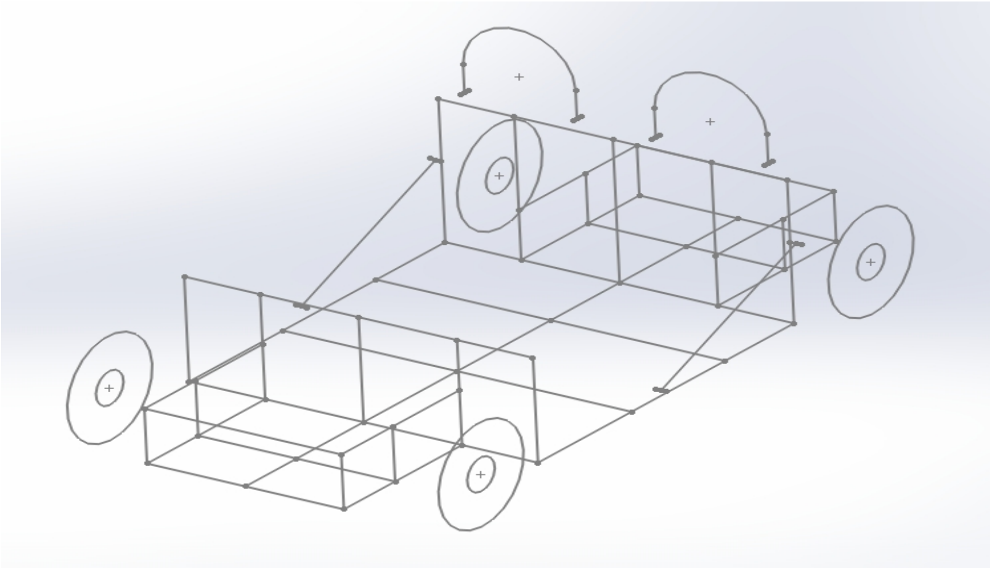

Figure 3.7. Wireframe design of the space frame chassis

Weldments toolbar in the software is used for converting the wireframes to profiles. Profile section geometries are used to create two types of design. First design consists of square hollow section profiles for main frame and circular hollow section tube profiles for support beams. Circular hollow section tube profiles are preferred for support beams rather than the square section profiles due to its easy formability characteristics and ease of the welding process. Second design consists of completely circular hollow section tube profiles. First design is referred to as square profile and second design is referred to as circular tube profile for simplicity of statements.

Commonly used section geometries for industrial purposes are selected considering the safety performances and weight of the chassis. Using similar profile dimensions increase the chassis comparison accuracy so square profile dimensions are selected as 40 mm side length and 2.5 mm thickness while circular tube profile dimensions are selected as 40 mm diameter and 2.5 mm thickness. Dimensions of the sections are generated as two-dimensional sketches in the software (www.solidworks.com). Section geometries and dimensions are given in Figure 3.8.

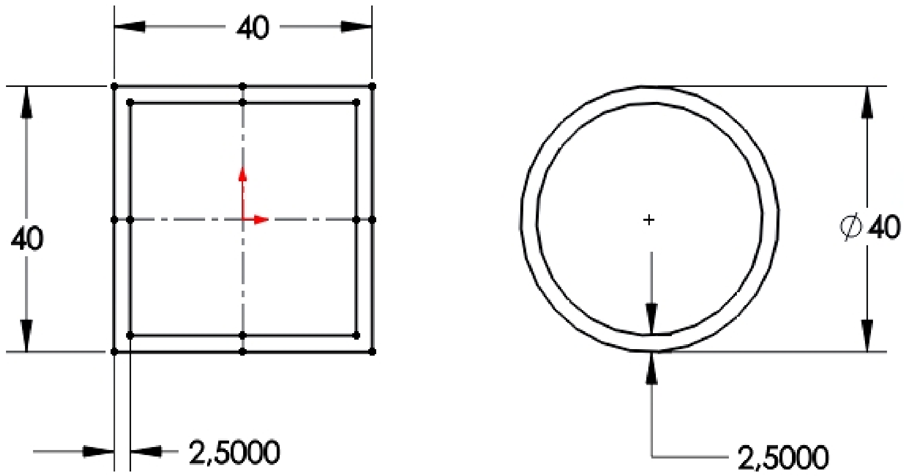

Figure 3.8. Section geometries and dimensions of square and circular profiles

Ladder frame chassis, backbone chassis and space frame chassis are modelled as solids using square and circular tube profiles. Profile joint locations are trimmed using trim/extend command due to having organised intersection points. Overlapped intersection points might be a problem in both manufacturing and analysis of the chassis. Each chassis type has two designs and they are called square profiled main frame and circular tube profiled frame.

Ladder frame chassis is modelled as a solid using square profiles for both side and cross members and circular tube profiles for cross members. X-bracing is used for the middle portion of the chassis to increase the torsional stiffness. Circular tube profiles are used in the X-bracing, front part and rear part of the chassis. Two different designs of ladder frame chassis are illustrated in Figures 3.9 and 3.10.

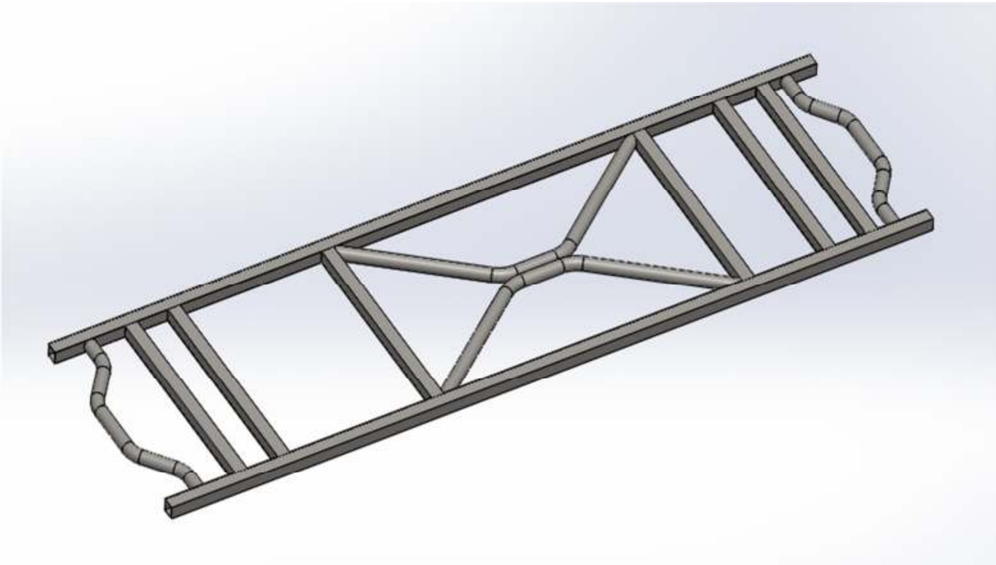

Figure 3.9. Ladder frame chassis as square profiled main frame

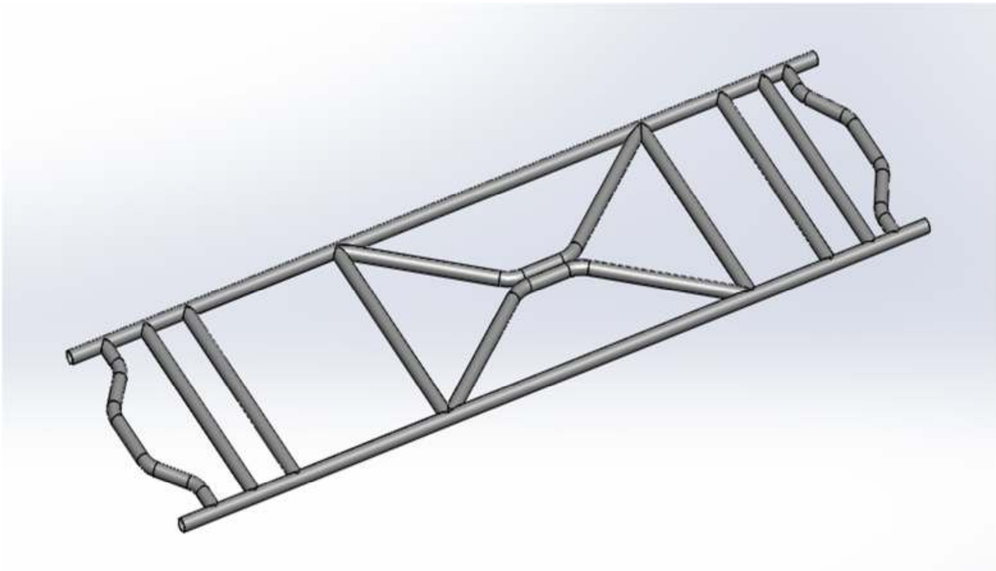

Figure 3.10. Ladder frame chassis as circular tube profiled frame

Backbone chassis is modelled as a solid using square profiles for main frame and circular tube profiles for center and front portion of the chassis in square profiled main frame chassis design. Circular tube profiles are used for the second design. Two different design of backbone chassis are given in Figures 3.11 and 3.12.

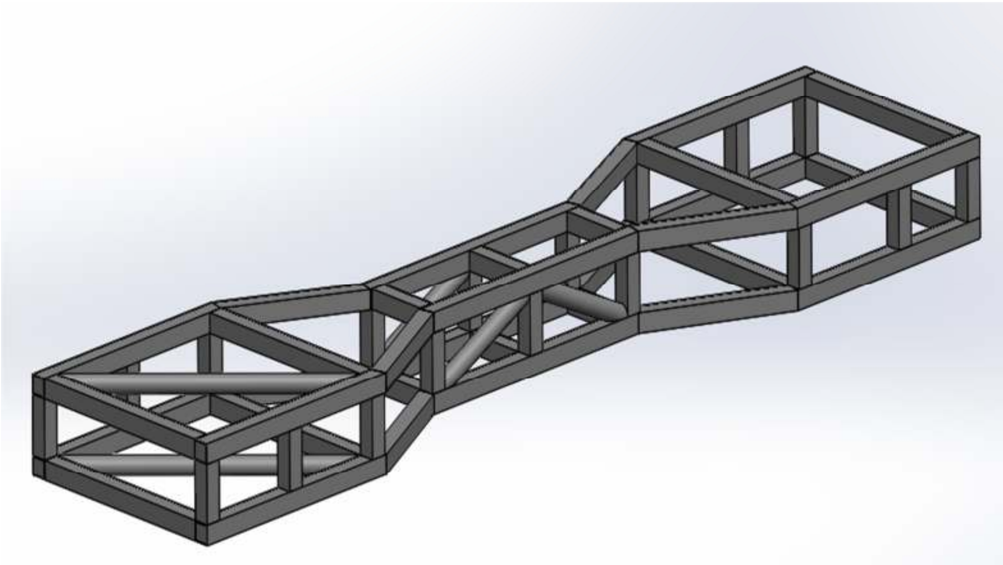

Figure 3.11. Backbone chassis as square profiled main frame

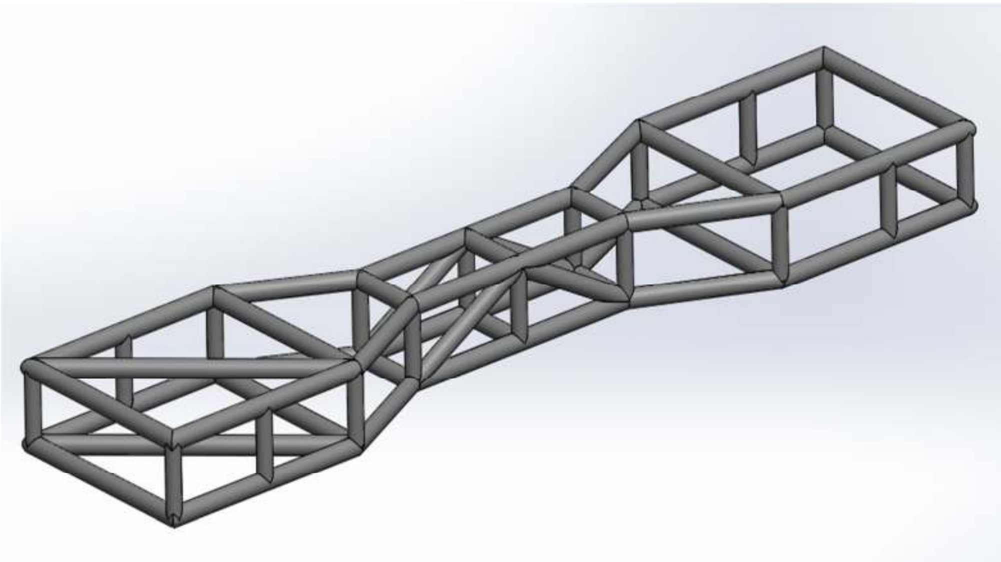

Figure 3.12. Backbone chassis as circular tube profiled frame

Space frame chassis is modelled as a solid using square profiles for main frame and circular tube profiles for roll bars and side members in square profiled main frame design. Second design consists of completely circular tube profiles. Two different designs of space frame chassis are illustrated in Figures 3.13 and 3.14.

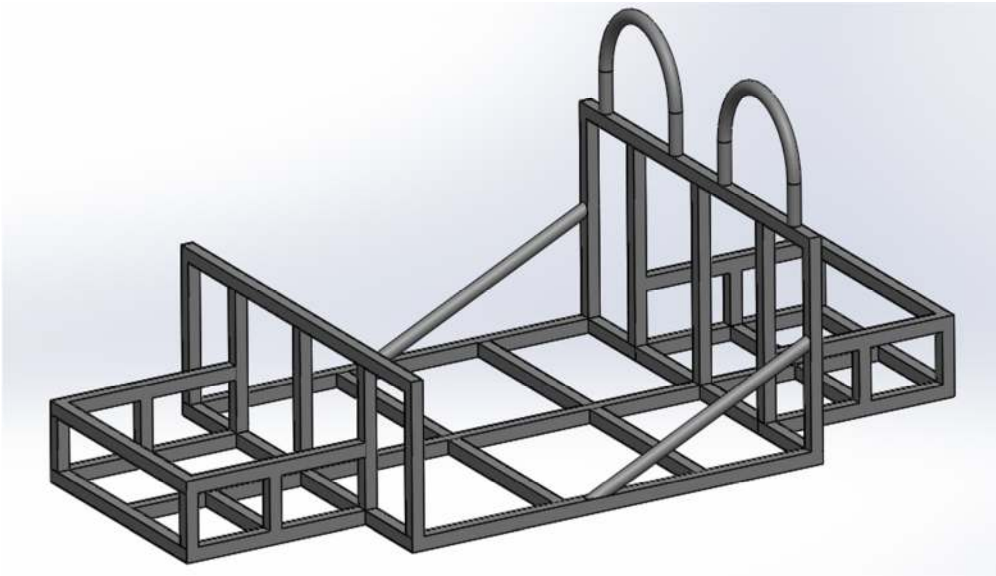

Figure 3.13. Space frame chassis as square profiled main frame

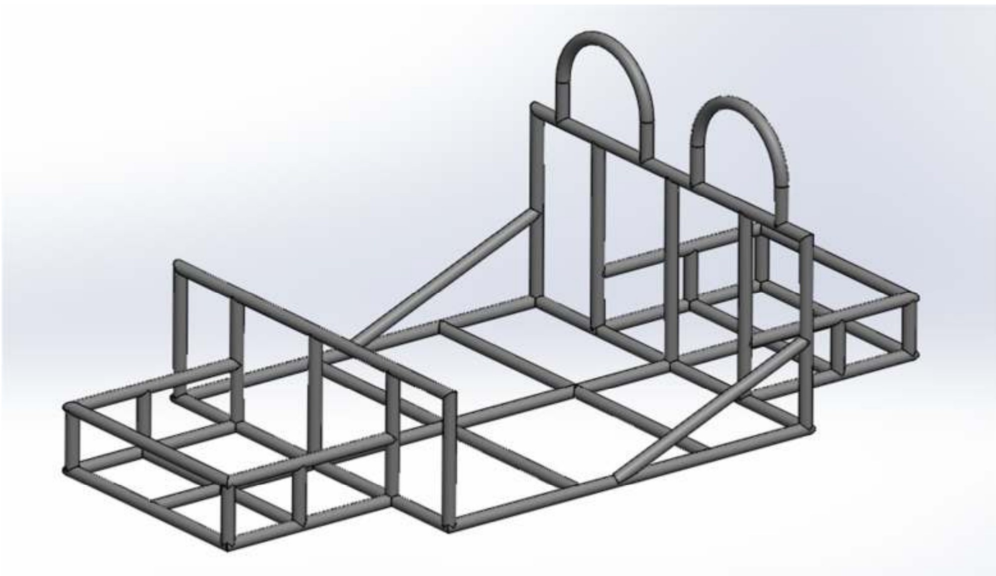

Figure 3.14. Space frame chassis as circular tube profiled frame

3.1.2.2. Design of the Vehicle Components

Chassis is designed considering the other vehicle components. Electric vehicle components like battery box, electric motor, seats, steering system, wheels and rear axle are designed. Dimensioning of the battery box, electric motor and seats are based on commercial products. Steering system and rear axle are designed for

1320 mm front and rear track width of the electric vehicle. All component designs are not fully functional; components are designed for the purpose of dimensioning the chassis and to observe the entire vehicle with chassis.

According to the racing rules, battery box is an obligatory structure that includes batteries and electrical components. Energy capacity of the batteries is limited by the rules with 3 kWh, so battery number and dimensions of battery box is calculated by considering this constraint. As a rechargeable battery type, lithium iron phosphate ($LiFePO_4$) is selected. One piece of battery; also called battery module has 3.2 V working voltage and 60 Ah capacity. 16 batteries are connected in series and it gives minimum 48 V working voltage. Multiplying this voltage with 60 Ah capacity, gives the battery pack's entire energy capacity as 2880 Wh which satisfies the racing rules. Specifications of the battery pack are listed in Table 3.2. Battery module and battery box designs are also shown in Figures 3.15 and 3.16.

Table 3.2. Specifications of battery module and battery pack

	Battery Module	**Battery Pack (16 Modules)**
Voltage (V)	3,2	48 - 51.2
Capacity (Ah)	60	60
Energy Capacity (W)	192	2880 - 3072

Figure 3.15. Designed battery module

Figure 3.16. Designed battery box including battery modules and electronic card

Electric vehicle is designed to have one electric motor. Electric motor power is selected as 3 kW and dimensions are based on the commercial products. Selected electric motor is illustrated in Figure 3.17.

Figure 3.17. Selected electric motor

Electric vehicle is designed to have two seats. Seat is designed as a racing car seat and dimensions are based on the commercial products. Protection of the driver is considered in the design according to the racing rules. Designed racing car seat is given in Figure 3.18.

Figure 3.18. Designed racing car seat

Steering system is designed with a steering wheel. System design depends on the chassis type. General steering system design is illustrated in Figure 3.19.

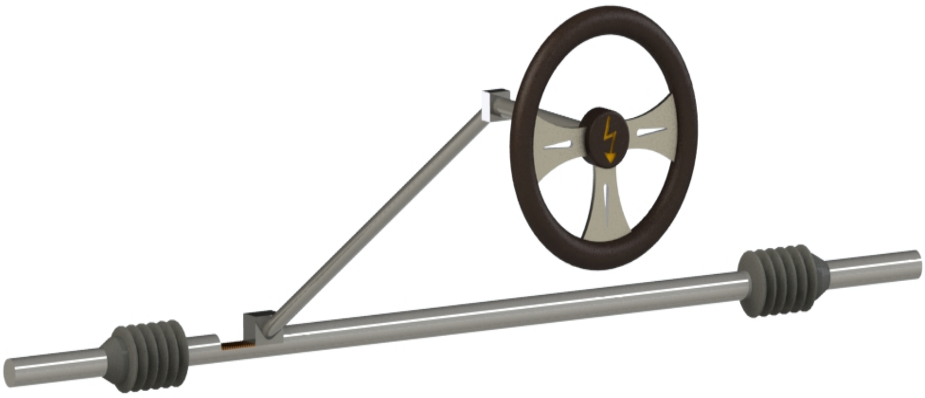

Figure 3.19. Design of the steering system

Electric vehicle's wheels are designed using 17" diameter rims. The only rule for wheels is having at least 80 mm tyre width. Wheels are designed using 90 mm tyre diameter. Rim and tyre designs are shown in Figure 3.20.

Figure 3.20. Designed rim and tyre

Electric vehicle's rear axle includes brake pad and gear wheel. Electric vehicle is designed for rear wheel drive. Rear axle is illustrated in Figure 3.21.

Figure 3.21. Design of the rear axle including brake pad and gear wheel

3.1.2.3 Assembly Design of Chassis and Vehicle Components

Assembly design includes chassis and the other vehicle components. Space frame chassis type is used for the assembly. Assembly also includes human models. One of the assembly designs includes thin sheets to have a closed structure. Assembly designs are illustrated in Figures 3.22 and 3.23.

Figure 3.22. Assembly design without sheets

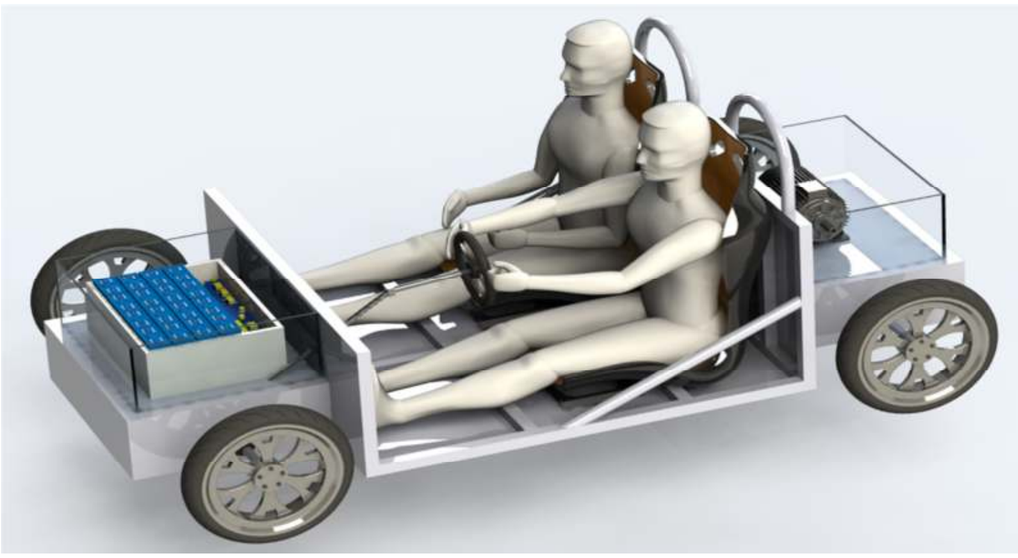

Figure 3.23. Assembly design with sheets and human models

3.2. Analysis of the Chassis Design

3.2.1. Finite Element Method and ANSYS

Analysis of a mechanical product is essential to investigate the product's performance. In this work, chassis is structurally analysed to observe the weight and safety characteristics. Safety characteristics of the chassis include stress and deformation values under static loading. Calculation of the weight, stress and deformation values of the chassis can be thought as a problem and this problem can be solved by analytically, experimentally and numerically. Analytical method includes hand calculation of the formulations. Analytical method could be time-consuming and error-prone process due to the complex structure of the chassis. Chassis could be analysed using an experimental setup, but it would be costly. Numerical solution of problems includes numerical approximations and by the help of the developing computer technology, it is possible to obtain rapid and accurate results. Numerical approach to the problems includes lots of theories and methods and one of these methods is finite element method.

Finite element method (FEM) is a computational method that gives approximate solutions to engineering problems. These engineering problems are also called boundary value problems. Investigation of the problem is performed within boundaries and most of the case these boundaries are physical structures. Dependent variables of these physical structures are governed by differential equations and these variables are called boundary conditions (Hutton, 2004).

Procedure of the FEM starts with the transformation of the engineering problem to a mathematical problem by dividing physical structure, also referred to as domain, into a finite number of subdomains. Subdomains are called elements and these elements could be a one-dimensional line, two-dimensional area and three-dimensional volume. Connection points of these elements are called nodes. Domain is defined by these nodes in the coordinate space. Degrees of freedom (DOF) of elements are defined by the DOF of these nodes. Systems of differential equations are generated on these nodes and converted into matrix form. Solution of the matrix form gives the desired results (Madenci and Guven, 2006).

There are many commercial computer software that give solutions to engineering problems using FEM. In this work, ANSYS v14.5 software package is used for the structural analysis of the chassis.

Static structural analysis procedure is started with the assignment of the material to the chassis and continued with the division of the domain into subdomains. In this work, domain is chassis and this division operation is called meshing in ANSYS workbench. After meshing, loads and support conditions are applied on the meshed model then stress and deformation values are obtained as a solution. Procedure of the analysis is same for the materials of steel and aluminium while composite material analysis includes modelling of the composite. Modelling of the composite is performed on ANSYS Composite PrepPost (ACP) software, which is a component software system of ANSYS.

3.2.2. Analysis Methodology in ANSYS

3.2.2.1. Material Selection

Structural analysis is started with importing the three-dimensional chassis model into ANSYS workbench in .STEP file extension then materials are assigned to the model. There is no limitation for material selection in electromobile racing rules. Three materials, steel, aluminium and composite, are selected for different reasons.

Steel is the most common used material in the automotive industry due to its high strength and low-cost characteristics. There are many choices for steel grades, AISI 4130 steel is selected for the chassis, which is widely used in automotive industry for many different applications.

Aluminium use in automotive applications is increasing due to its lightweight characteristic (Hirsch and Al-Samman, 2013). 5000 series alloys of aluminium have good forming and corrosion resistance properties. Aluminium 5042-H19 is selected for chassis material and it is also used for chassis applications in series production.

Composite material use in chassis applications is a new and trending option (Bambach, 2013). Composite materials are seen as a replacement by steel due its lightweight and high strength characteristics, but main obstacle to achieve this goal is price. Composite material production and application is very expensive compared to steel. Some of the commercial electric vehicles use composite materials for chassis applications. Composite materials are consisting of a reinforcement material and a matrix material. For the composite material, woven carbon fiber is selected as reinforcement material and epoxy polymer is selected as matrix material.

Material properties of steel and aluminium are obtained from an online database of engineering material website MatWeb (www.matweb.com) and material property data are entered in the ANSYS material library. ANSYS material library already has composite material properties of carbon fiber epoxy. Steel and aluminium have isotropic mechanical properties while carbon fiber epoxy has orthotropic mechanical properties. Material properties of steel, aluminium and carbon fiber epoxy are listed in Tables 3.3, 3.4 and 3.5, respectively.

Table 3.3. Material properties of AISI 4130 Steel

Property	**Value**	**Unit**
Density	7850	kg/m^3
Young's Modulus	205000	MPa
Poisson’s Ratio	0,29	
Tensile Yield Strength	360	MPa
Tensile Ultimate Strength	560	MPa

Table 3.4. Material properties of Aluminium 5042-H19

Property	**Value**	**Unit**
Density	2670	kg/m^3
Young's Modulus	70000	MPa
Poisson's Ratio	0,33	
Tensile Yield Strength	345	MPa
Tensile Ultimate Strength	360	MPa

Table 3.5. Material properties of Carbon Fiber Epoxy

Property	Value	Unit
Density	1480	kg/m^3
Young's Modulus X Direction	91820	MPa
Young's Modulus Y Direction	91820	MPa
Young's Modulus Z Direction	9000	MPa
Poisson's Ratio XY	0,05	
Poisson's Ratio YZ	0,3	
Poisson's Ratio XZ	0,3	
Shear Modulus XY	19500	MPa
Shear Modulus YZ	3000	MPa
Shear Modulus XZ	3000	MPa

3.2.2.2. Mesh Generation

Generating mesh is a critical phase in the structural analysis procedure. Dividing structure into smaller portions, in other words generating more mesh, could increase the accuracy of the analysis, but the software will spend more time to solve the problem (www.ansys.com). Using few number of mesh spends less time, but analysis results would not be reliable. Element and node numbers of steel and aluminium are the same while the composite material is different from them. The reason of difference is the different element types. Solid elements are used for the aluminium and steel mesh generation while shell elements are used for the composite material mesh generation and solid meshing method is different from the surface meshing method. In this work, mesh is generated automatically using maximum relevance to having finer mesh. Mesh generated models of ladder frame chassis are shown in Figures 3.24 and 3.25.

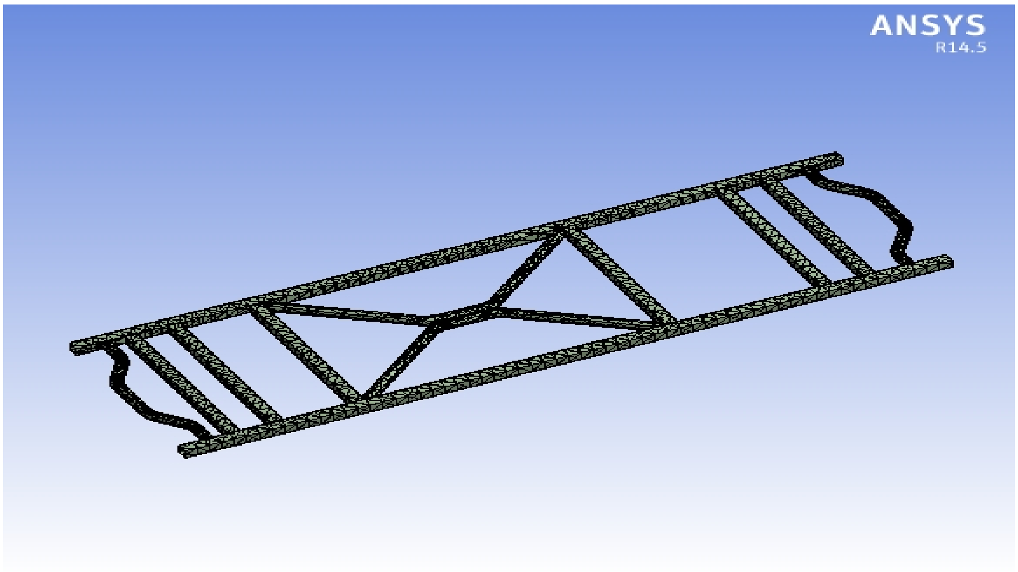

Figure 3.24. Mesh generation on the square profiled ladder frame chassis

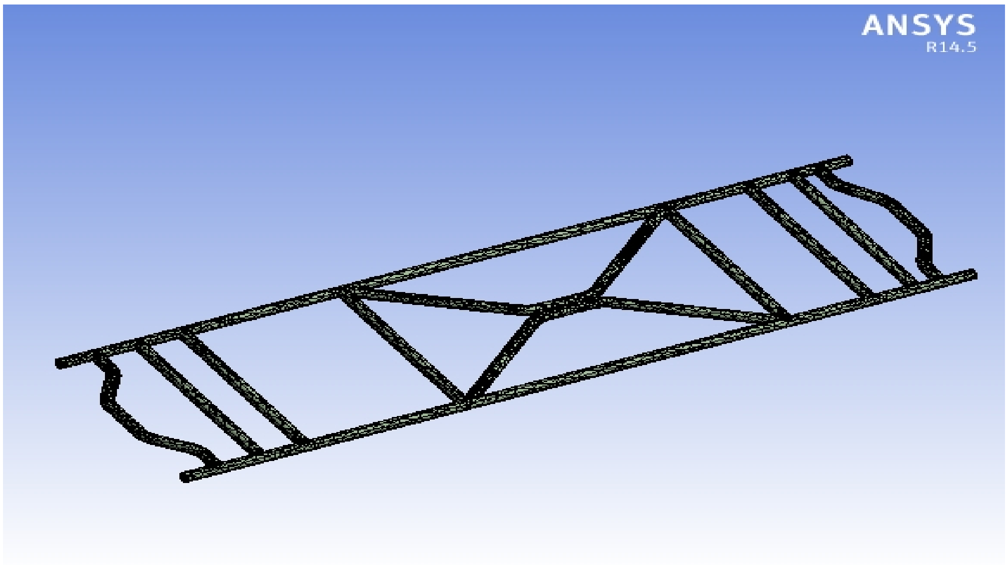

Figure 3.25. Mesh generation on the circular tube profiled ladder frame chassis

Element and node numbers of square profiled ladder frame chassis are 16033 and 30422 respectively for steel and aluminium materials and for composite material, element and node numbers are 11928 and 11849. Element and node numbers of circular tube profiled ladder frame chassis are 28148 and 52870, respectively for steel and aluminium materials and for composite material, element and node numbers are 27979 and 27904, respectively.

Backbone chassis mesh generation is illustrated in Figures 3.26 and 3.27.

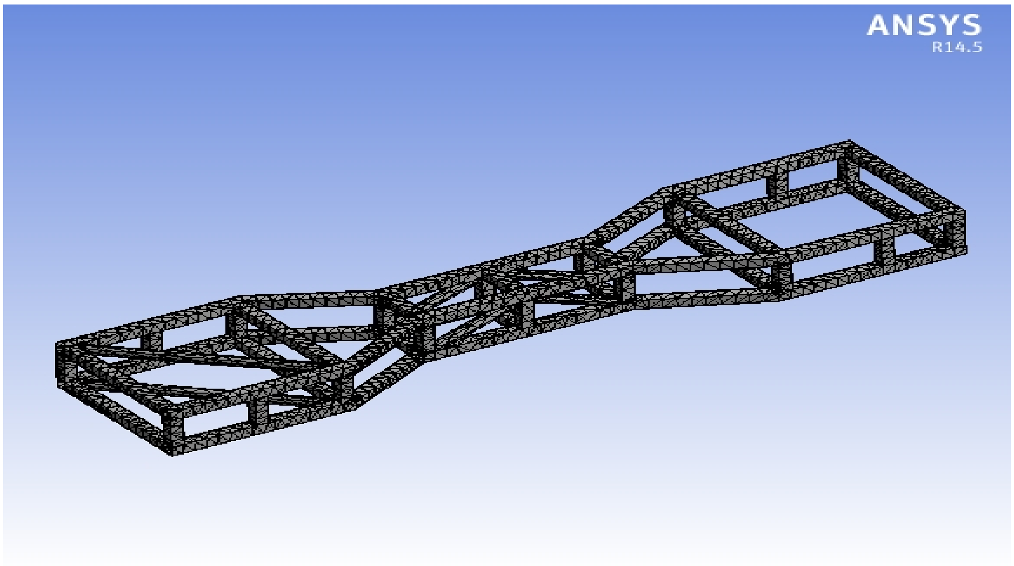

Figure 3.26. Mesh generation on the square profiled backbone chassis

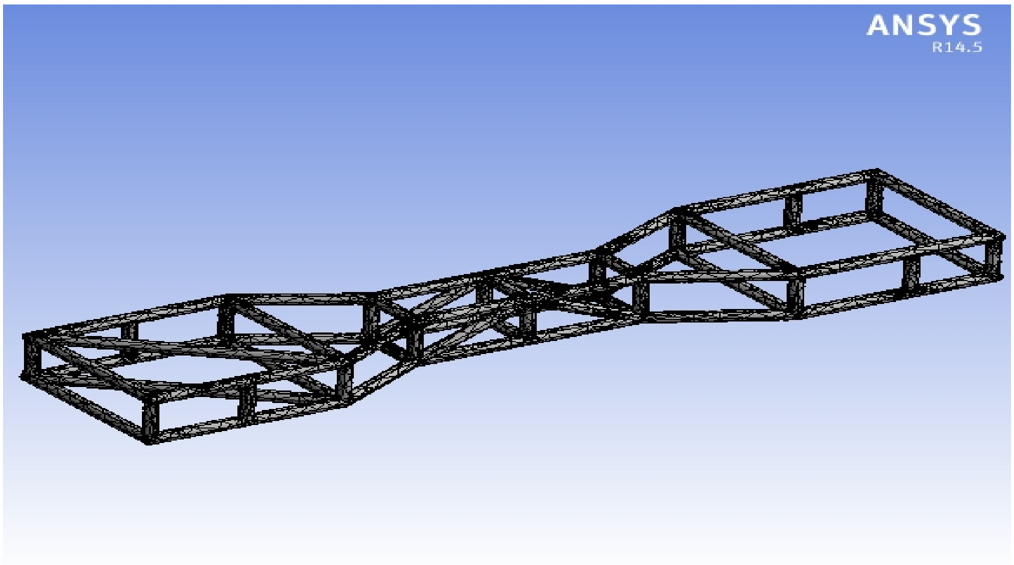

Figure 3.27. Mesh generation on the circular tube profiled backbone chassis

Element and node numbers of square profiled backbone chassis are 20700 and 38758 for steel and aluminium materials and for composite material, element and node numbers are 18181 and 18665, respectively. Element and node numbers of circular tube profiled backbone chassis are 40939 and 76536 for steel and aluminium materials and for composite material, element and node numbers are 32679 and 32531, respectively.

Space frame chassis mesh generation is given in Figures 3.28 and 3.29.

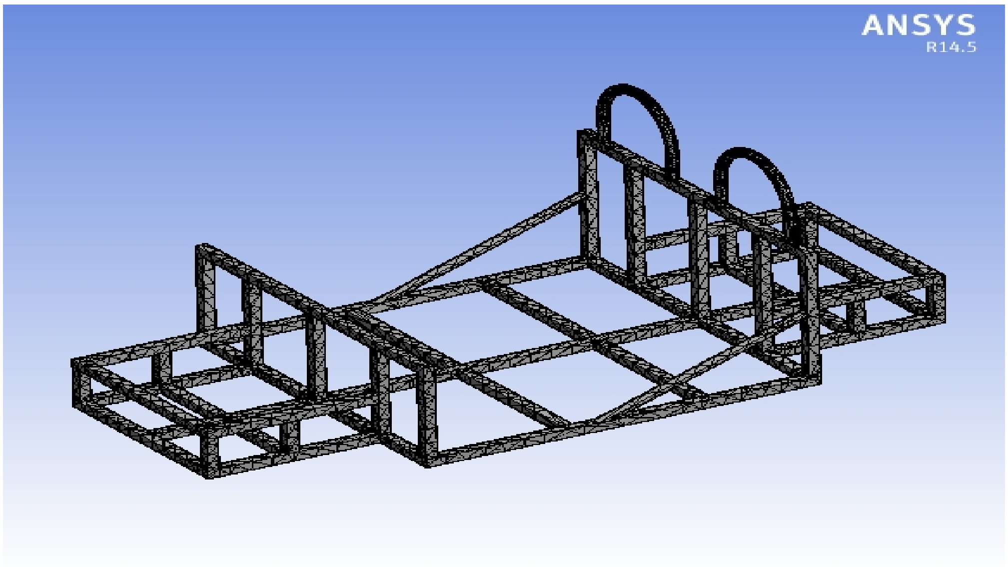

Figure 3.28. Mesh generation on the square profiled space frame chassis

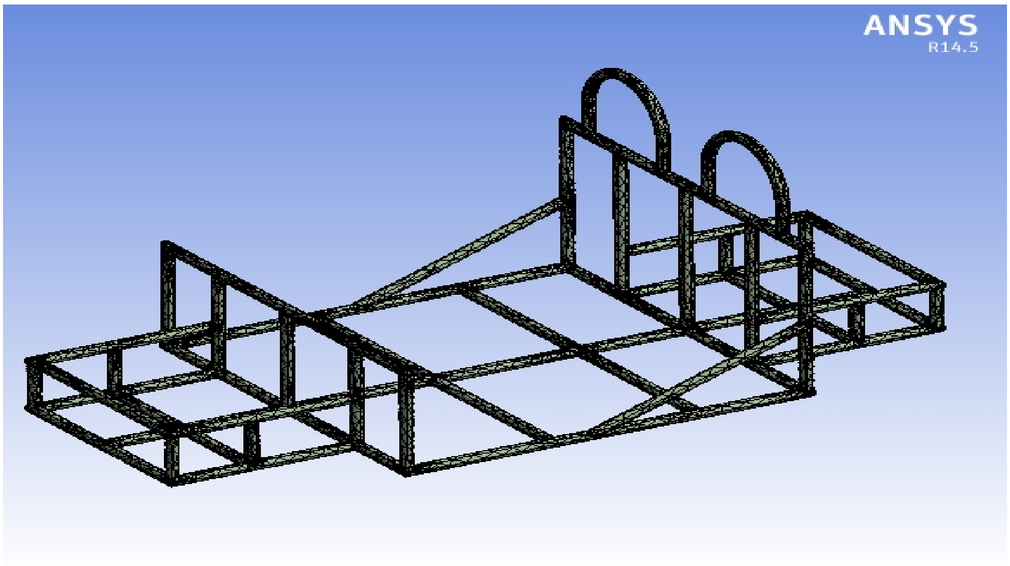

Figure 3.29. Mesh generation on the circular tube profiled space frame chassis

Element and node numbers of square profiled space frame chassis are 24006 and 44993 for steel and aluminium materials and for composite material, element and node numbers are 15360 and 15235, respectively. Element and node numbers of circular tube profiled space frame chassis are 60074 and 113020 for steel and aluminium materials and for composite material, element and node numbers are 42799 and 42622, respectively.

3.2.2.3. Loading and Support Conditions

Loading procedure of the chassis is performed considering two different conditions, which are distributed loading and torsional loading. As a result of the distributed loading, maximum von-Mises stress and maximum deformation values are obtained. Torsional loading is performed to find the maximum torsional deformation value and these torsional deformation values are used to calculate the torsional stiffness of the chassis.

Distributed loading process includes the weight of all vehicle components, one driver and one passenger. Location of the distributed loads considered for front, middle and rear sections of the chassis. Weights of these sections are calculated before loading the chassis in ANSYS. Front section of the chassis includes battery pack and steering system, weighs about 60 kg. Middle section of the chassis includes driver, passenger and two seats, weighs about 170 kg. Rear section of the chassis includes electric motor and rear axle, weighs about 35 kg. A lightweight electric vehicle body is considered for the analysis and 35 kg weight of this body is added to the all sections of the chassis as roughly 60 N each. Total weight of the electric vehicle is about 300 kg and roughly, 3000 N of forces are applied to the system. Weights and considering forces are illustrated in Table 3.6.

Table 3.6. Weights and forces of distributed loading

	Weight (kg)	**Force (N)**
Battery Box	45	450
Steering System	15	150
Seats x 2	20	200
Passengers x 2	150	1500
Electric Motor	20	200
Rear Axle	15	150
Vehicle Body	35	350
Total	**300**	**3000**

Distributed forces are applied to the mounting locations of the components. Forces are divided into two and each force applied to the one side of the chassis. Locations of the forces are determined in the design phase. Different chassis types have different locations due to different designs, but all chassis types have the same magnitudes of the forces. Exact locations of the forces are applied to the chassis using coordinate systems and for the front section 720 N force applied to the 2 sides of the chassis frame each having 360 N force. 1820 N force is applied to the 2 sides of the middle section of the chassis each having 910 N forces and for the rear section 470 N force applied to the two sides of the frame each having 235 N. After applying the forces on the chassis, support conditions are determined. Chassis is supported from the ground by its four wheels and to simulate this situation, mounting points of the wheels are fixed, using fixed supports. Distributed load locations and support conditions of the ladder frame are illustrated in Figures 3.30 and 3.31.

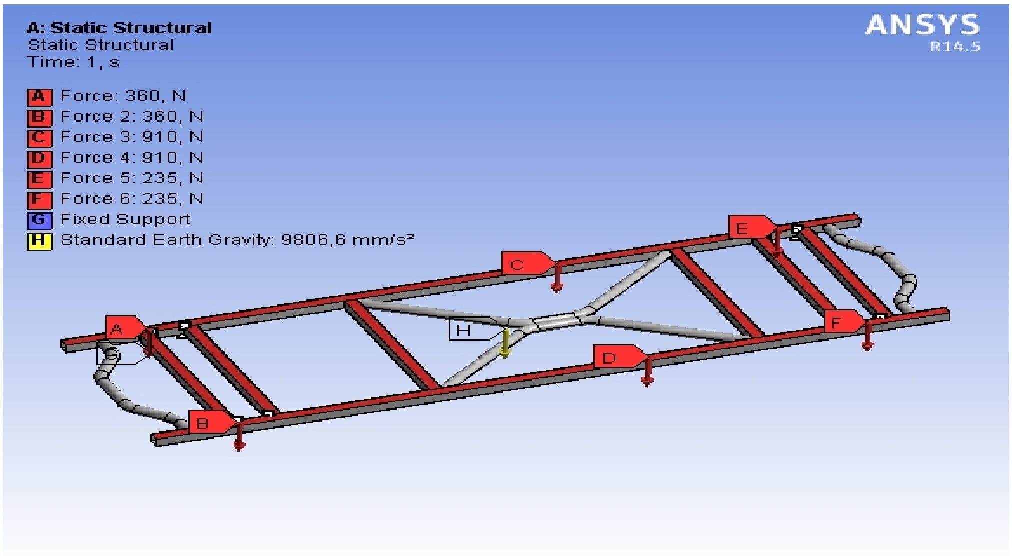

Figure 3.30. Distributed loads of the square profiled ladder frame chassis

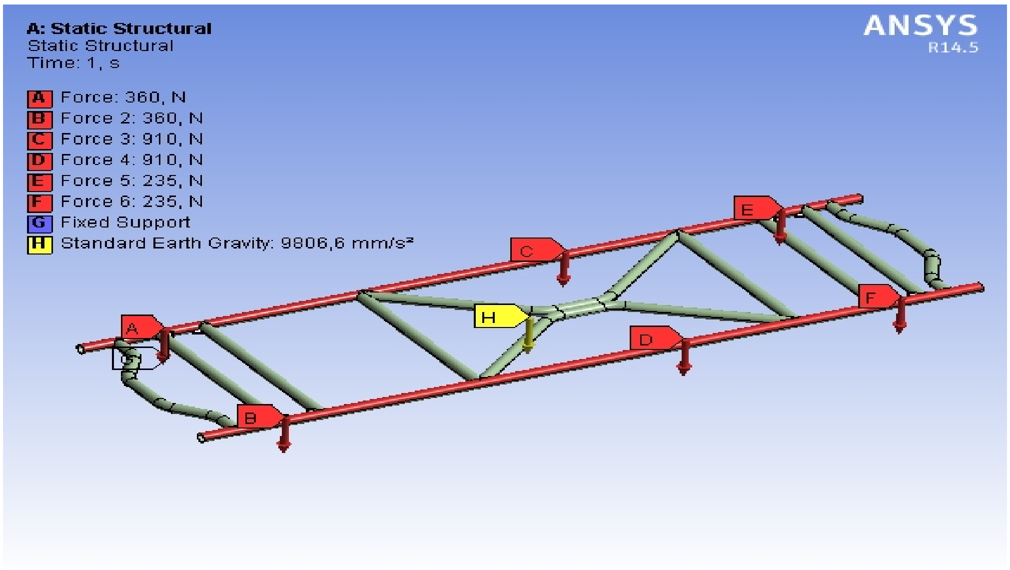

Figure 3.31. Distributed loads of the circular tube profiled ladder frame chassis

Distributed load locations and support conditions of the backbone chassis are given in Figures 3.32 and 3.33.

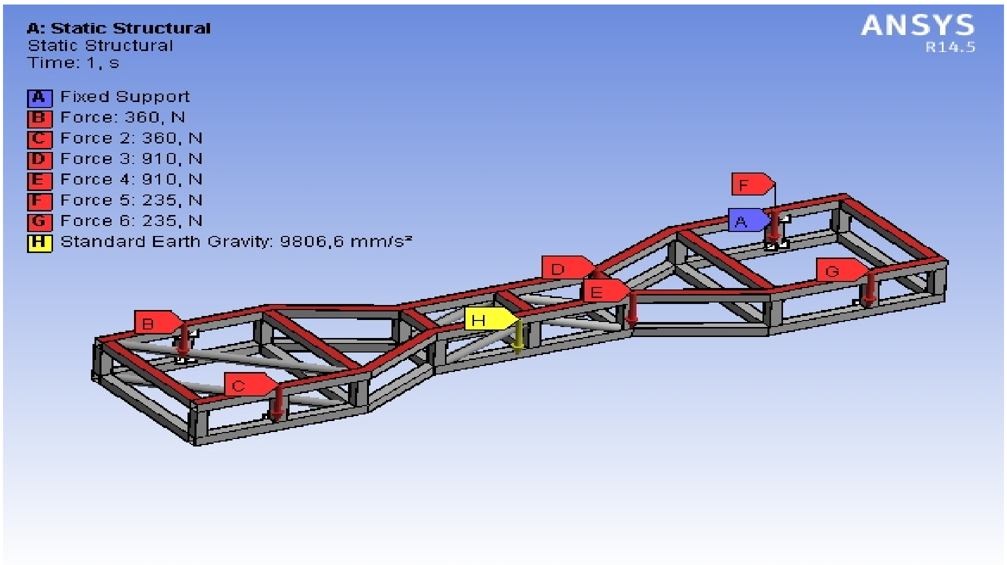

Figure 3.32. Distributed loads of the square profiled backbone chassis

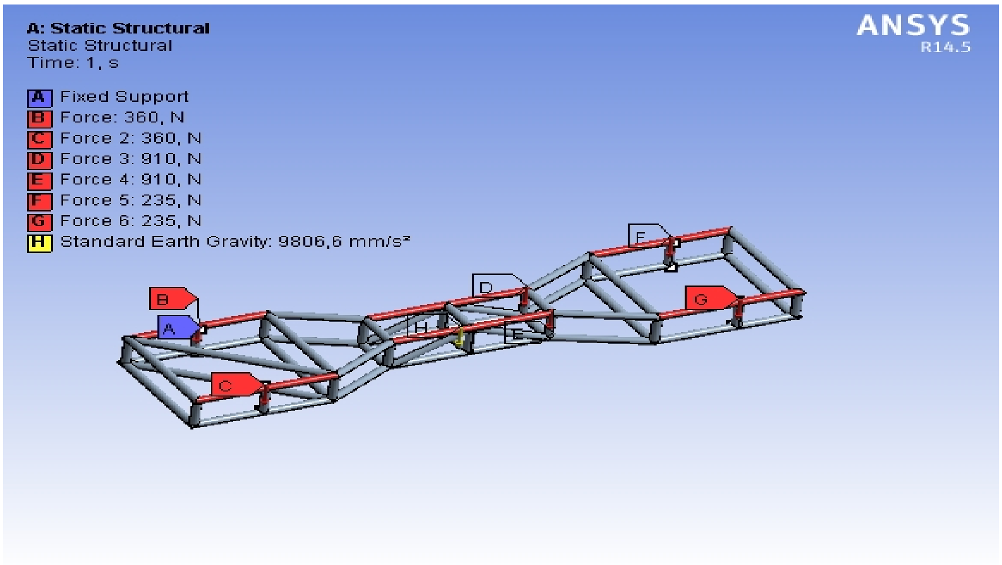

Figure 3.33. Distributed loads of the circular tube profiled backbone chassis

Distributed load locations and support conditions of the space frame chassis are illustrated in Figures 3.34 and 3.35.

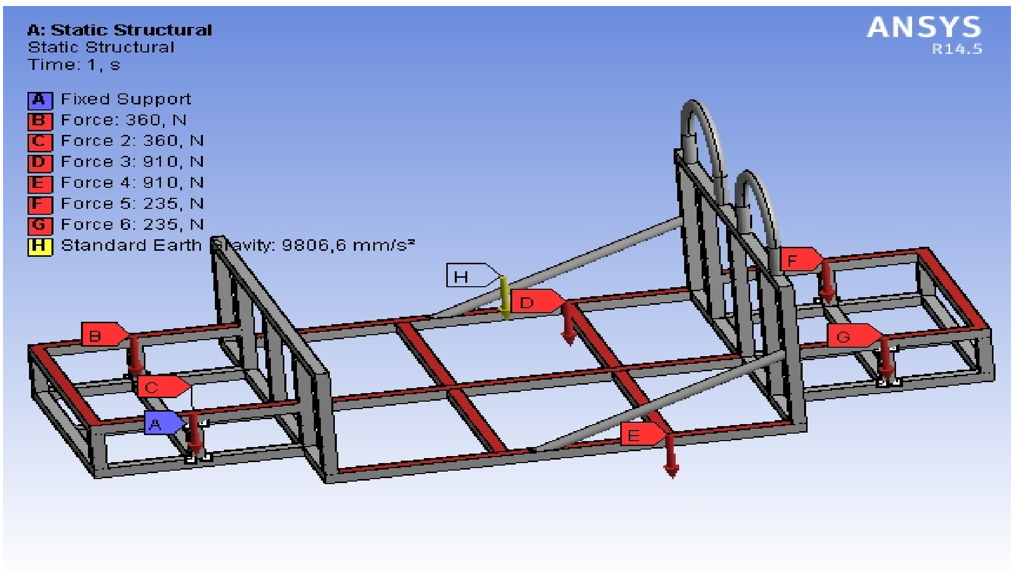

Figure 3.34. Distributed loads of the square profiled space frame chassis

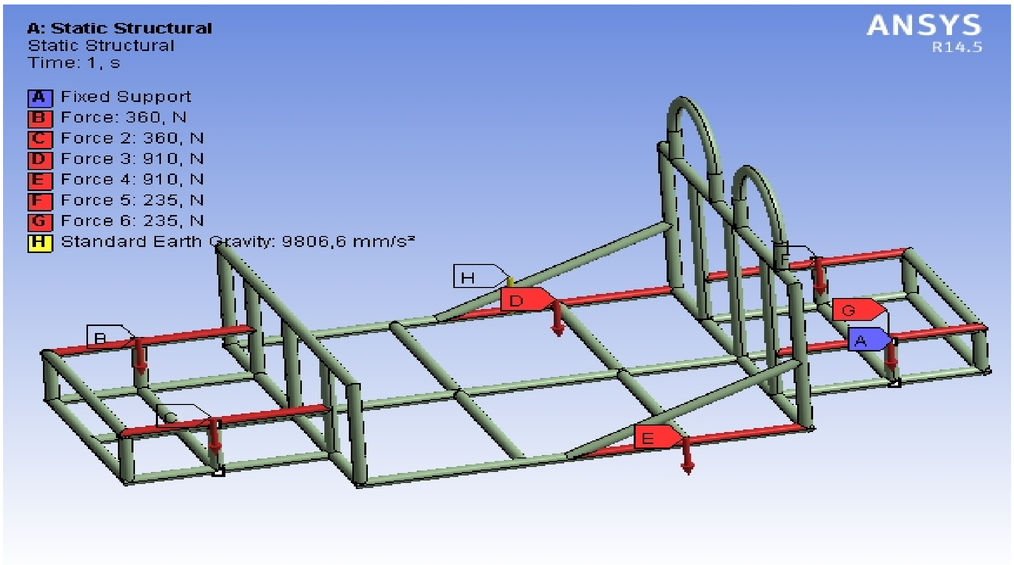

Figure 3.35. Distributed loads of the circular tube profiled space frame chassis

The other condition for the loading procedure is torsional loading. Torsional loading of the chassis is performed to obtain torsional deformation values of the chassis. Torsional stiffness of the chassis is calculated using the values of the torsional deformation.

Handling of a vehicle is the capability of keeping four wheels on the road. Especially on bumpy roads or cornering at high speeds, this situation is harder and comfort of the vehicle is directly related to the chassis of the vehicle because all the loads are transmitted to the chassis. In this situation, torsional stiffness of the vehicle becomes a critical value. As the name state, torsional stiffness of the vehicle is considered under the torsional loading. If chassis is designed as torsionally stiff then the entire vehicle will be torsionally stiff (Adams, 1993). Torsional stiffness is the resistance capacity of a chassis under torsional loading. Torsional loading is simulated in ANSYS software and torsional stiffness of the chassis is calculated using torsional deformation values obtained by the analysis results.

Torsional loading on the chassis is simulated using 198 Nm torque. This value is selected to have exact 150 N of force for ease of the analysis and calculations. Torque is divided into front track width of the vehicle, which is 1320 mm, and resulting two 150 N forces are applied to the front of the chassis in opposite directions where two wheels are mounted. Chassis width is smaller than the track width so these forces are applied as remote forces to achieve 1320 mm track width. Mountings of the rear wheels are fixed using fixed supports as support conditions. As a result of this torsional loading, chassis is deformed and maximum total deformation values are obtained from the analysis results. These maximum total deformation values are called maximum torsional deformation. Torsional loading locations and support conditions of the ladder frame chassis is illustrated in Figures 3.36 and 3.37.

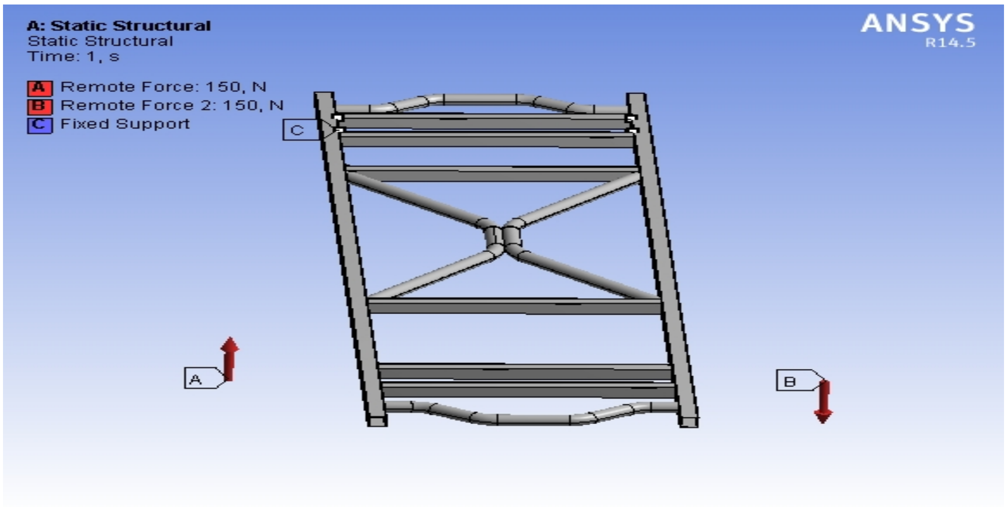

Figure 3.36. Torsional loading of the square profiled ladder frame chassis

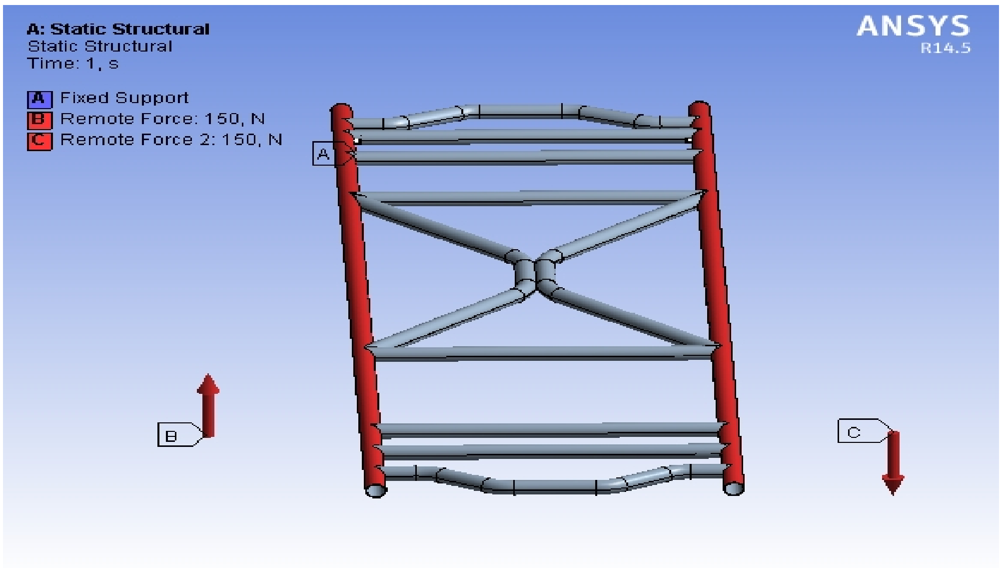

Figure 3.37. Torsional loading of the circular tube profiled ladder frame chassis

Torsional loading locations and support conditions of the backbone chassis is given in Figures 3.38 and 3.39.

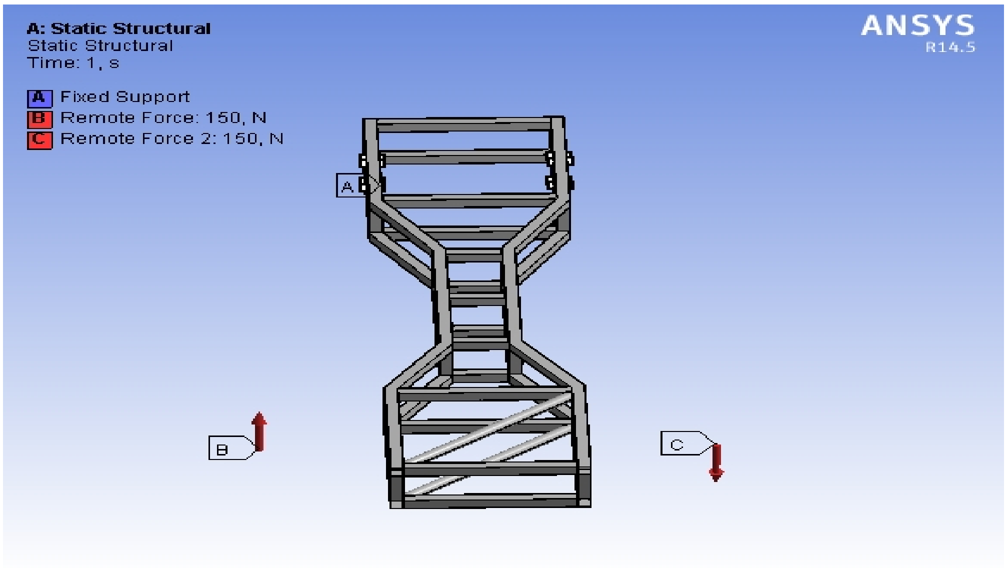

Figure 3.38. Torsional loading of the square profiled backbone chassis

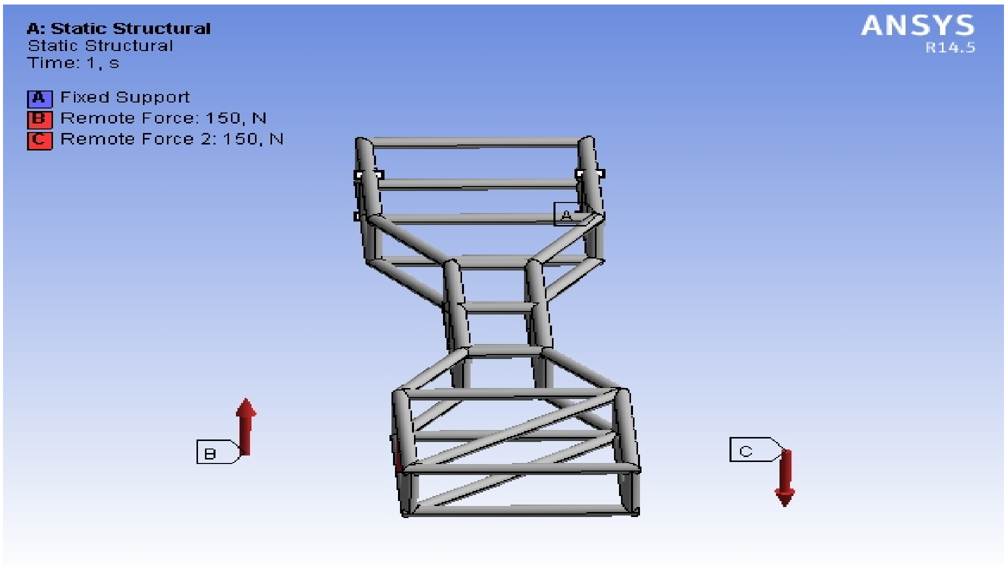

Figure 3.39. Torsional loading of the circular tube profiled backbone chassis

Torsional loading locations and support conditions of the space frame chassis is shown in Figures 3.40 and 3.41.

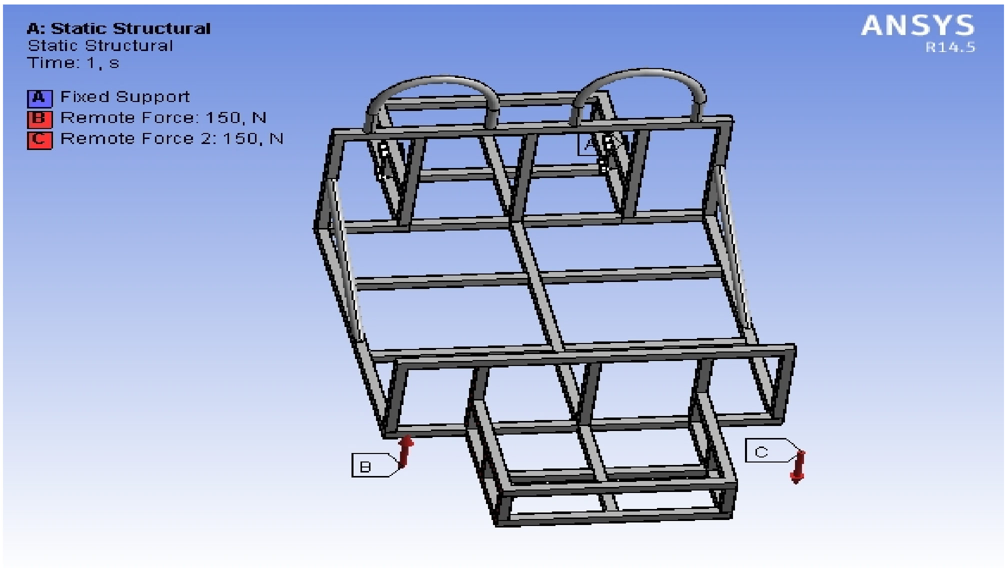

Figure 3.40. Torsional loading of the square profiled space frame chassis

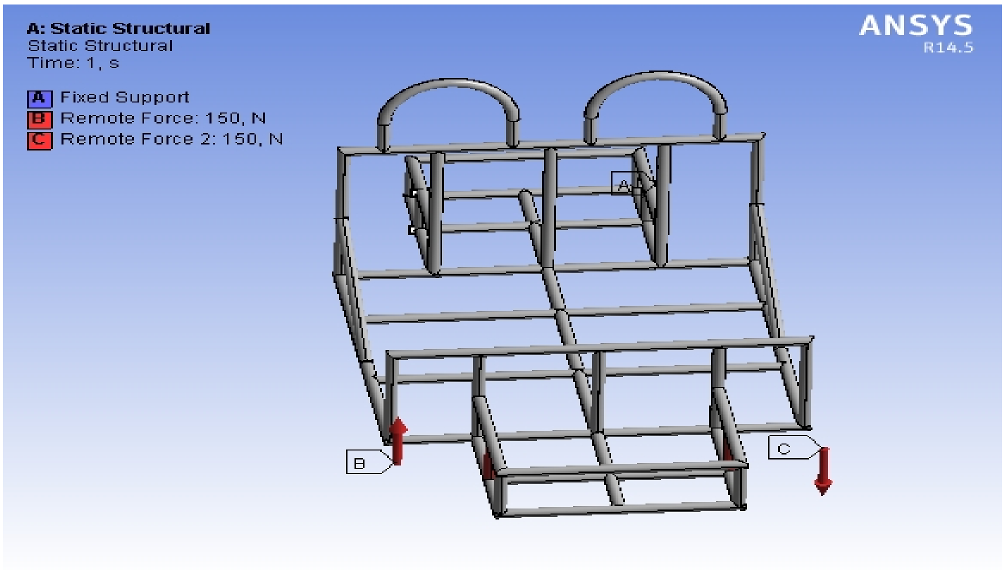

Figure 3.41. Torsional loading of the circular tube profiled space frame chassis

Torsional stiffness of the chassis is calculated using the structural analysis results of the torsional loading. Torsional stiffness (K) is equal to the; torque (T) divided by angular deformation (θ). Angular deformation value (θ) of the chassis is equal to the; arctangent of the maximum torsional deformation (Δy) divided by track width (L) (Riley and George, 2002).

Angular deformation (θ) has a unit of radian so it is converted to degree. Steps of the torsional stiffness calculation are expressed in Equations 3.1 and 3.2.

$$\theta = \tan^{-1}\left[\frac{(\Delta y)}{L}\right] \tag{3.1}$$

$$K = \frac{T}{\theta} \tag{3.2}$$

The unit of the angular deformation (θ) is after multiplying with the approximately 57.296 (1 radian is taken as 57.296 degree) degree and unit of the torque is Nm, so resulting unit of the torsional stiffness is Nm/degree.

Square profiled aluminium space frame chassis' torsional stiffness is calculated as an example. Calculation of the torsional stiffness (K) started with the calculation of the angular deformation (θ). Arctangent value is calculated by dividing torsional deformation value, which is 3.217 mm obtained from the torsional loading analysis, to the front track width of the chassis, which is 1320 mm for all chassis designs. Resulting 0.002437 value is in radians and multiplying this value with 57.296 gives angular deformation (θ) value, which is 0.1396 degree. Dividing 198 Nm torque (T) to this 0.1396 degree angular deformation (θ) value results in approximately 1418 Nm/deg. All other calculations are based on this procedure.

Torsional stiffness values of the chassis types are compared and besides 198 Nm of torque, additional torque magnitudes of 297 Nm and 396 Nm are used to obtain exact 225 N and 300 N of forces to observe the torsional stiffness characteristics of the chassis.

3.2.2.4. Composite Modelling

Composite analysis have the same procedure with the other materials used in chassis analysis but in the material assignment step, composite material is modelled using ANSYS Composite PrepPost (ACP) software which is a component system of ANSYS. Before the modelling procedure, composite material type and thickness is selected. Square and circular section geometries have 2.5 mm of thickness and to make a reliable comparison among the materials and chassis types, composite material thickness is also selected as 2.5 mm. As a composite material carbon fiber epoxy is selected from the material library of the software.

Before starting to the modelling, three-dimensional models of the all chassis types are imported to the software in .STEP file extension and models are converted to surface body using ANSYS design modeller and mesh is generated on this surface.

Composite modelling process started with the definition of the fabric. Fabrics are selected from the composite material library of the software. Composite material is selected as carbon fiber epoxy so fabric is also selected as woven carbon fiber and fabric thickness is considered as 0.25 mm. Selected composite material and fabric thickness are shown in Figure 3.42.

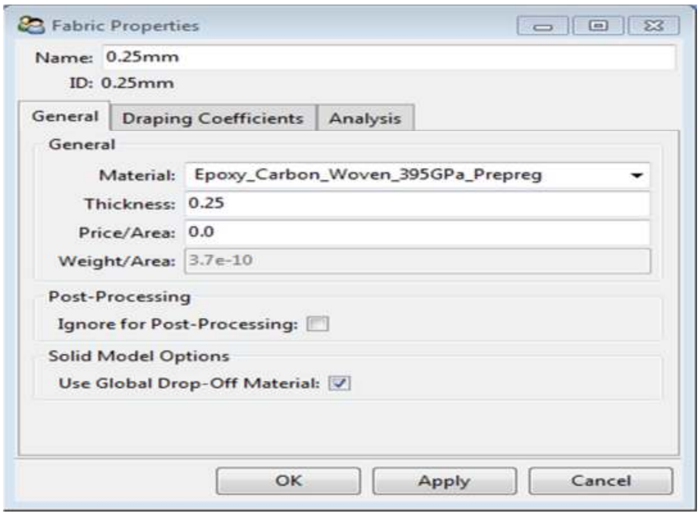

Figure 3.42. Selected composite material and fabric thickness

Certain numbers of fabrics are used to create the composite laminate. Lamination process is organized using stack-up section of the software. A stack-up is the combination of the fabrics. 10 plies are used in the stack-up creation due to the total 2.5 mm thickness of the laminate. Ply angles are defined in the software. Special case cross-ply is considered for the stack-up. Cross-ply laminate has only 0° and 90° plies and order of the angles are used as $[0/90_2/0/90]$ (Kaw, 2006). Also even symmetry is used and 2.5 mm laminate thickness is obtained from the 10 plies. Stack-up design is given in Figure 3.43.

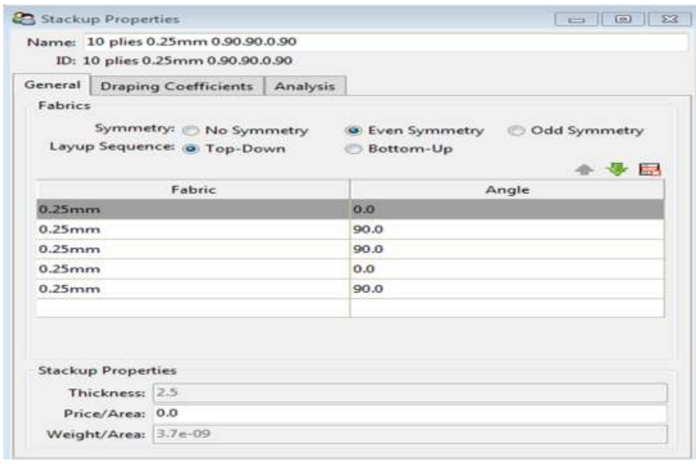

Figure 3.43. Stack-up design using cross-ply laminate

Directions of the fibers are determined using rosettes section of the software. Rosettes are defined as parallel type and orientation of the plies are based on this fiber direction. Orientation of the plies is defined in the oriented element sets section and direction of them is selected outward.

Fiber direction of 0° angle fibers is always parallel to the surface of the chassis and plies are laid down from bottom to top. Fabric selection, fiber direction and oriented element sets are defined as entire composite material in modelling ply group section and imported as layered section to the structural analysis. ACP software general view is illustrated in Figure 3.44.

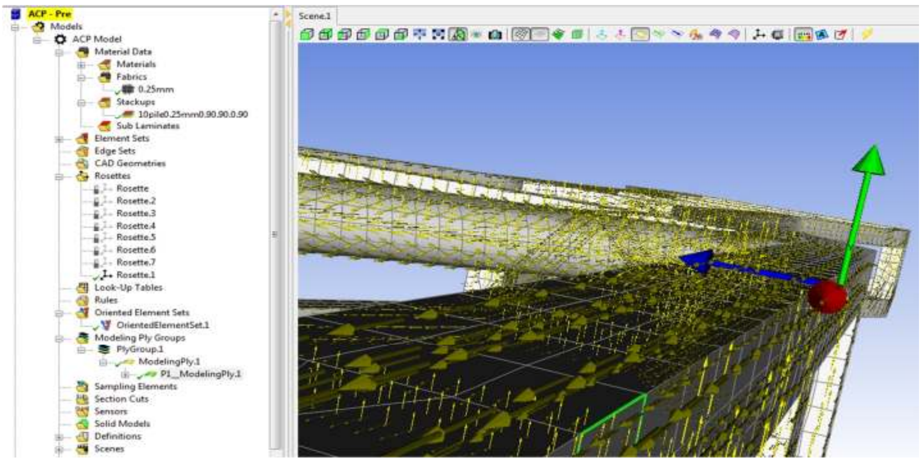

Figure 3.44. General view of the ACP software

3.3. Design Optimization of the Chassis

Analysis results of the chassis include weight, safety and comfort data of all chassis types with different materials. Three chassis types including two different section geometries are structurally analysed considering three materials. Analysis results include weight, maximum von-Mises stress, maximum deformation, maximum torsional deformation and torsional stiffness data. Torsional stiffness is obtained from the results of the torsional deformation so there are finally four different results data to be considered. As a result of the all designs and analysis, there are 72 different data of chassis types, section geometries and materials. Selection of the optimum design is performed considering two different methods. First method is the parametric optimization of the data. As a result of the parametric optimization, five chassis designs are selected which have the highest parametric performance and these chassis designs are compared. Chassis is designed considering the rules of the electromobile race so comparison and selection criteria are made regarding electromobile race rules. Finally, selected design is structurally optimized as a second method to improve the racing performance of the vehicle via chassis.

3.3.1. Parametric Optimization of the Chassis

Parametric optimization of the chassis is performed to find the optimum data of the analysis results (Cavazzuti et. al., 2011). Chassis design includes many factors with variables and performance of the chassis is directly affected from them. Taguchi method is used for the selection of the optimum design among the many factors. It is a statistical method based on the design of experiments (DOE) methodology and is developed by Genichi Taguchi. In Taguchi method, variations of the system are divided into two categories. The first one is control factors and the other one is noise factors. Control factors are the design parameters of the system and noise factor are the non-controllable factors like environmental variables. Control factors generate responses over noise factors and generated signal to noise ratio is the function of these responses over noises.

Signal to noise ratio is calculated for desired output and this output could be maximum, minimum or nominal value (JMP, 2009). General steps of the Taguchi method are given in Figure 3.45.

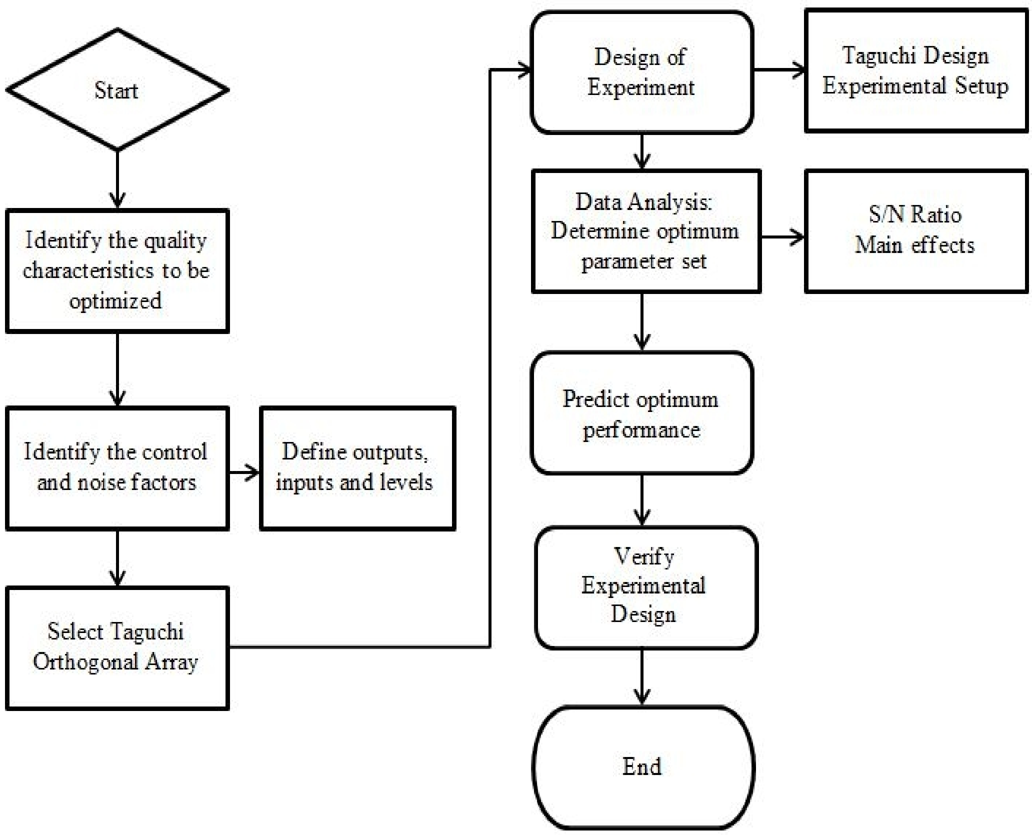

Figure 3.45. General steps of the Taguchi method

Selection of the optimum design is performed on the Minitab 17 statistical software using Taguchi method. Creating Taguchi design in the software is started with determining the factors of the system as section geometry, material and chassis type. Levels of these three factors are determined (Ziaulhaq et. al., 2013). Section geometry as a factor has two levels which are the square profiled main frame with circular tube profiled support beams and complete circular tube profiled chassis and levels of the section geometry is named as square and circular. Material as a factor has three levels, which are AISI 4130 steel, aluminium 5042-H19 and carbon fiber epoxy and levels are named as steel, aluminium and composite. Chassis type as a factor has three levels, which are ladder frame chassis, backbone chassis and space frame chassis, and levels are named as ladder frame, backbone and space frame. Taguchi design has three factors and one of the factors has two levels while the other two factors have three levels so Taguchi design is created using mixed level design with number of factor of three. Taguchi orthogonal array is selected as L18. Factors with levels in coded units and selection of the orthogonal array are illustrated in Figures 3.46 and 3.47.

Section Geometry	Material	Chassis Type
1	1	1
1	1	2
1	1	3
1	2	1
1	2	2
1	2	3
1	3	1
1	3	2
1	3	3
2	1	1
2	1	2
2	1	3
2	2	1
2	2	2
2	2	3
2	3	1
2	3	2
2	3	3

Figure 3.46. Factors with levels in coded units

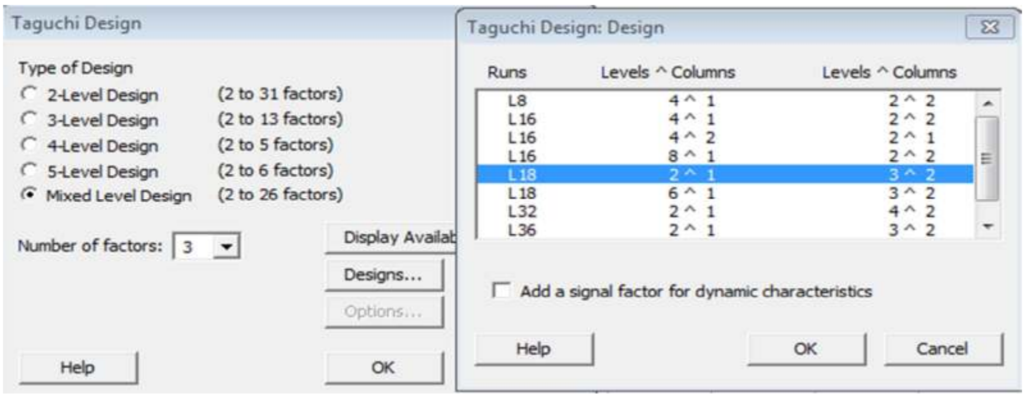

Figure 3.47. Selection of the orthogonal array

Taguchi design is created after entering the uncoded units of the factors and levels into the worksheet and then analysis results of these factors and levels are entered into the worksheet. Analysis results include maximum von-Mises stress, maximum deformation and maximum torsional deformation and weight values. Created Taguchi design is given in Figure 3.48.

↓	C1-T	C2-T	C3-T	C4	C5	C6	C7
	Section Geometry	Material	Chassis Type	von-Mises Stress (MPa)	Maximum Deformation (mm)	Max Torsional Deformation (mm)	Weight (kg)
1	Square	Steel	LadderFrame	26,344	0,697	1,578	34,810
2	Square	Steel	Backbone	17,834	0,163	0,463	56,961
3	Square	Steel	SpaceFrame	13,587	0,505	1,086	88,842
4	Square	Aluminium	LadderFrame	24,379	1,882	4,712	11,840
5	Square	Aluminium	Backbone	15,319	0,427	1,367	19,374
6	Square	Aluminium	SpaceFrame	12,706	1,356	3,217	30,218
7	Square	Composite	LadderFrame	43,251	1,844	5,926	9,467
8	Square	Composite	Backbone	17,607	0,599	2,538	14,861
9	Square	Composite	SpaceFrame	24,222	1,526	5,310	17,447
10	Circular	Steel	LadderFrame	53,220	1,599	2,227	29,406
11	Circular	Steel	Backbone	43,591	0,306	0,679	47,175
12	Circular	Steel	SpaceFrame	30,826	0,782	1,757	71,898
13	Circular	Aluminium	LadderFrame	50,408	4,443	6,638	10,002
14	Circular	Aluminium	Backbone	40,018	0,824	1,999	16,046
15	Circular	Aluminium	SpaceFrame	27,998	2,104	5,225	24,455
16	Circular	Composite	LadderFrame	99,614	4,367	10,560	7,834
17	Circular	Composite	Backbone	68,968	2,031	6,093	9,312
18	Circular	Composite	SpaceFrame	81,688	3,437	12,078	14,115

Figure 3.48. Taguchi design in Minitab

Taguchi design is analysed using analysis results as response factors and signal to noise ratios are obtained from these response factors (www.minitab.com). Main goal of the study is having minimum stress, deformation and weight values so smaller is better option is used for the signal to noise ratio.

Signal to noise ratios of designs are generated and highest five signal to noise ratios are selected. All five designs have square section geometry with aluminium and composite materials. Chassis type having the highest signal to noise ratio is backbone chassis while ladder frame comes second and space frame has the smallest value. Among the designs, square profiled aluminium space frame chassis is selected although this design have the smallest value of signal to noise ratio among the five of designs. According to the racing rules, vehicles must have roll bars and installing roll bar needs extra work for the ladder frame and backbone chassis. Moreover, ladder frame and backbone chassis also need extra work for the mounting and casing of the battery box and electric motor. Using composite material makes the vehicle lighter but composite materials are expensive. Electric vehicle will be used for race only so composite material use is not feasible for this one-time use. Although space frame has structural advantage for mounting of the components, it has less signal to noise ratio than the square profiled composite backbone chassis, which has the highest value of signal to noise ratio. Square profiled aluminium chassis also has less torsional stiffness and higher weight value then the square profiled composite backbone chassis. Structural optimization of the space frame chassis is performed to increase the torsional stiffness value and decrease the weight of the chassis.

3.3.2. Structural Optimization of the Chassis

As a result of the structural optimization new design has completely closed structure. Smaller dimensions are used for the section geometries to decrease the weight of the chassis. For the square section, 30 mm side length and for the circular section 30 mm diameter is used while 2.5 mm thickness is the same with the old design. Design and analysis procedure of the optimized structure is performed and procedure is the same as the previous chassis designs. Optimized square profiled space frame design is illustrated in Figure 3.49.

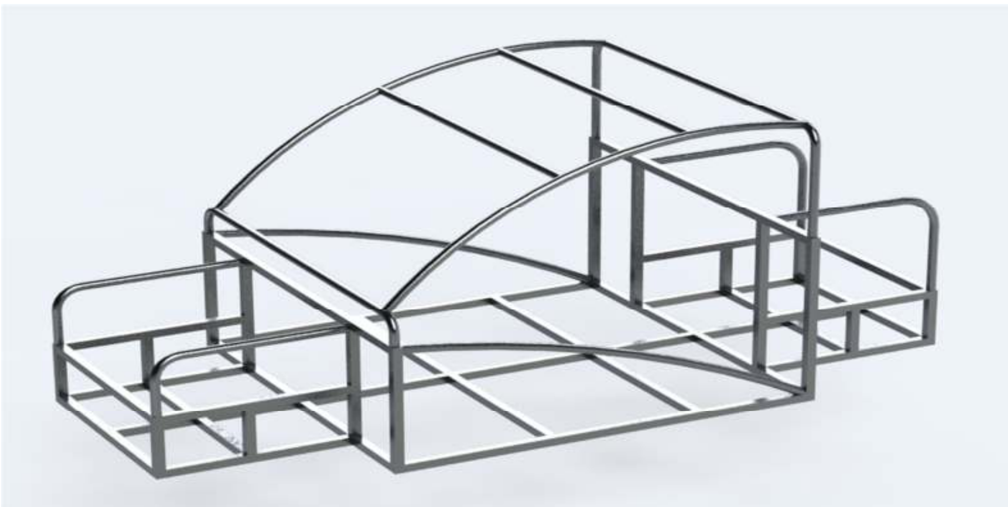

Figure 3.49. Structurally optimized square profiled space frame chassis

Structurally optimized design is analysed. Mesh is generated on the chassis and mesh generated model is shown in Figure 3.50.

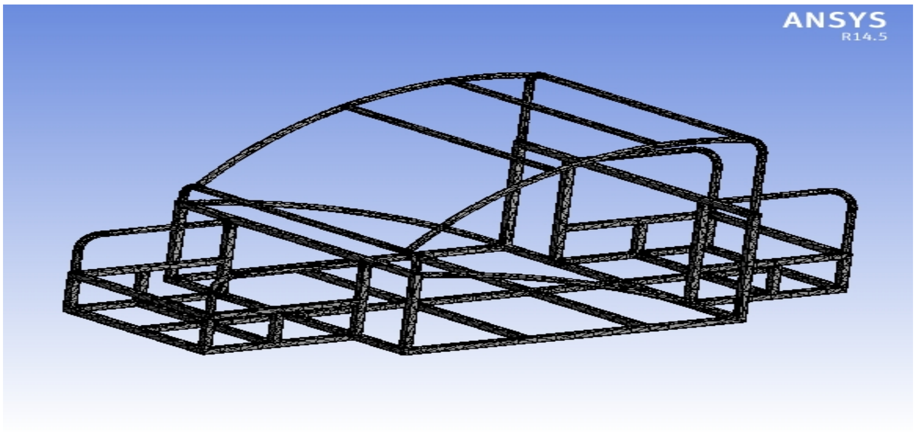

Figure 3.50. Mesh generation on structurally optimized space frame chassis

Loading and support conditions are determined for the chassis. Distributed loading and torsional loading conditions are illustrated in Figures 3.51 and 3.52.

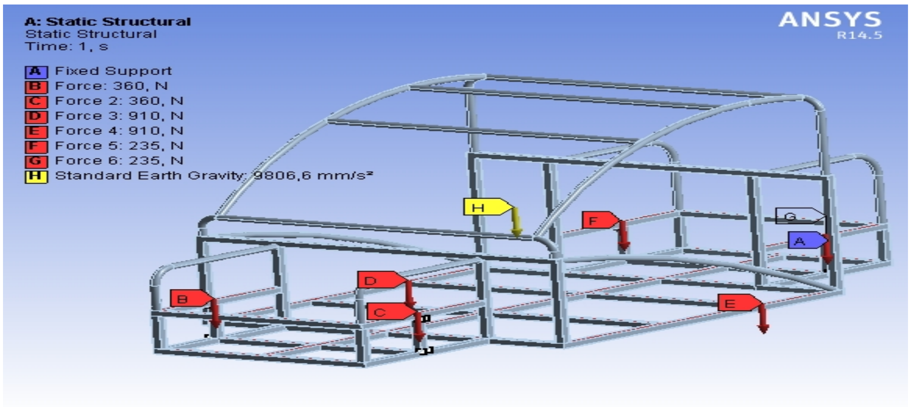

Figure 3.51. Distributed loads of the optimized space frame chassis

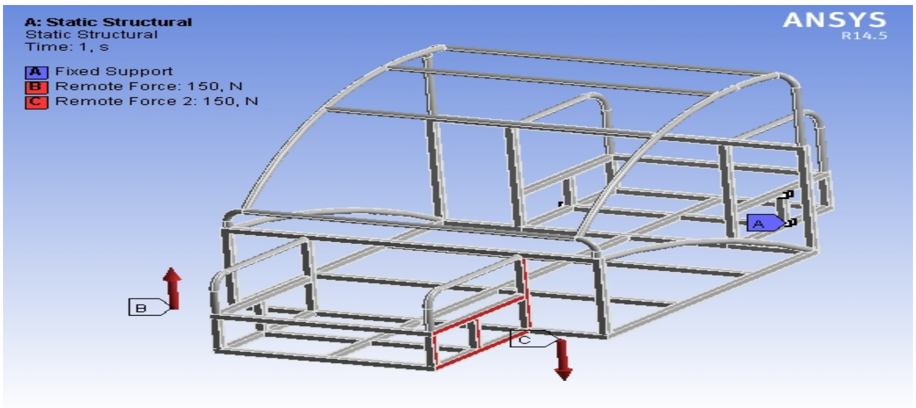

Figure 3.52. Torsional loading of the optimized space frame chassis

Body of the electric vehicle is designed using Solidworks. Composite material is considered for the body with a weight of 35 kg. Electric vehicle bodies from different perspectives are shown in Figures 3.53 and 3.54.

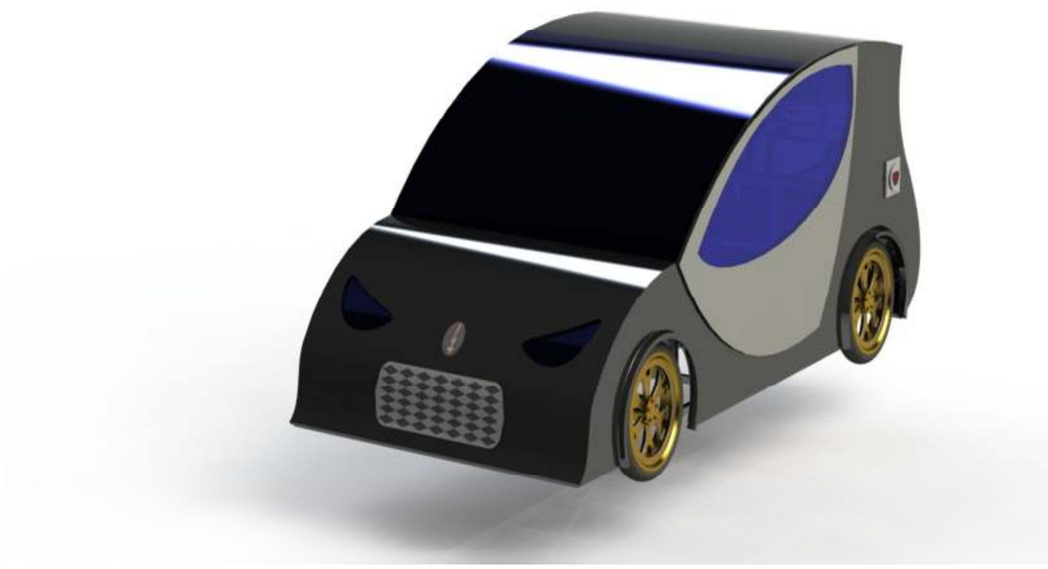

Figure 3.53. Front view of the electric vehicle body

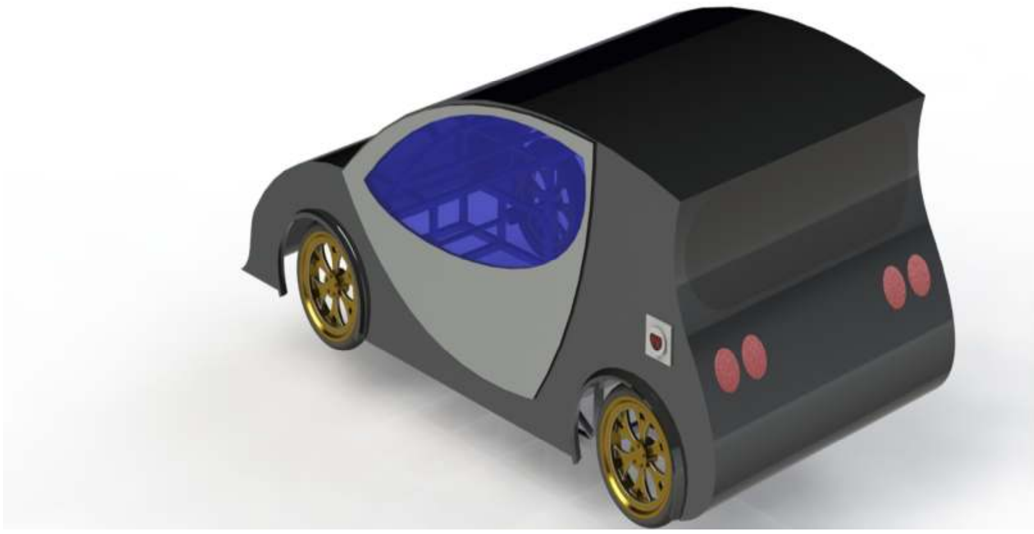

Figure 3.54. Rear view of the electric vehicle body

4. RESULTS AND DISCUSSION

4.1. Chassis Analysis Results

4.1.1. Chassis Weight

Weight data are obtained from the ANSYS software. As a result of the various chassis designs due to different section geometries, different chassis types and different materials, totally 18 weight data are obtained. Weight data of different designs are listed in Table 4.1.

Table 4.1. Weight data of the different chassis designs

Chassis Type	**Material**	**Section Geometry**	**Weight (kg)**
Ladder Frame	AISI 4130 Steel	Square	**34.810**
Ladder Frame	Aluminium 5042-H19	Square	**11.840**
Ladder Frame	Carbon Fiber	Square	**9.467**
Ladder Frame	AISI 4130 Steel	Circular	**29.406**
Ladder Frame	Aluminium 5042-H19	Circular	**10.002**
Ladder Frame	Carbon Fiber	Circular	**7.834**
Backbone	AISI 4130 Steel	Square	**56.961**
Backbone	Aluminium 5042-H19	Square	**19.374**
Backbone	Carbon Fiber	Square	**14.861**
Backbone	AISI 4130 Steel	Circular	**47.175**
Backbone	Aluminium 5042-H19	Circular	**16.046**
Backbone	Carbon Fiber	Circular	**9.312**
Space Frame	AISI 4130 Steel	Square	**88.842**
Space Frame	Aluminium 5042-H19	Square	**30.218**
Space Frame	Carbon Fiber	Square	**17.447**
Space Frame	AISI 4130 Steel	Circular	**71.898**
Space Frame	Aluminium 5042-H19	Circular	**24.455**
Space Frame	Carbon Fiber	Circular	**14.115**

4.1.2. Analysis Results of the Distributed Loading

Distributed loading results include maximum von-Mises stresses and maximum deformations. Maximum von-Mises stress results of the square and circular tube profiled ladder frame chassis with assigned materials of steel, aluminium and composite are illustrated in Figures 4.1 - 4.6.

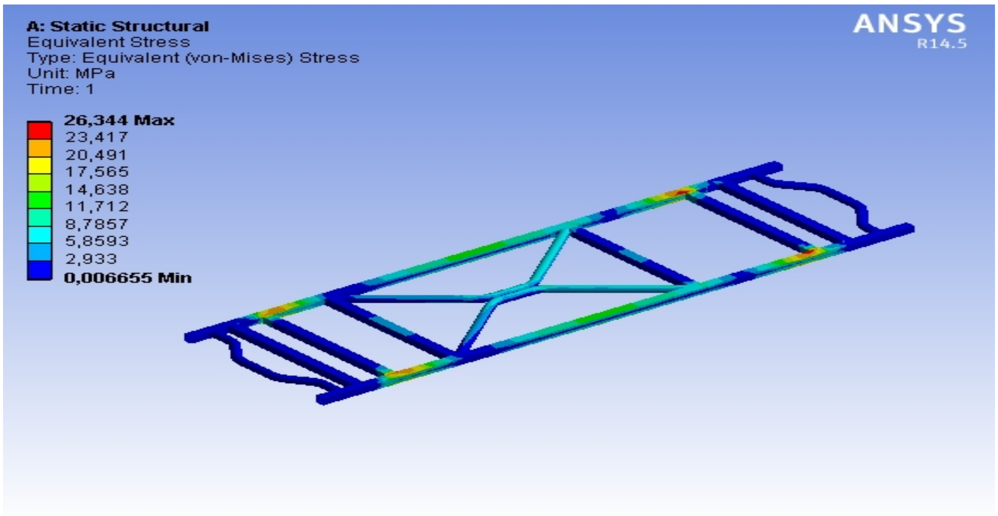

Figure 4.1. Maximum von-Mises stress of the square profiled AISI 4130 steel ladder frame

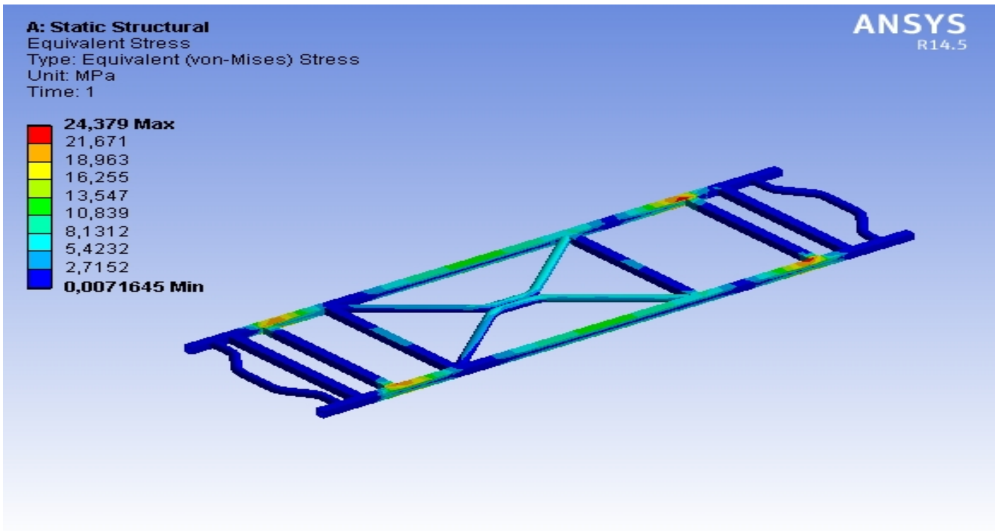

Figure 4.2. Maximum von-Mises stress of the square profiled aluminium 5042-H19 ladder frame

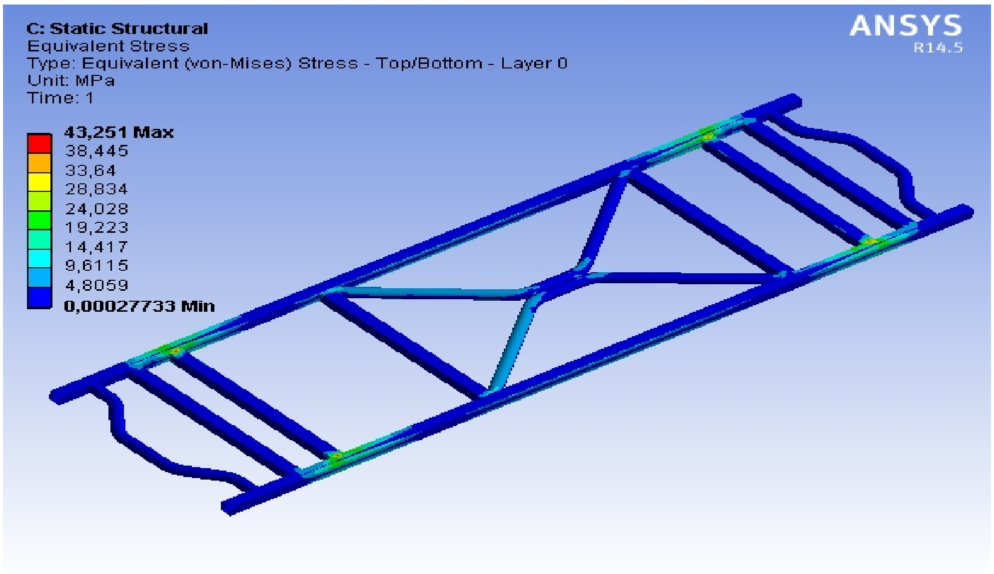

Figure 4.3. Maximum von-Mises stress of the square profiled carbon fiber ladder frame

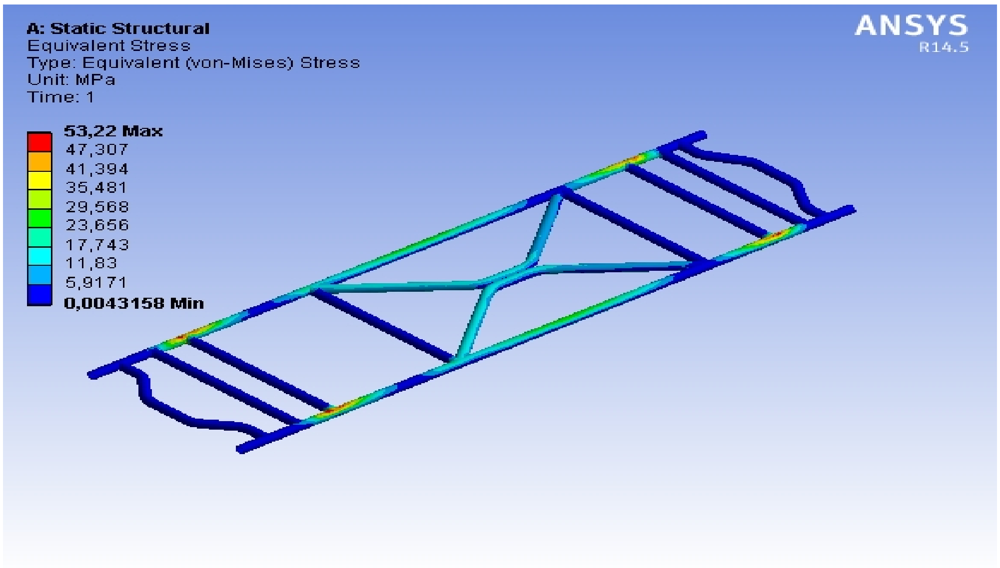

Figure 4.4. Maximum von-Mises stress of the circular tube profiled AISI 4130 steel ladder frame

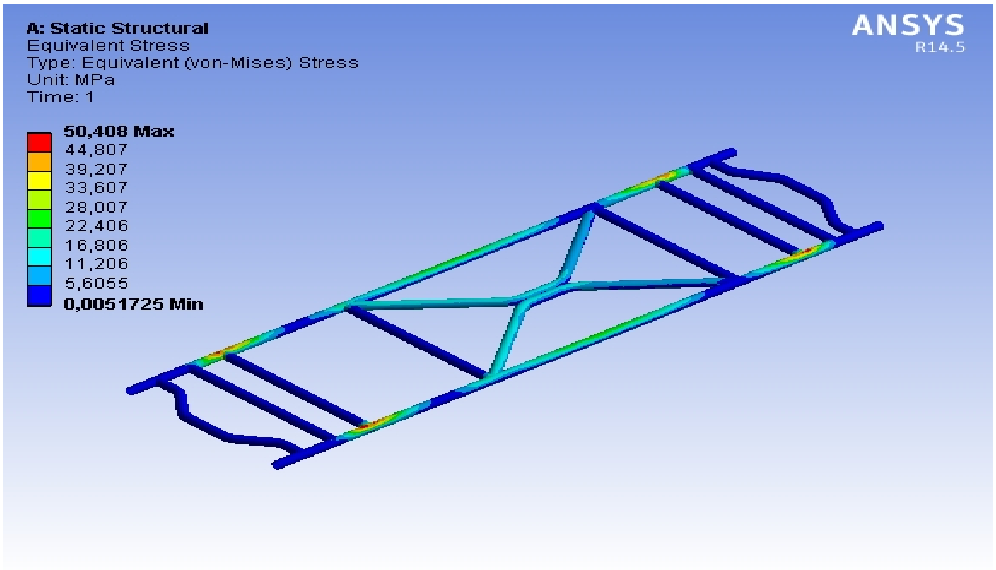

Figure 4.5. Maximum von-Mises stress of the circular tube profiled aluminium 5042-H19 ladder frame

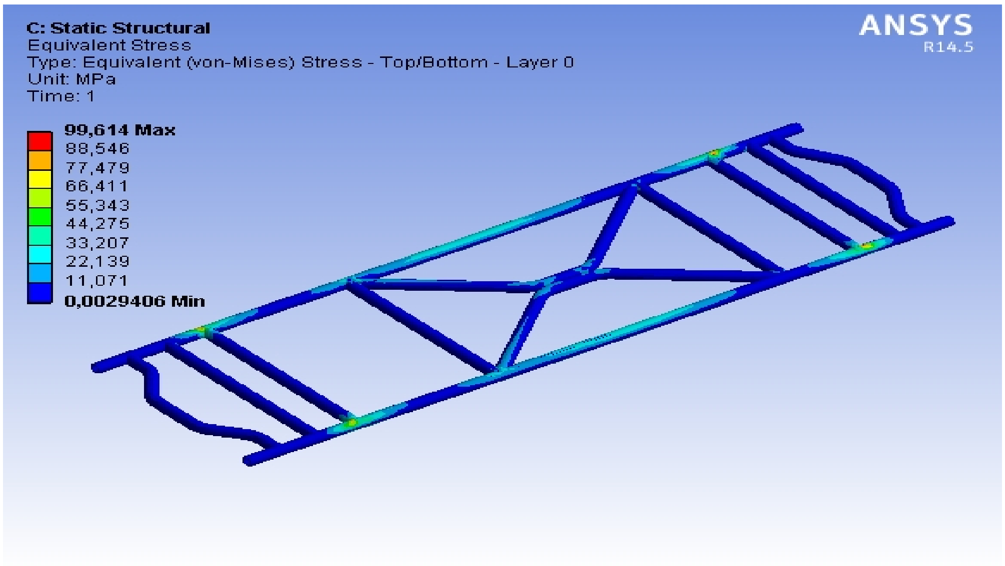

Figure 4.6. Maximum von-Mises stress of the circular tube profiled carbon fiber ladder frame

Maximum von-Mises stresses of the square and circular tube profiled backbone chassis with assigned materials of steel, aluminium and composite are given in Figures 4.7- 4.12.

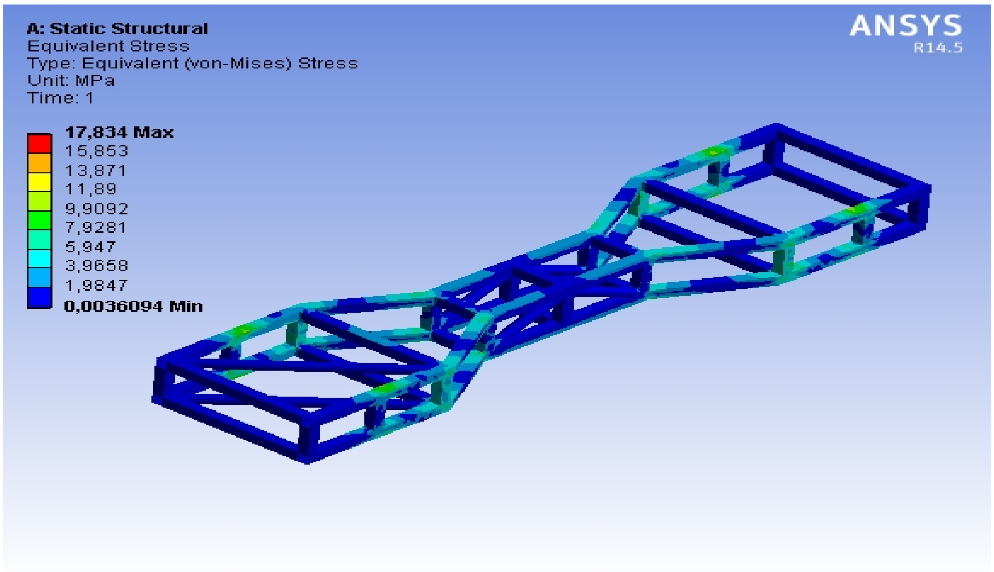

Figure 4.7. Maximum von-Mises stress of the square profiled AISI 4130 steel backbone chassis

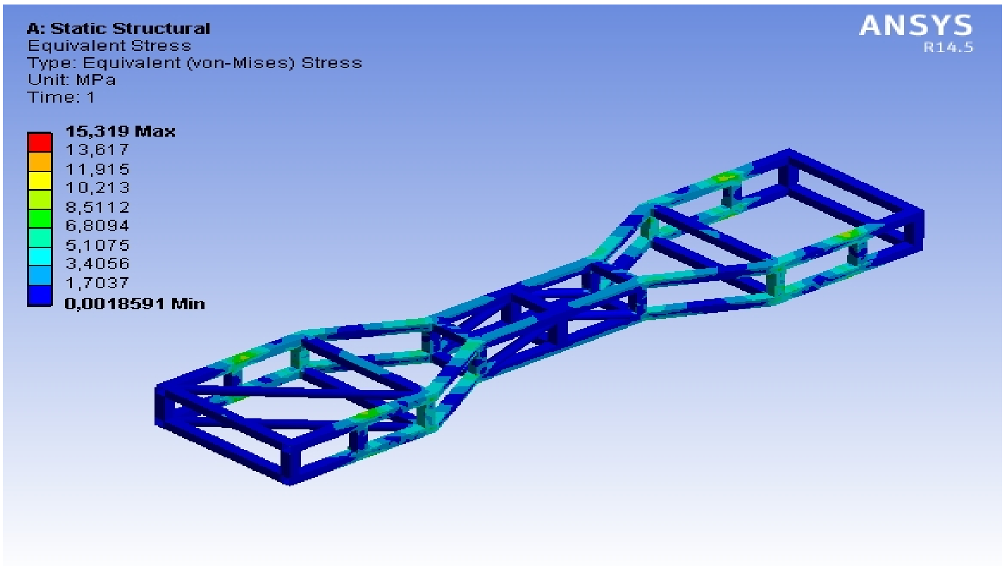

Figure 4.8. Maximum von-Mises stress of the square profiled aluminium 5042-H19 backbone chassis

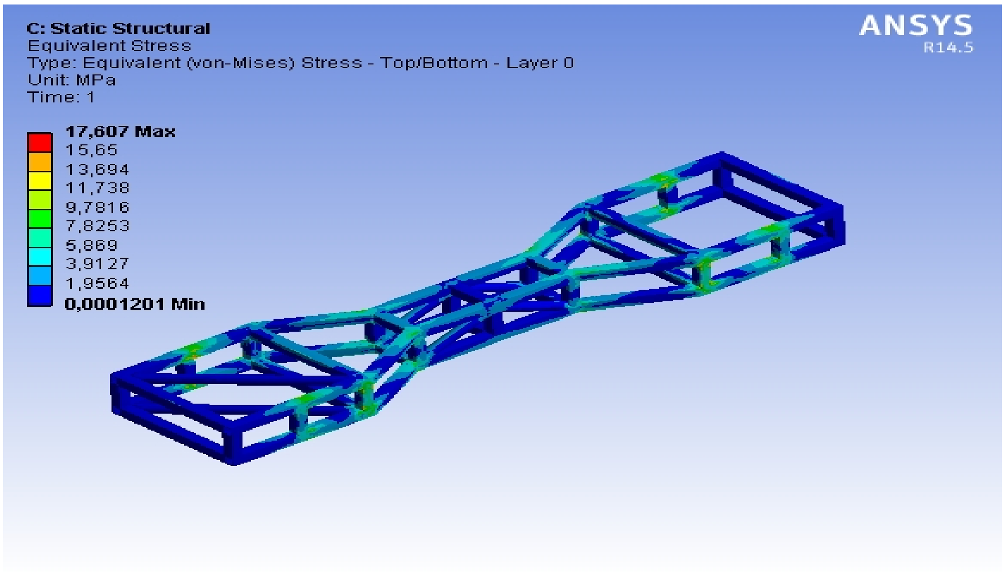

Figure 4.9. Maximum von-Mises stress of the square profiled carbon fiber backbone chassis

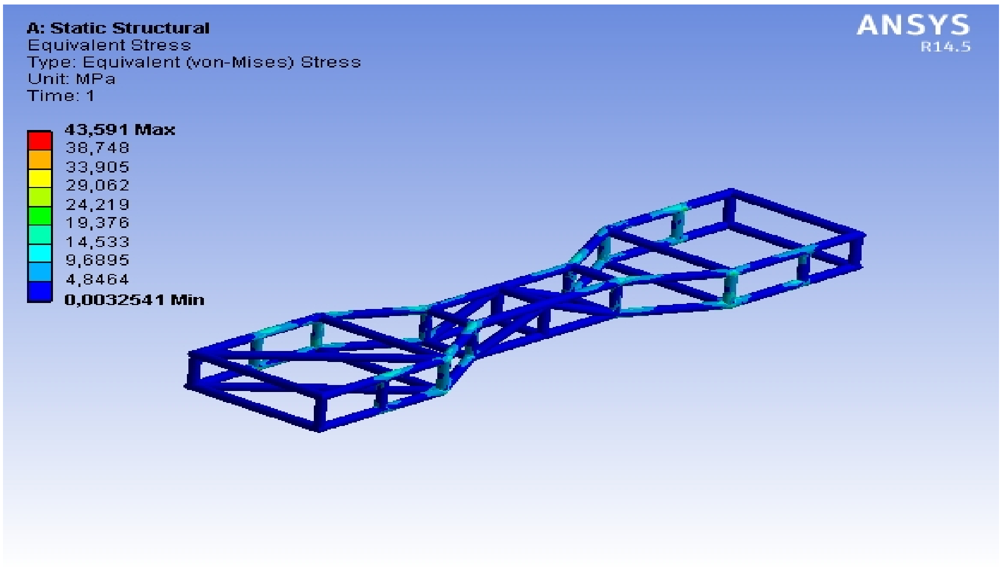

Figure 4.10. Maximum von-Mises stress of the circular tube profiled AISI 4130 steel backbone chassis

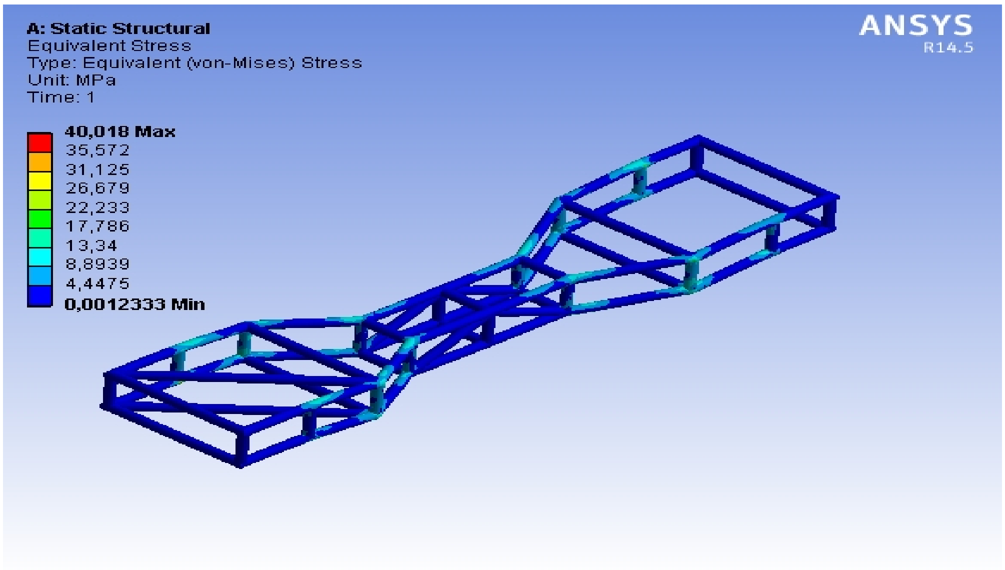

Figure 4.11. Maximum von-Mises stress of the circular tube profiled aluminium 5042-H19 backbone chassis

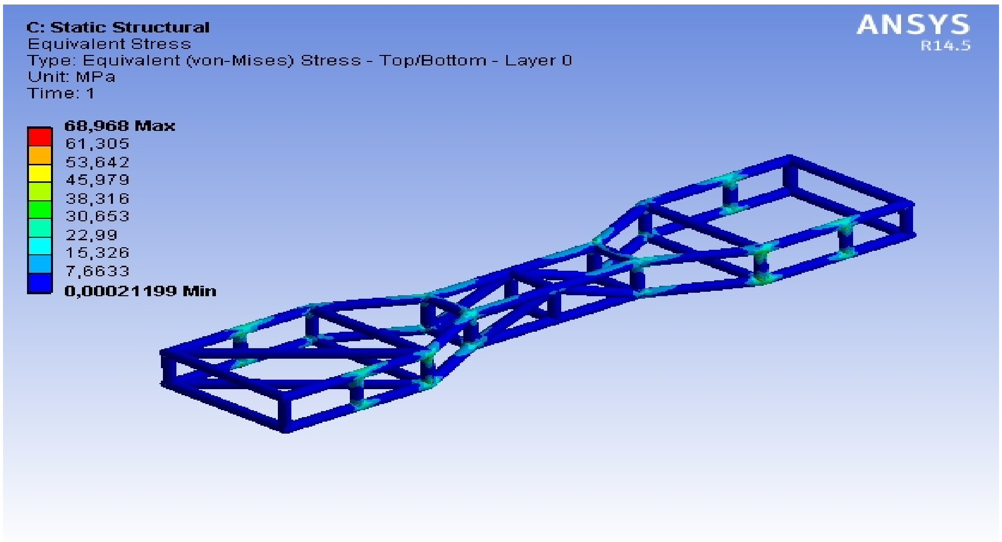

Figure 4.12. Maximum von-Mises stress of the circular tube profiled carbon fiber backbone chassis

Maximum von-Mises stresses of the square and circular tube profiled space frame chassis with assigned materials of steel, aluminium and composite are illustrated in Figures 4.13 - 4.18.

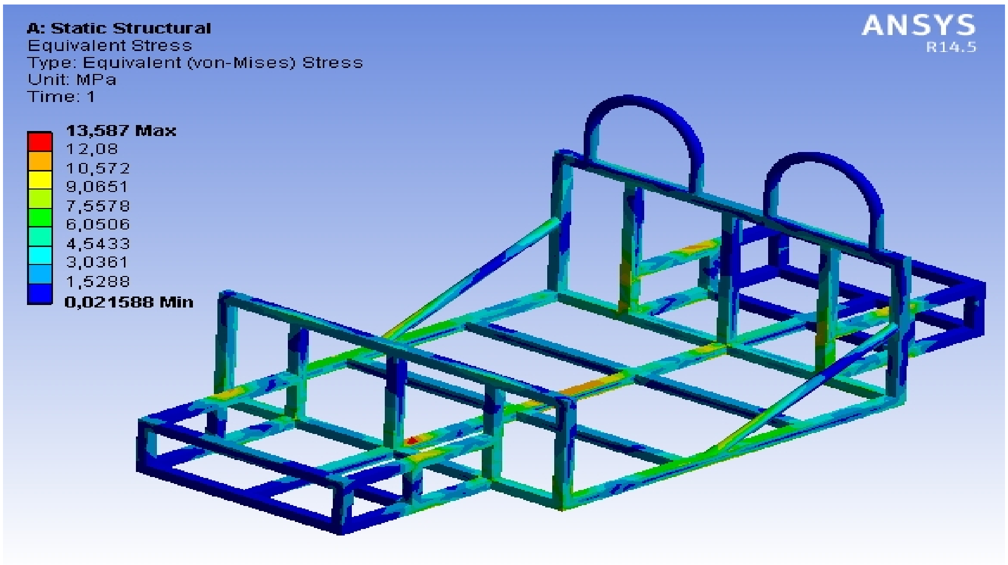

Figure 4.13. Maximum von-Mises stress of the square profiled AISI 4130 steel space frame

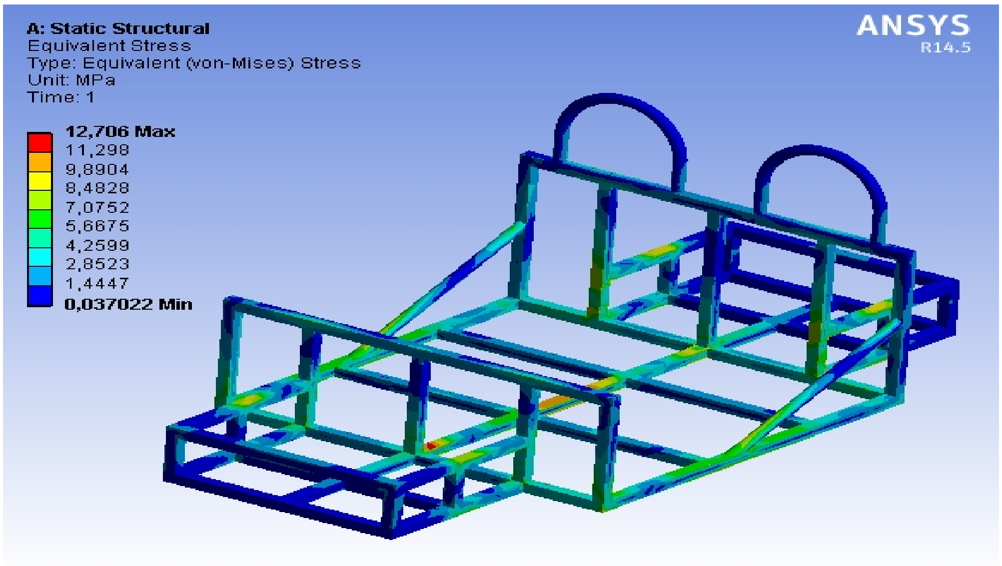

Figure 4.14. Maximum von-Mises stress of the square profiled aluminium 5042-H19 space frame

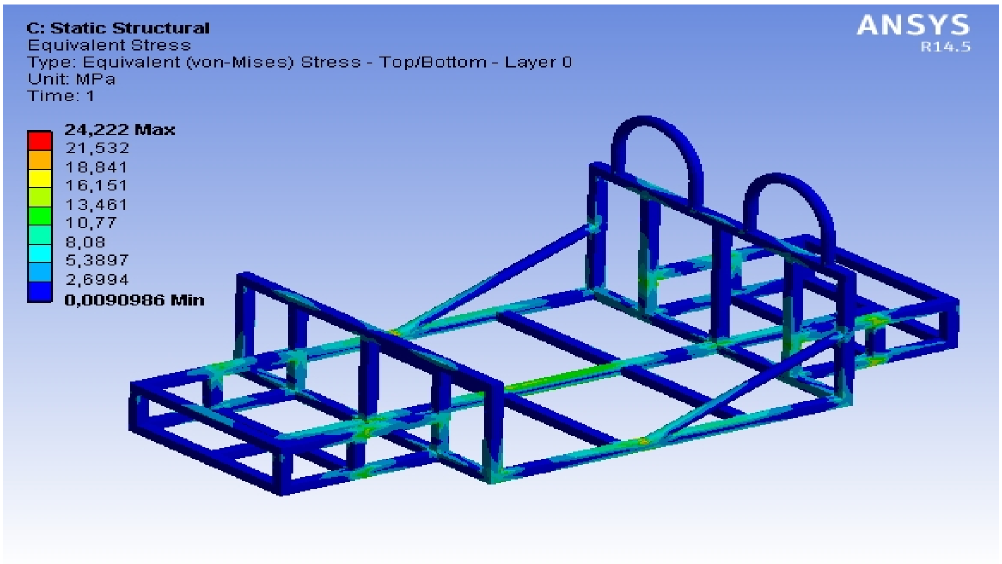

Figure 4.15. Maximum von-Mises stress of the square profiled carbon fiber space frame

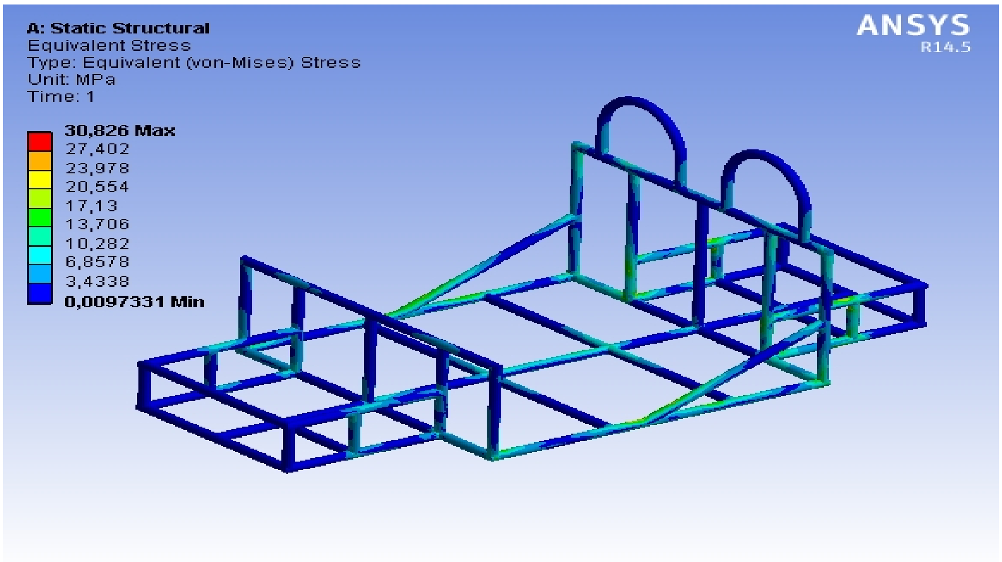

Figure 4.16. Maximum von-Mises stress of the circular tube profiled AISI 4130 steel space frame

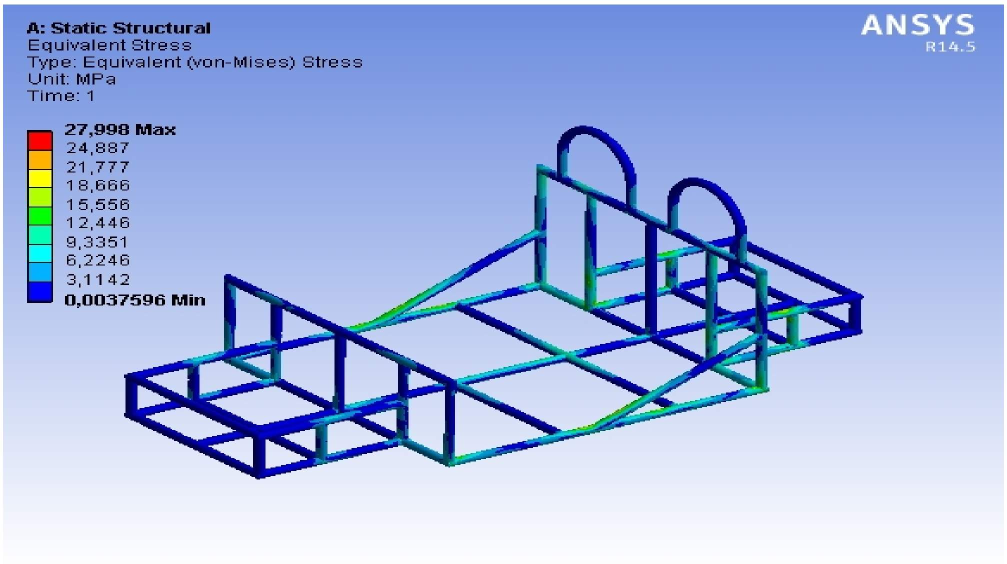

Figure 4.17. Maximum von-Mises stress of the circular tube profiled aluminium 5042-H19 space frame

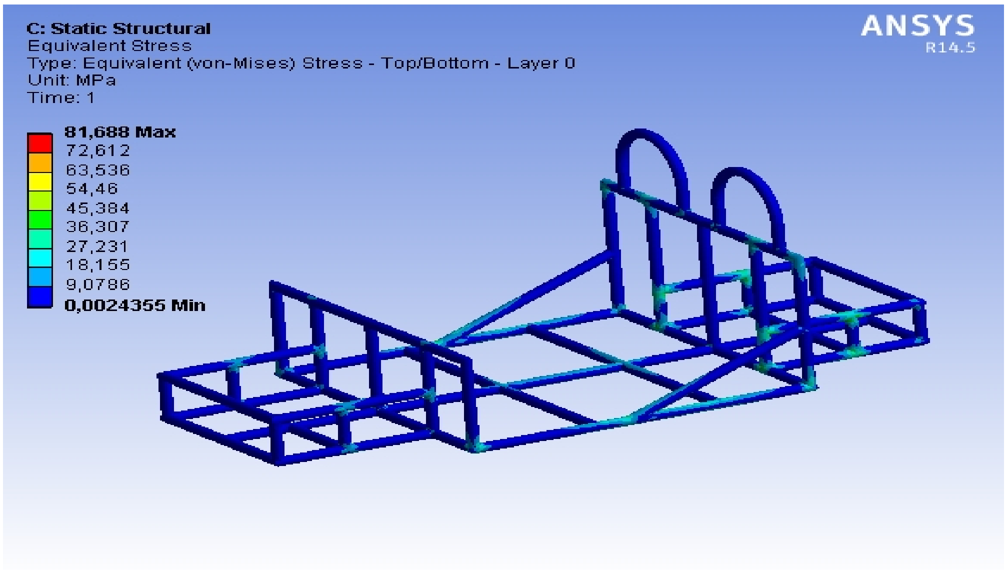

Figure 4.18. Maximum von-Mises stress of the circular tube profiled carbon fiber space frame

Maximum deformation results of the square and circular tube profiled ladder frame chassis with assigned materials of steel, aluminium and composite are shown in Figures 4.19 - 4.24.

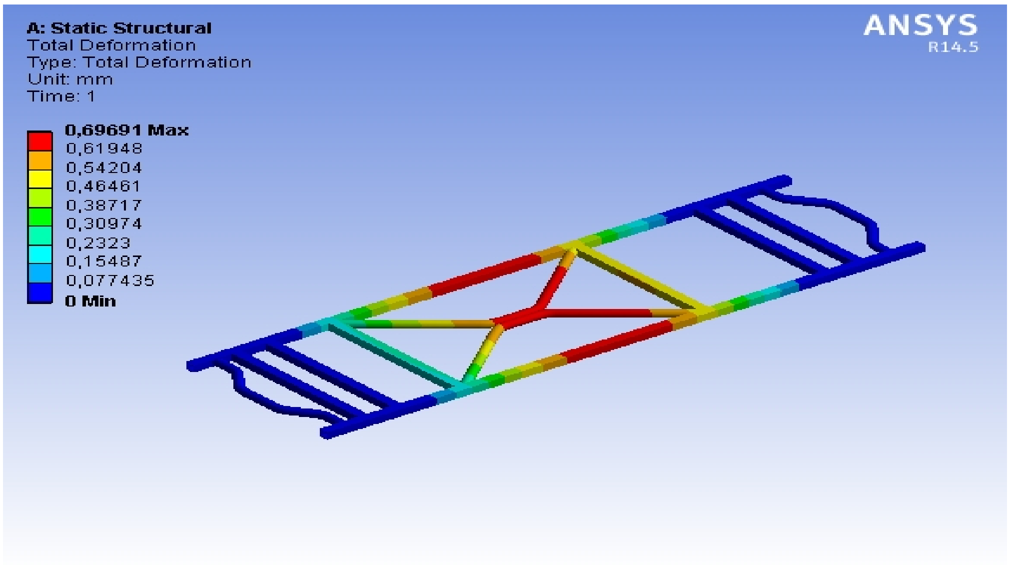

Figure 4.19. Maximum deformation of the square profiled AISI 4130 steel ladder frame

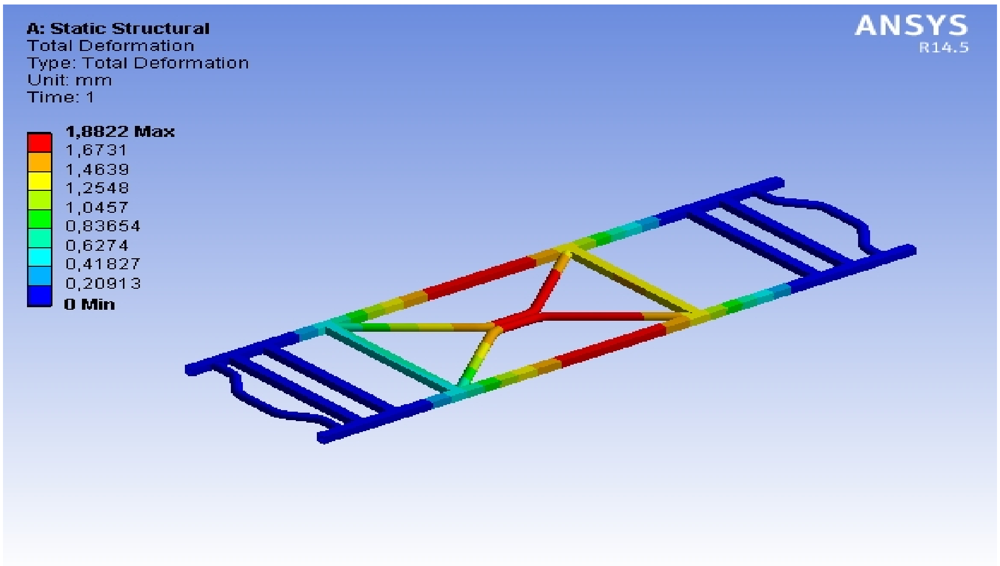

Figure 4.20. Maximum deformation of the square profiled aluminium 5042-H19 ladder frame

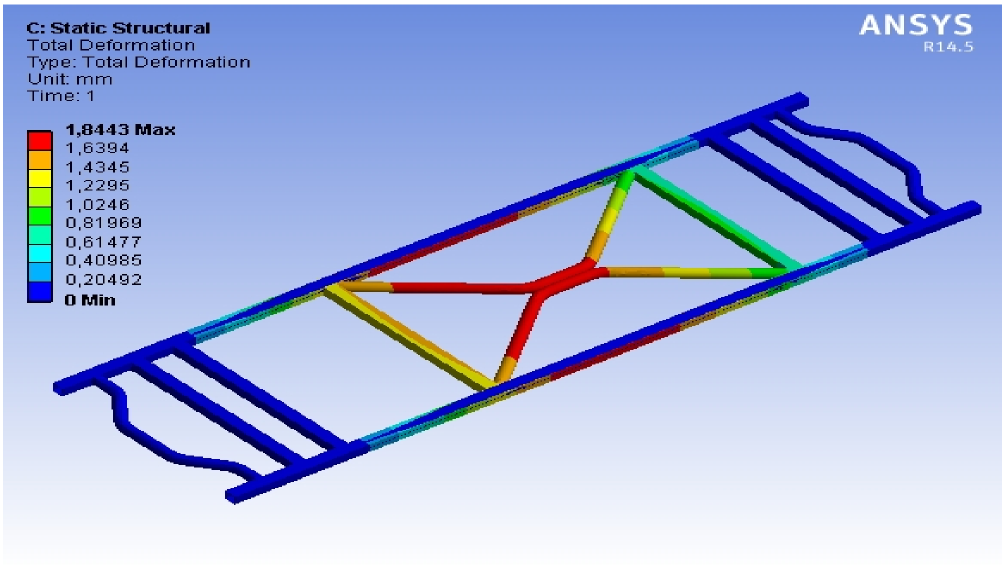

Figure 4.21. Maximum deformation of the square profiled carbon fiber ladder frame

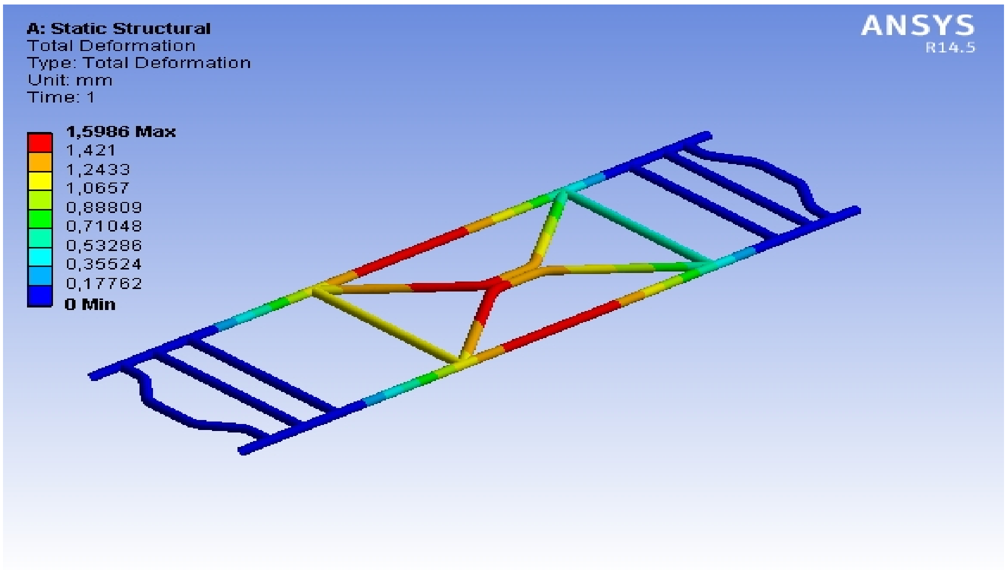

Figure 4.22. Maximum deformation of the circular tube profiled AISI 4130 steel ladder frame

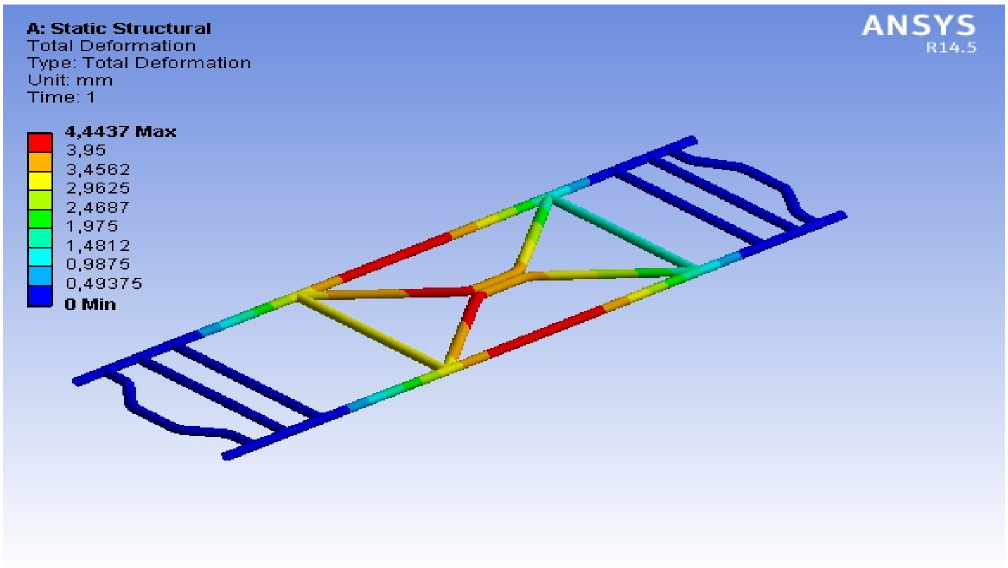

Figure 4.23. Maximum deformation of the circular tube profiled aluminium 5042-H19 ladder frame

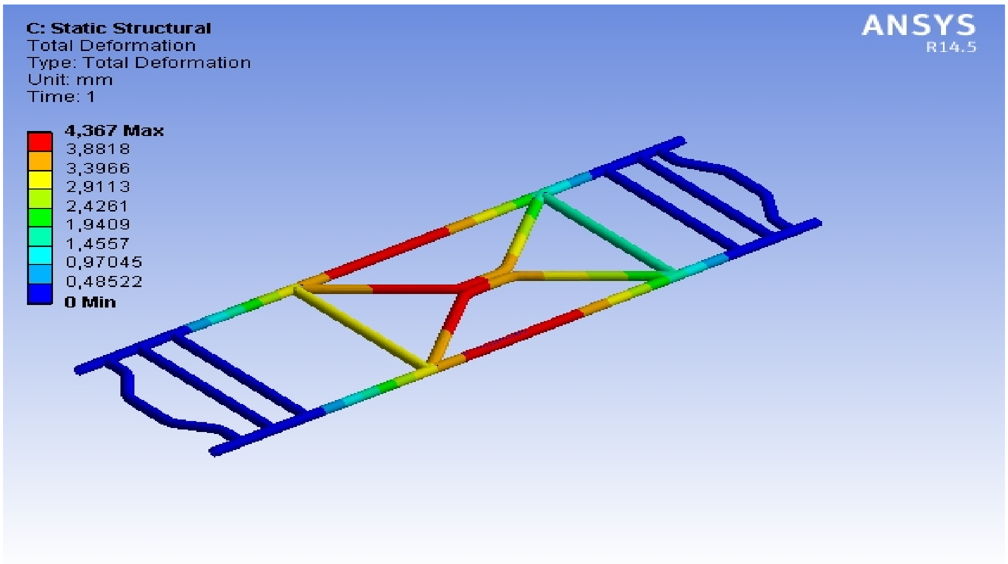

Figure 4.24. Maximum deformation of the circular tube profiled carbon fiber ladder frame

Maximum deformation results of the square and circular tube profiled backbone chassis with assigned materials of steel, aluminium and composite are illustrated in Figures 4.25 - 4.30.

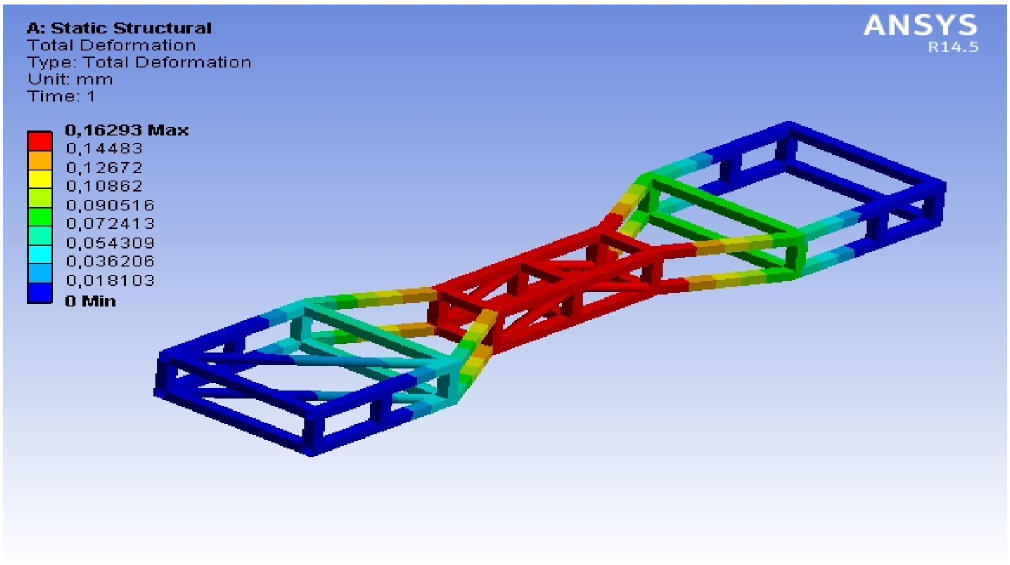

Figure 4.25. Maximum deformation of the square profiled AISI 4130 steel backbone chassis

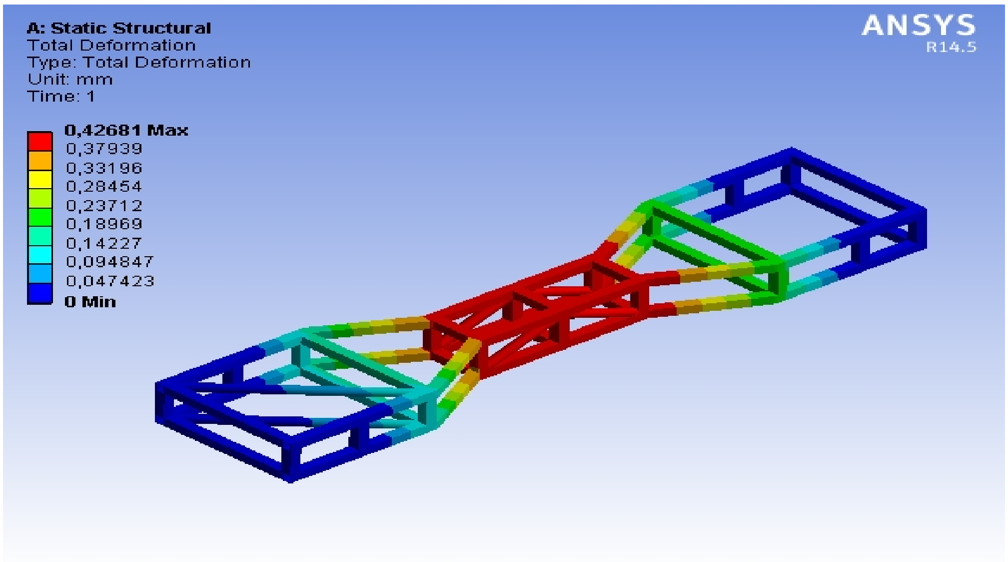

Figure 4.26. Maximum deformation of the square profiled aluminium 5042-H19 backbone chassis

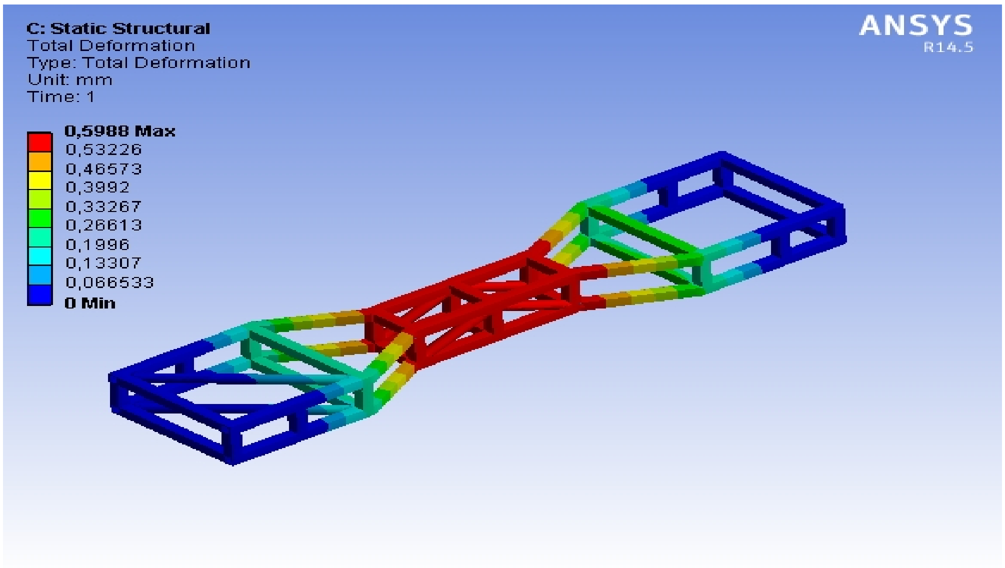

Figure 4.27. Maximum deformation of the square profiled carbon fiber backbone chassis

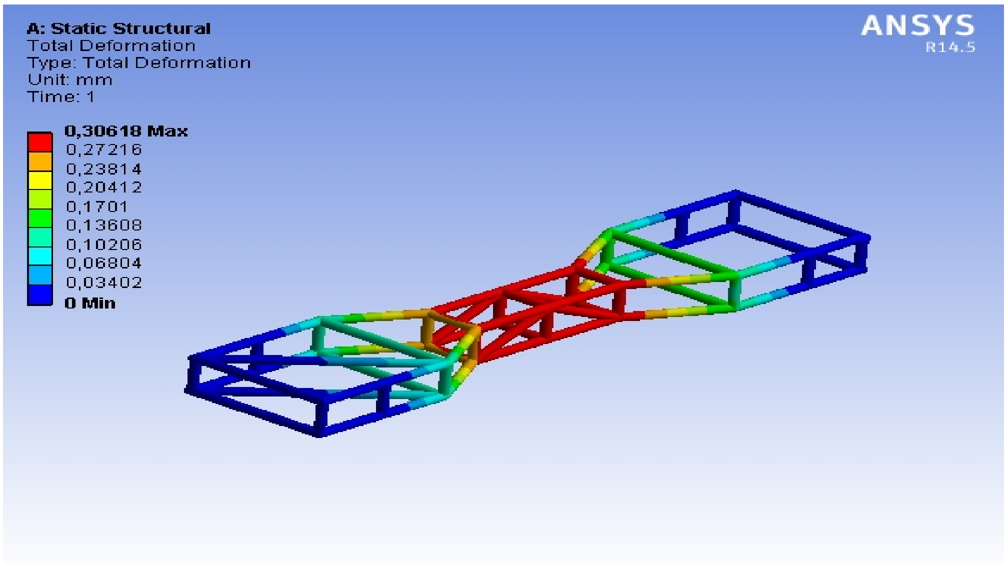

Figure 4.28. Maximum deformation of the circular tube profiled AISI 4130 steel backbone chassis

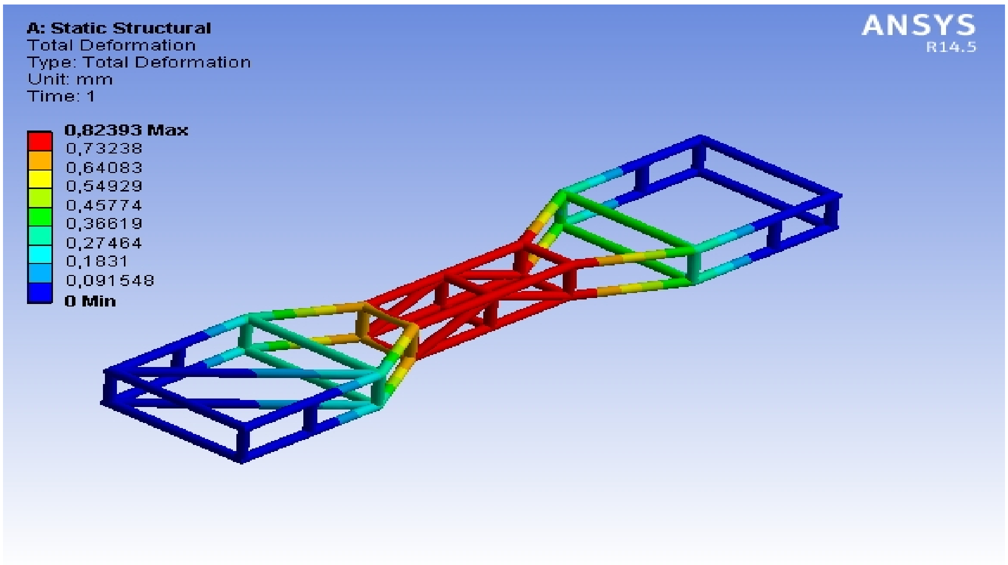

Figure 4.29. Maximum deformation of the circular tube profiled aluminium 5042-H19 backbone chassis

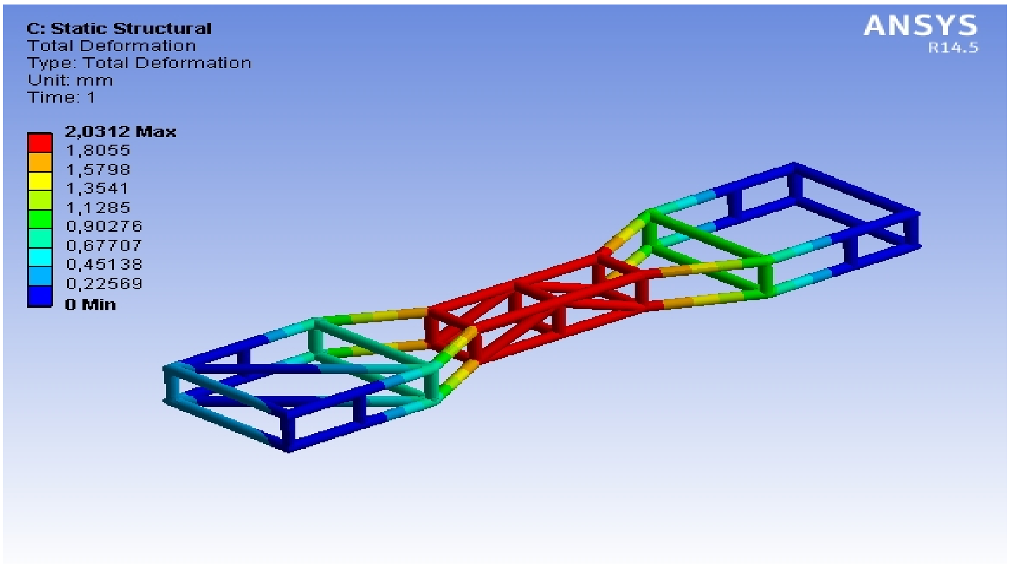

Figure 4.30. Maximum deformation of the circular tube profiled carbon fiber backbone chassis

Maximum deformation results of the square and circular tube profiled space frame chassis with assigned materials of steel, aluminium and composite are given in Figures 4.31 - 4.36.

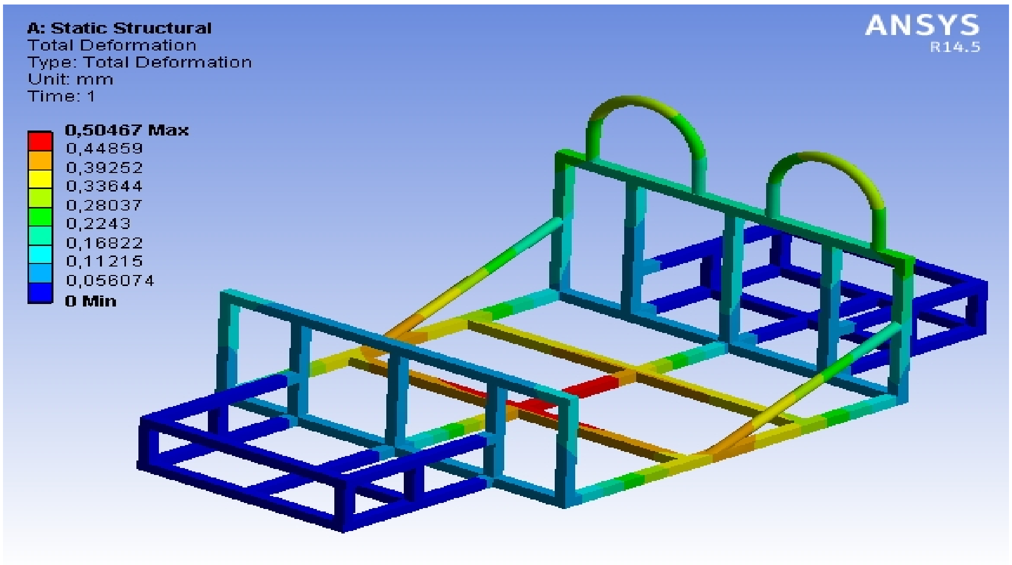

Figure 4.31. Maximum deformation of the square profiled AISI 4130 steel space frame

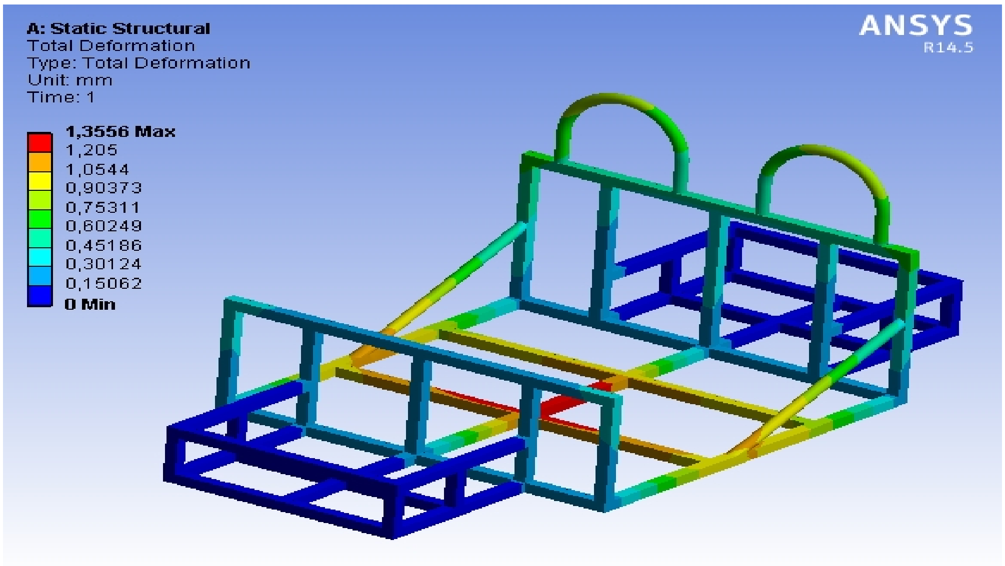

Figure 4.32. Maximum deformation of the square profiled aluminium 5042-H19 space frame

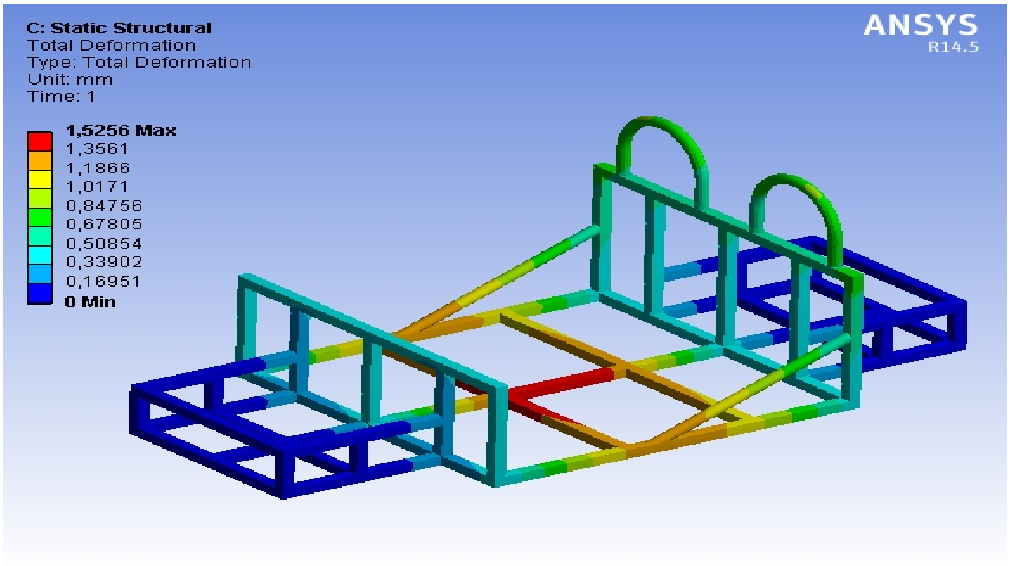

Figure 4.33. Maximum deformation of the square profiled carbon fiber space frame

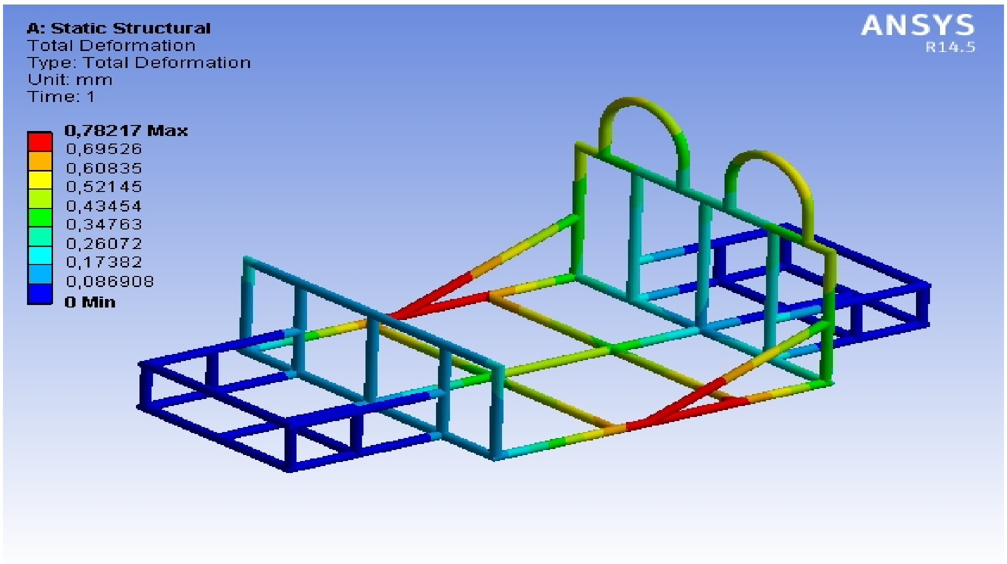

Figure 4.34. Maximum deformation of the circular tube profiled AISI 4130 steel space frame

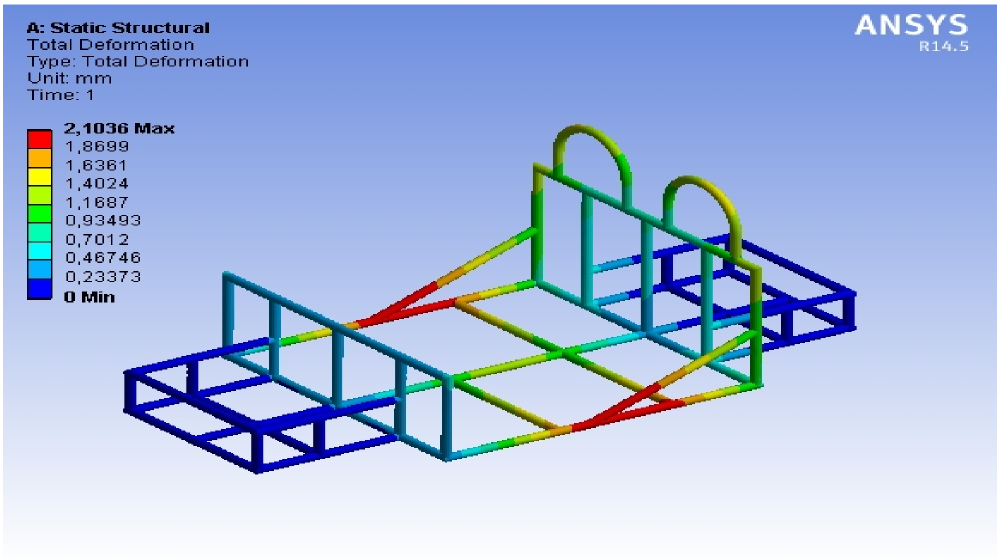

Figure 4.35. Maximum deformation of the circular tube profiled aluminium 5042-H19 space frame

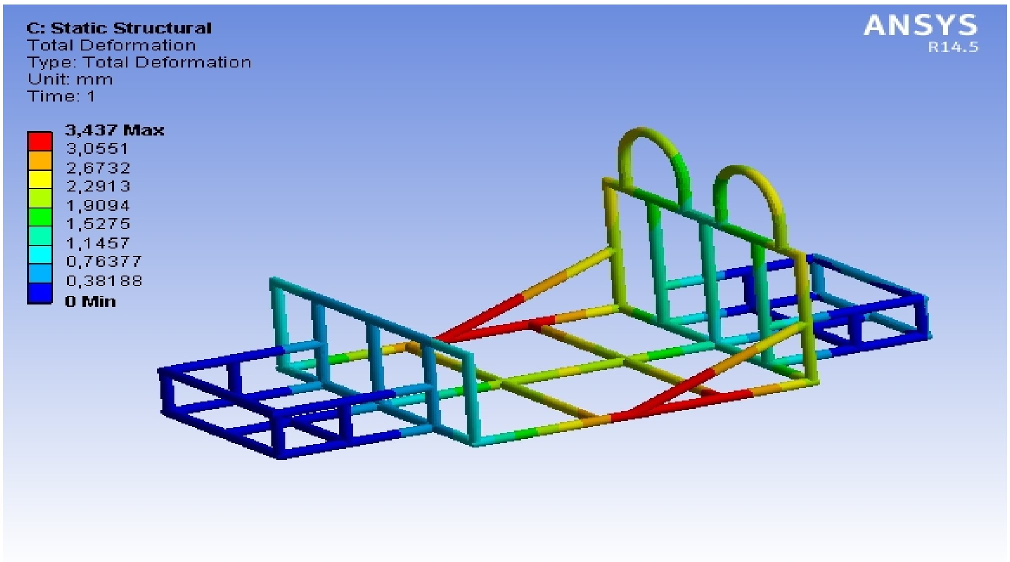

Figure 4.36. Maximum deformation of the circular tube profiled carbon fiber space frame

Comparative chart of the maximum von-Mises stresses for the square and circular hollow sections are illustrated in Figures 4.37 and 4.38

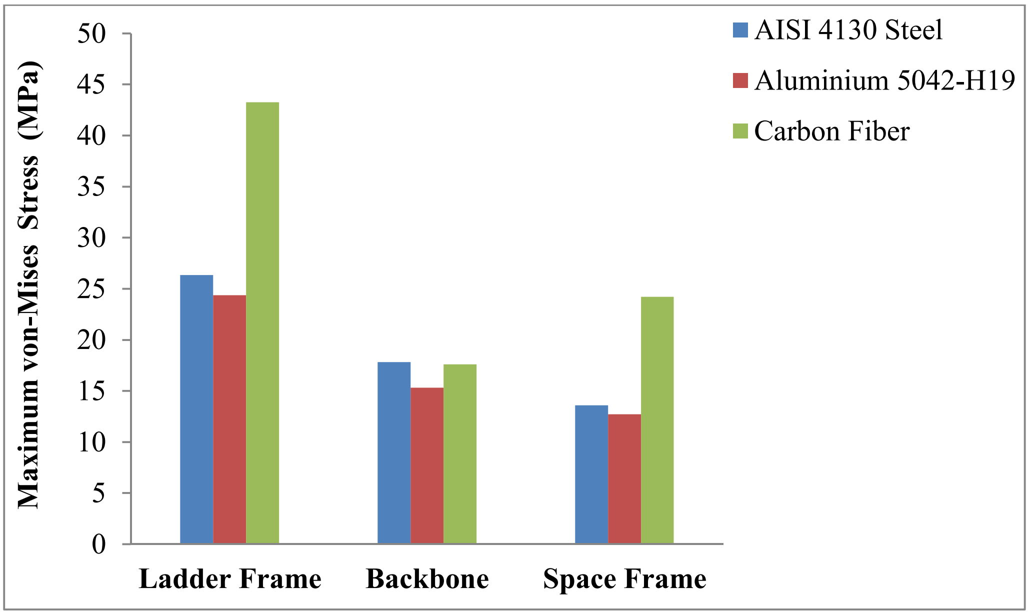

Figure 4.37. Comparative maximum von-Mises stress chart of the square hollow section profiled chassis types with assigned materials

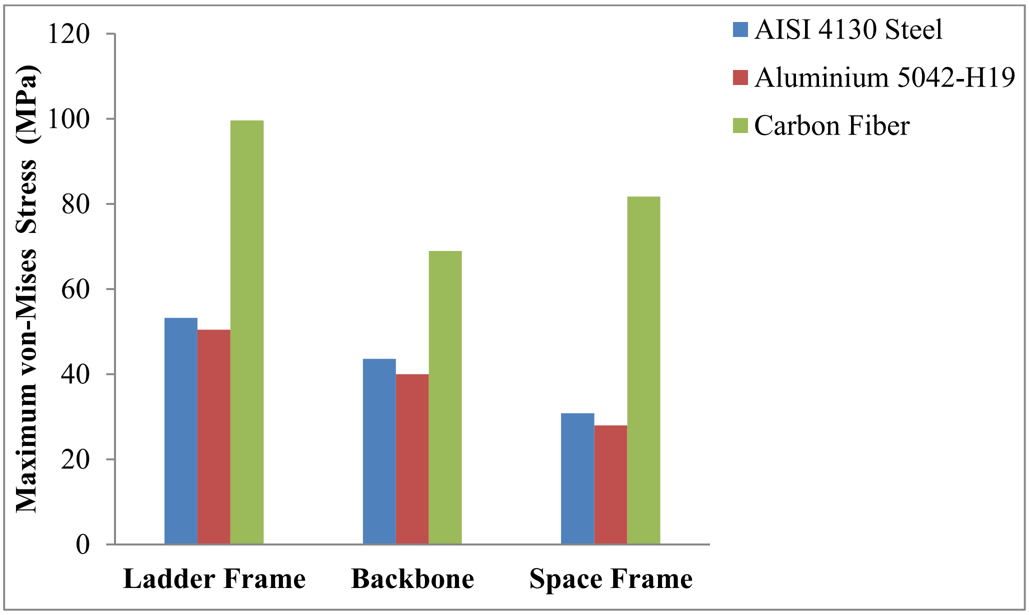

Figure 4.38. Comparative maximum von-Mises stress chart of the circular hollow section profiled chassis types with assigned materials

Comparative chart of the maximum deformation values for the square and circular hollow sections are given in Figures 4.39 and Figure 4.40.

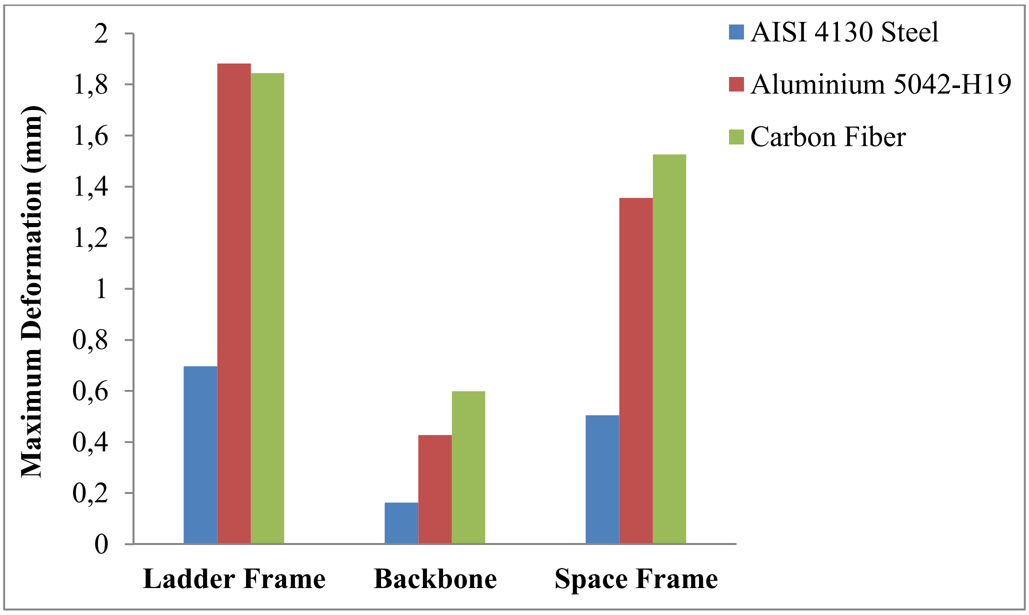

Figure 4.39. Comparative maximum deformation chart of the square hollow section profiled chassis types with assigned materials

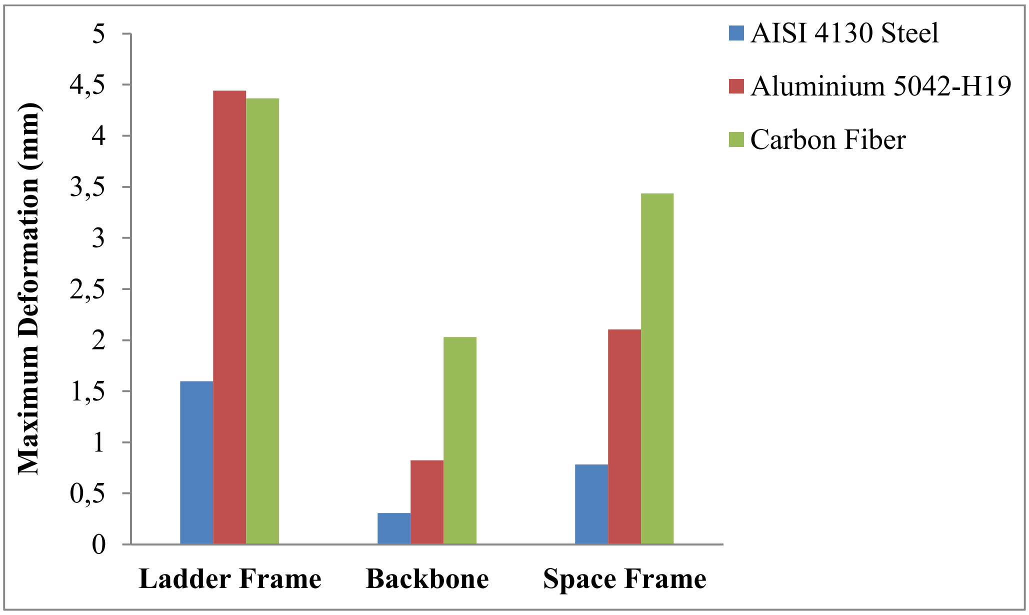

Figure 4.40. Comparative maximum deformation chart of the circular hollow section profiled chassis types with assigned materials

Results indicate that for materials of AISI 4130 steel and aluminium 5052-H19, maximum von-Mises stress values are less than the yield strength of the materials. There is no specific yield strength to discuss of the composite materials and ultimate strength of the carbon fiber is much higher than the AISI 4130 steel and aluminium 5042-H19, so all designs are in the safe region. Results also indicate that square hollow section profiled chassis has lower maximum von-Mises stress when compared to circular hollow profiled section. Chassis types with carbon fiber have the highest stress values except square profiled backbone chassis while aluminium has the lowest. 5042 series aluminium alloys are used for the series production in chassis applications for their high strength (Hirsch, 2011) and all chassis designs of assigned material of aluminium 5042-H19 have the lowest stress values.

Safest chassis material is the steel when considering the maximum deformation of the chassis. Carbon fiber chassis has the higher maximum deformation values than the aluminium 5042-H19 chassis except ladder frame chassis, both square and circular section profiled carbon fiber ladder frame chassis has smaller maximum deformation values than the aluminium 5042-H19 ones.

4.1.3. Analysis Results of the Torsional Loading

Torsional loading results include maximum torsional deformation results of the chassis. Total deformation values are obtained from the torsional loading of the chassis and gathered as maximum torsional deformation data and used in the calculation of the torsional stiffness of the chassis. Maximum torsional deformation results of the square and circular tube profiled ladder frame chassis with assigned materials of AISI 4130 steel, aluminium 5042-H19 and carbon fiber are illustrated in Figures 4.41 – 4.46.

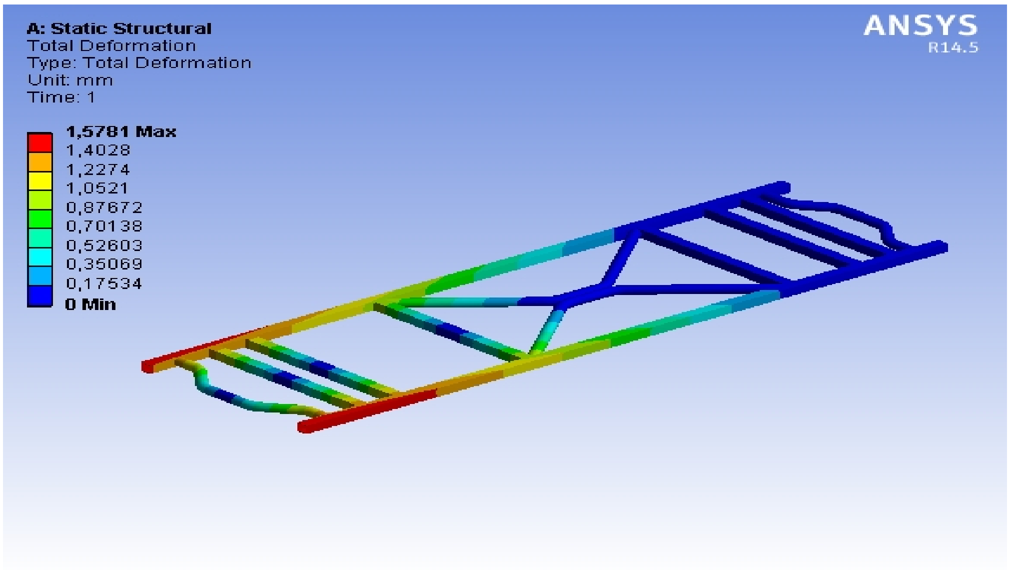

Figure 4.41. Maximum torsional deformation of the square profiled AISI 4130 steel ladder frame

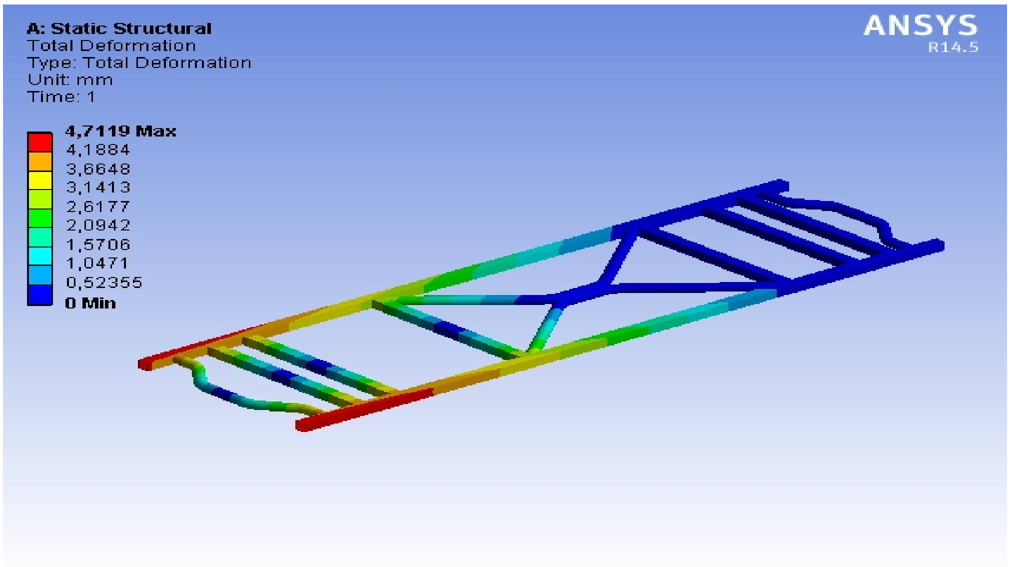

Figure 4.42. Maximum torsional deformation of the square profiled aluminium 5042-H19 ladder frame

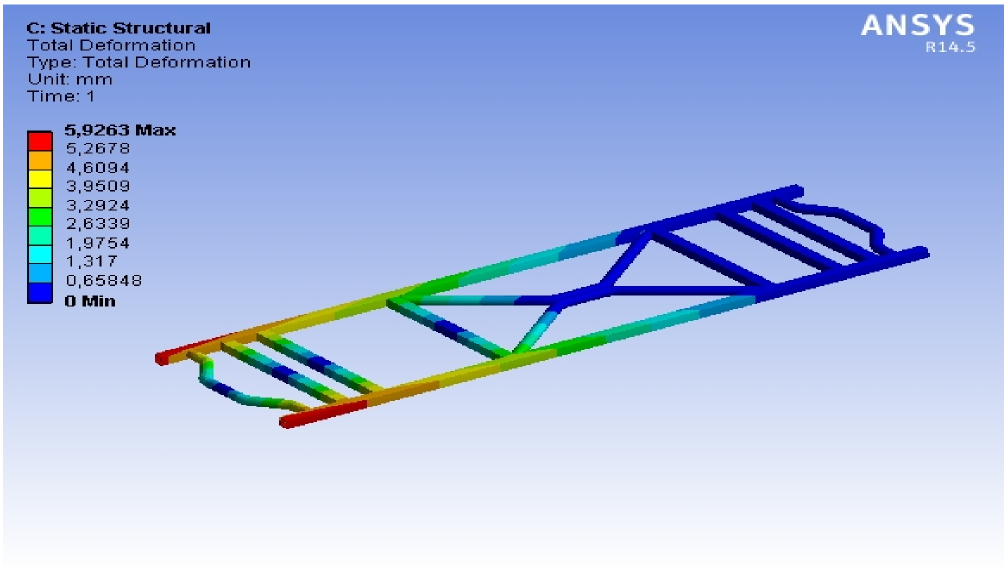

Figure 4.43. Maximum torsional deformation of the square profiled carbon fiber ladder frame

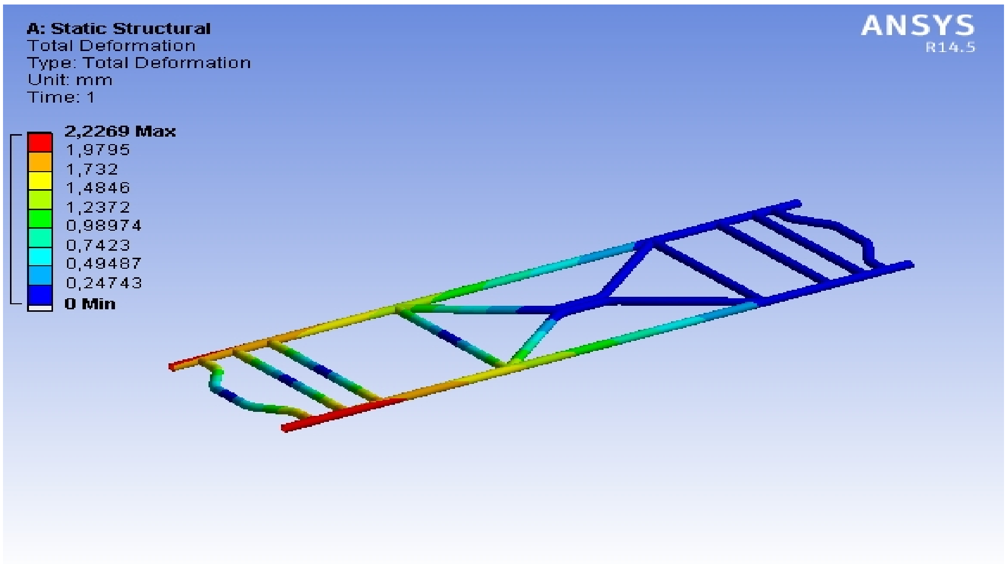

Figure 4.44. Maximum torsional deformation of the circular tube profiled AISI 4130 steel ladder frame

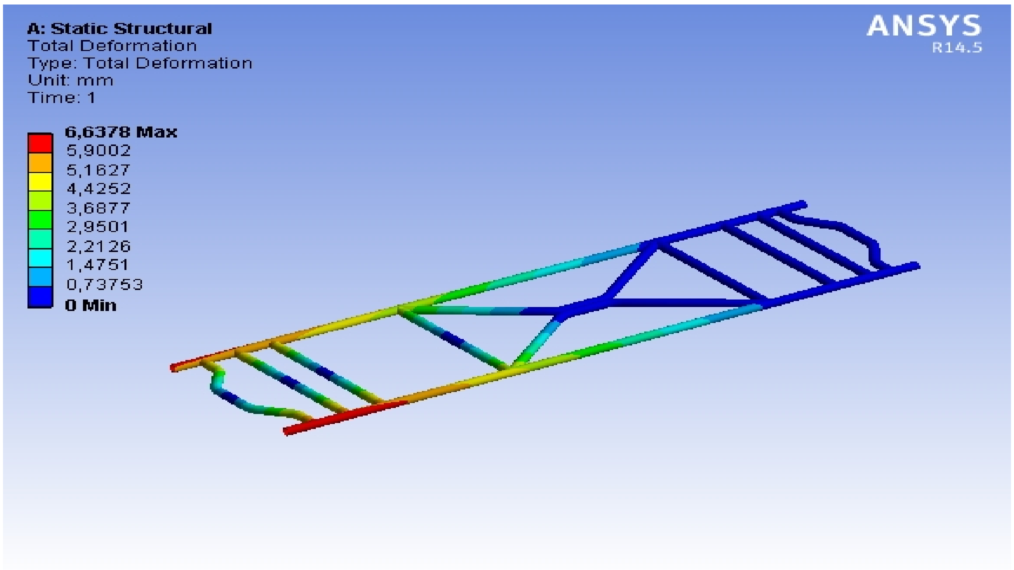

Figure 4.45. Maximum torsional deformation of the circular tube profiled aluminium 5042-H19 ladder frame

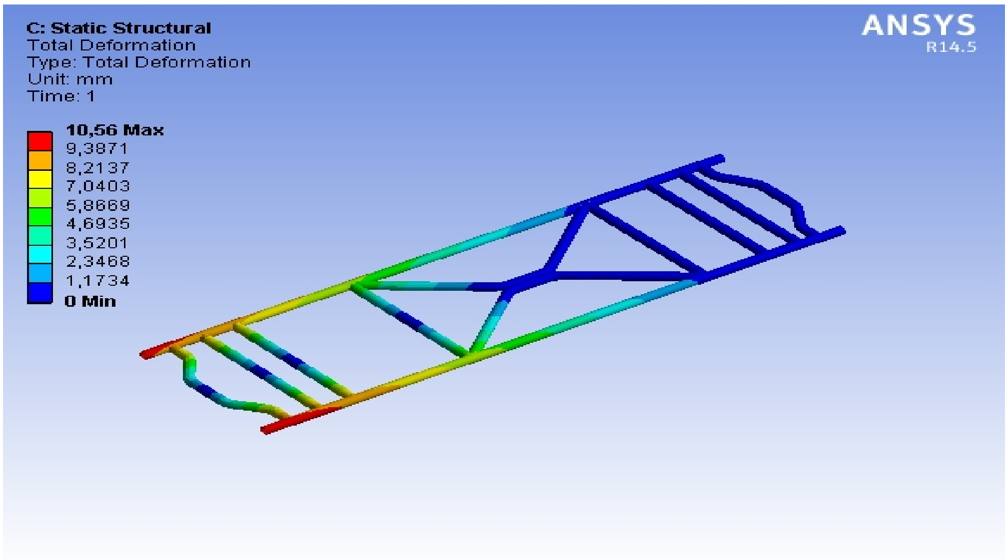

Figure 4.46. Maximum torsional deformation of the circular tube profiled carbon fiber ladder frame

Maximum torsional deformation values of the square and circular tube profiled backbone chassis with assigned materials of steel, aluminium and composite are shown in Figures 4.47- 4.52.

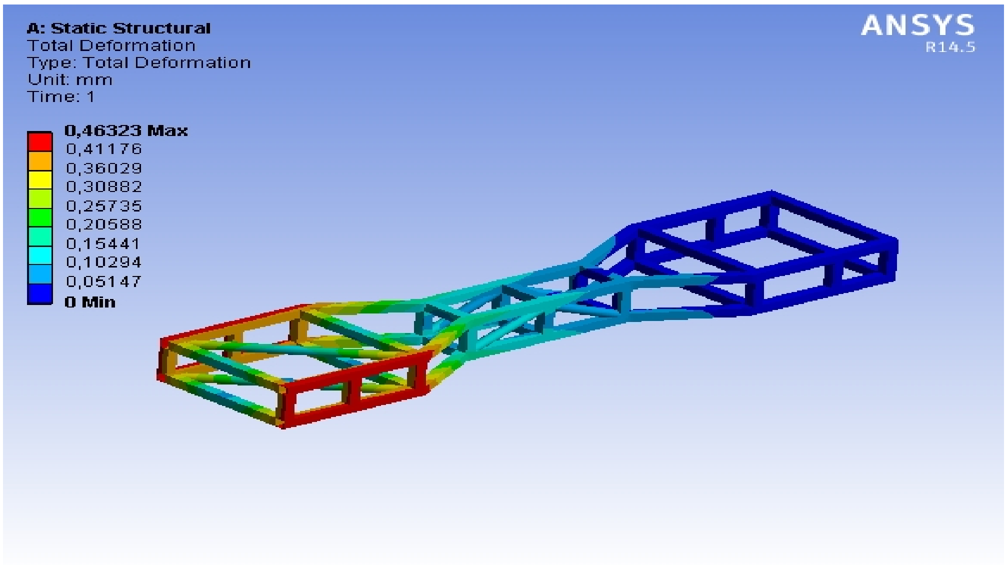

Figure 4.47. Maximum torsional deformation of the square profiled AISI 4130 steel backbone chassis

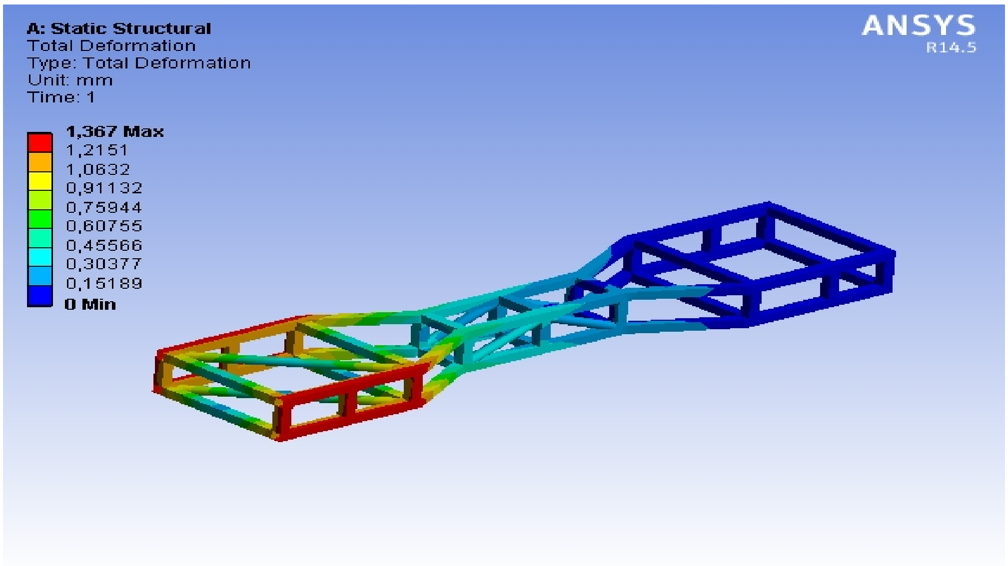

Figure 4.48. Maximum torsional deformation of the square profiled aluminium 5052-H19 backbone chassis

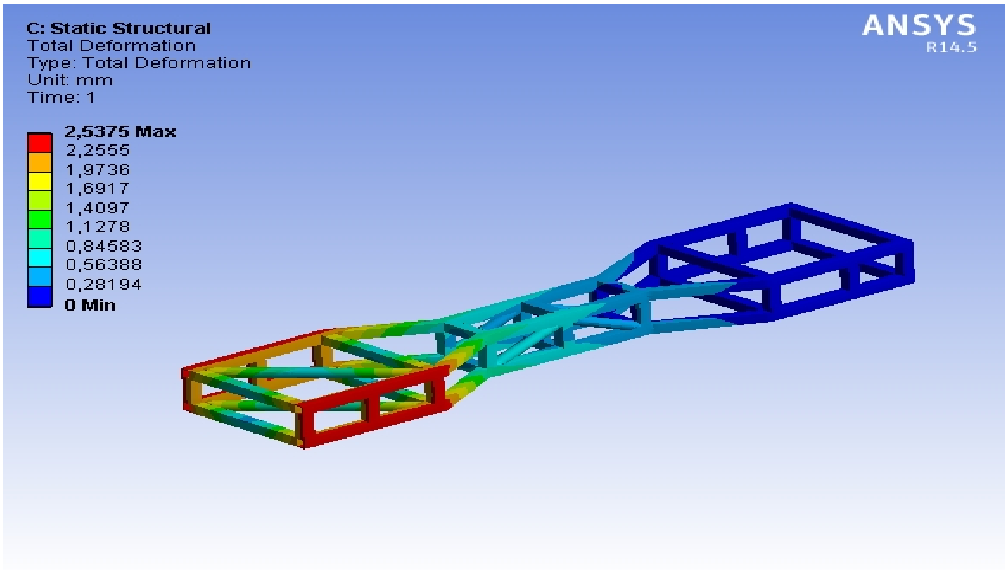

Figure 4.49. Maximum torsional deformation of the square profiled carbon fiber backbone chassis

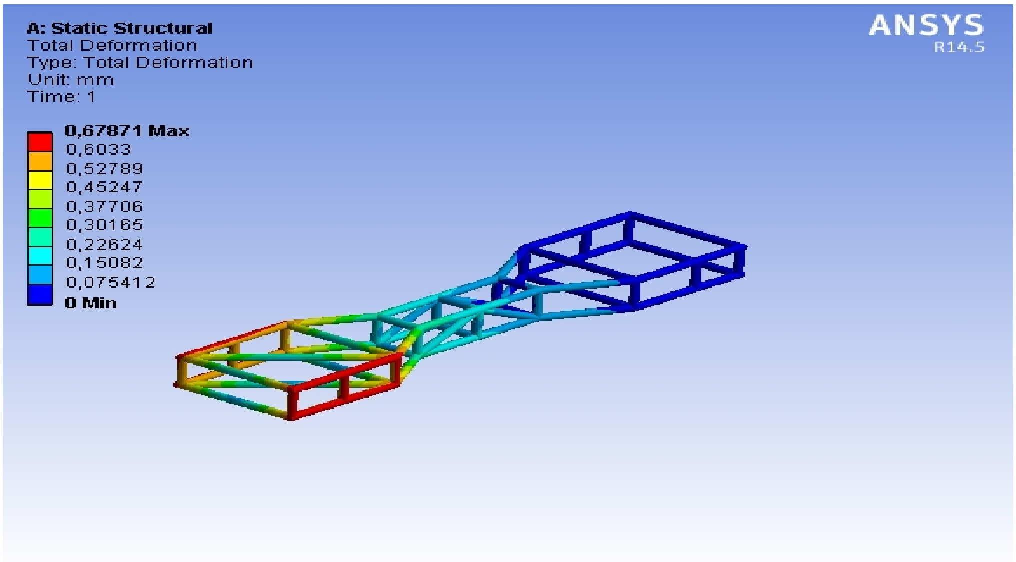

Figure 4.50. Maximum torsional deformation of the circular tube profiled AISI 4130 steel backbone chassis

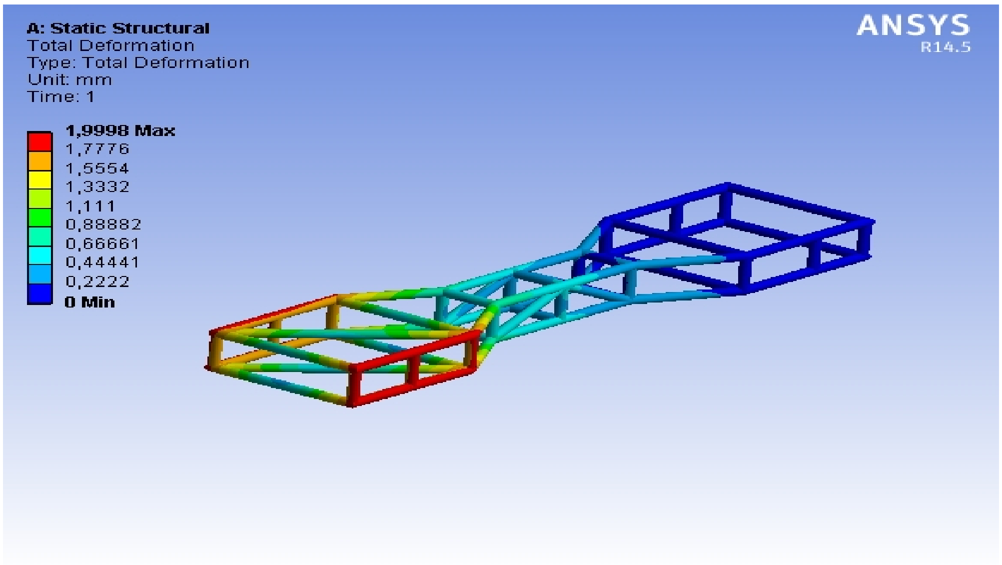

Figure 4.51. Maximum torsional deformation of the circular tube profiled aluminium 5042-H19 backbone chassis

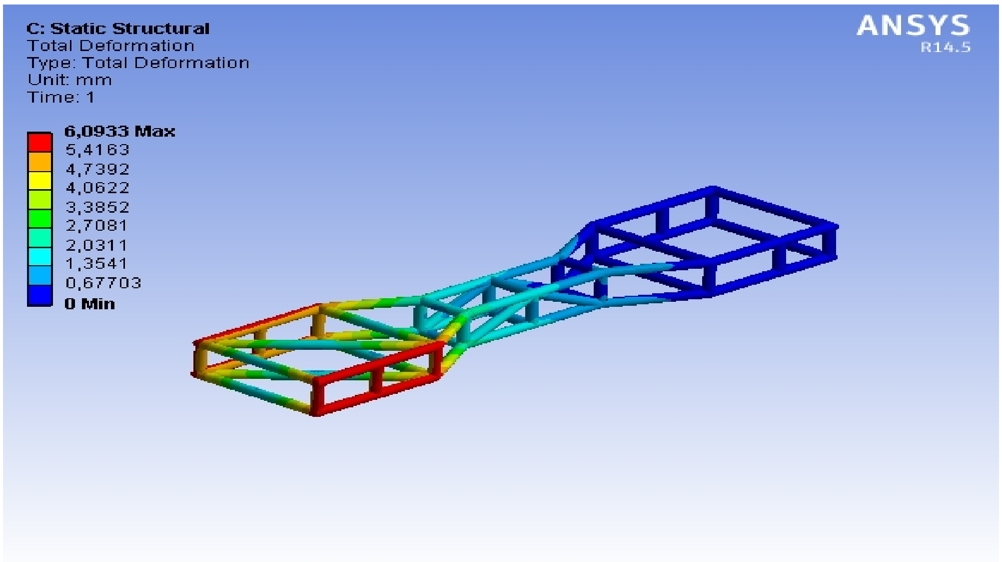

Figure 4.52. Maximum torsional deformation of the circular profiled carbon fiber backbone chassis

Maximum torsional deformation results of the square and circular tube profiled space frame chassis with assigned materials of AISI 4130 steel, aluminium 5042-H19 and carbon fiber are illustrated in Figures 4.53 - 4.58.

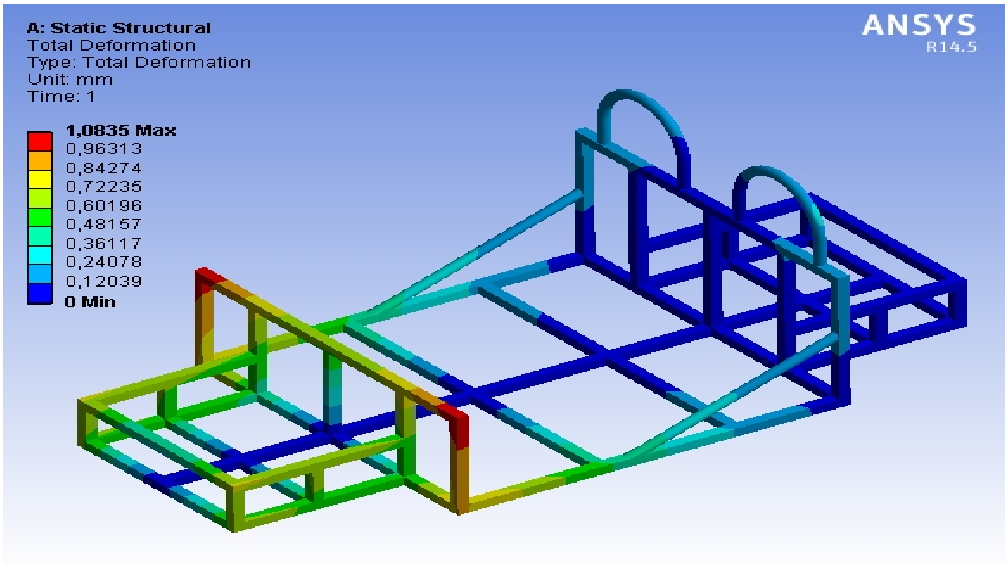

Figure 4.53. Maximum torsional deformation of the square profiled AISI 4130 steel space frame

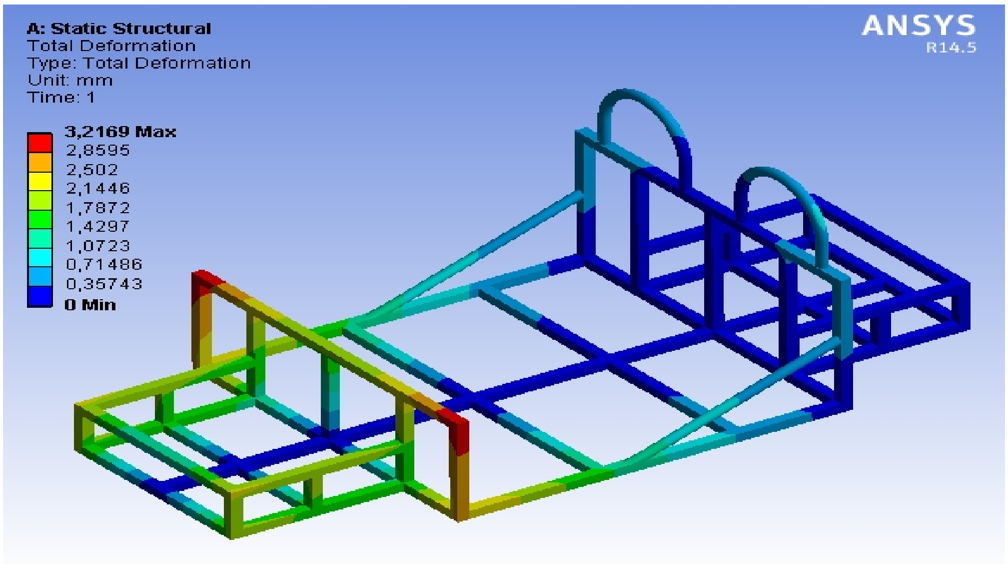

Figure 4.54. Maximum torsional deformation of the square profiled aluminium 5042-H19 space frame

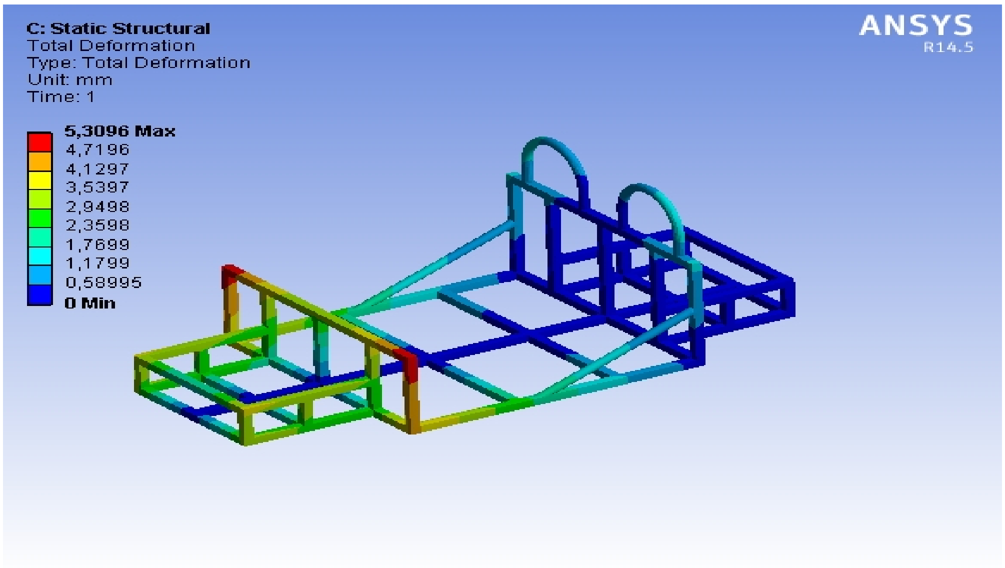

Figure 4.55. Maximum torsional deformation of the square profiled carbon fiber space frame

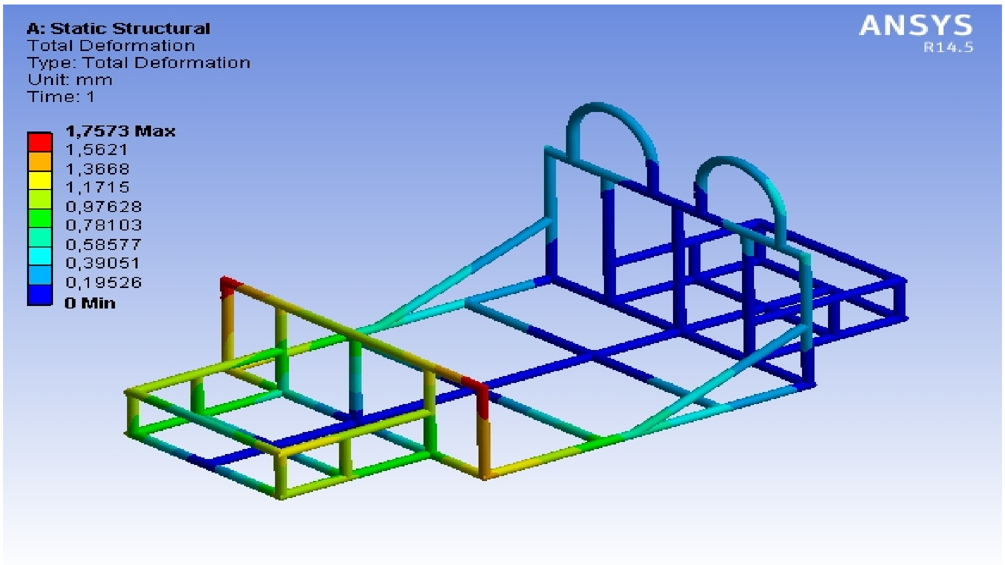

Figure 4.56. Maximum torsional deformation of the circular tube profiled AISI 4130 steel space frame

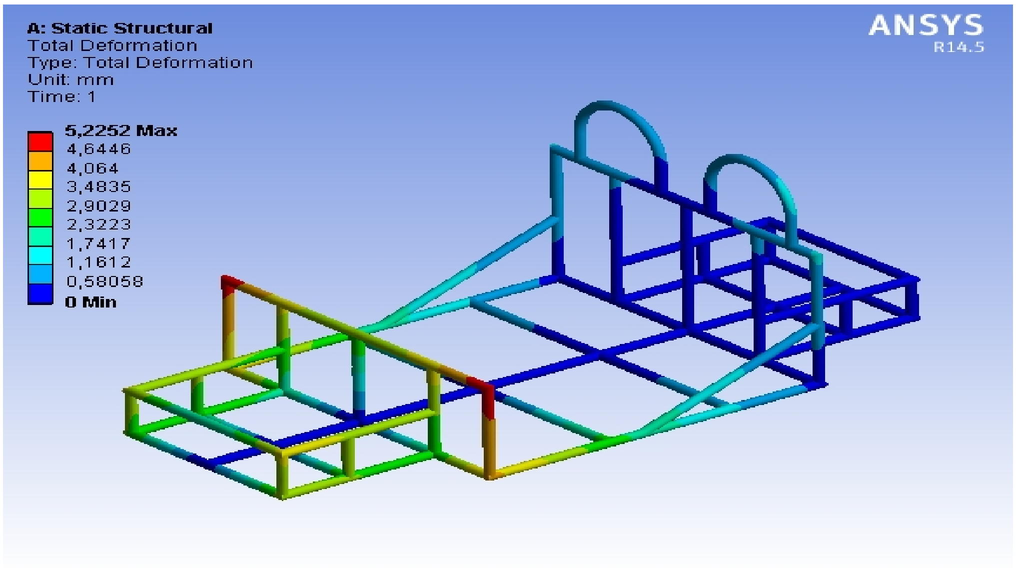

Figure 4.57. Maximum torsional deformation of the circular profiled aluminium 5042-H19 space frame

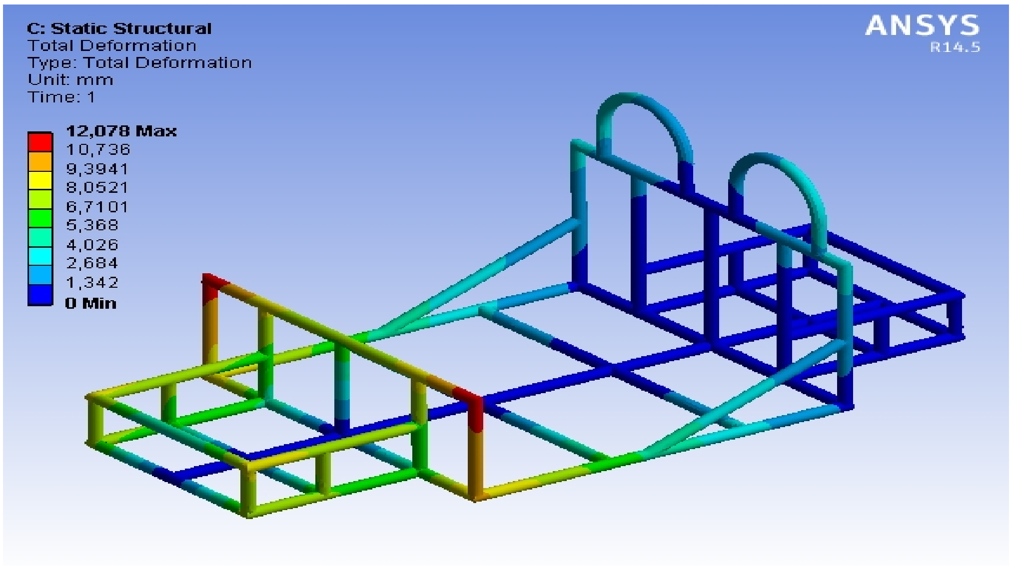

Figure 4.58. Maximum torsional deformation of the circular tube profiled carbon fiber space frame

Comparative chart of the maximum torsional deformation values for the square and circular hollow sections are given in Figures 4.59 and Figure 4.60.

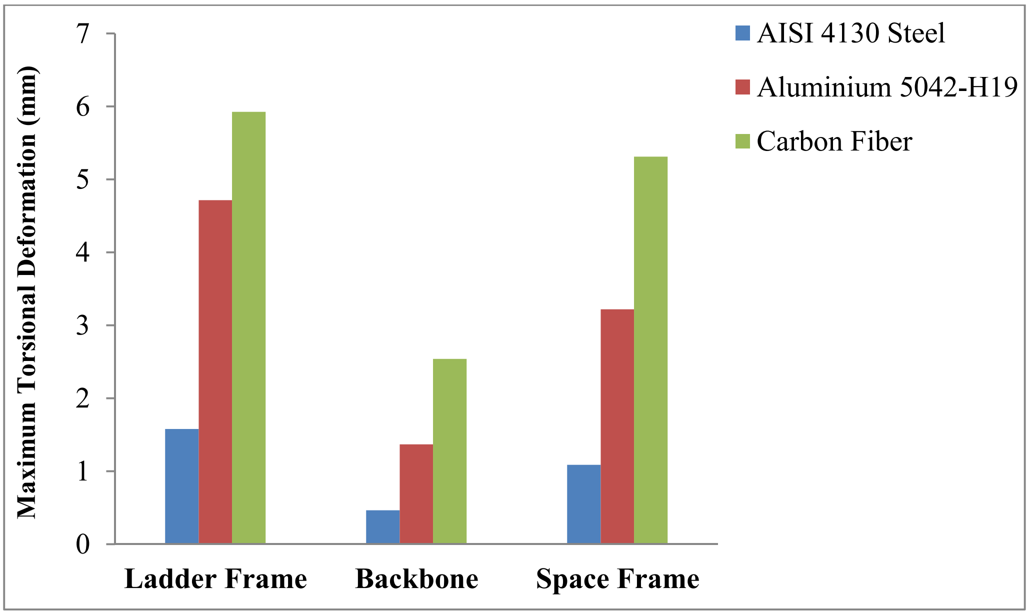

Figure 4.59. Comparative maximum torsional deformation chart of the square hollow section profiled chassis types with assigned materials

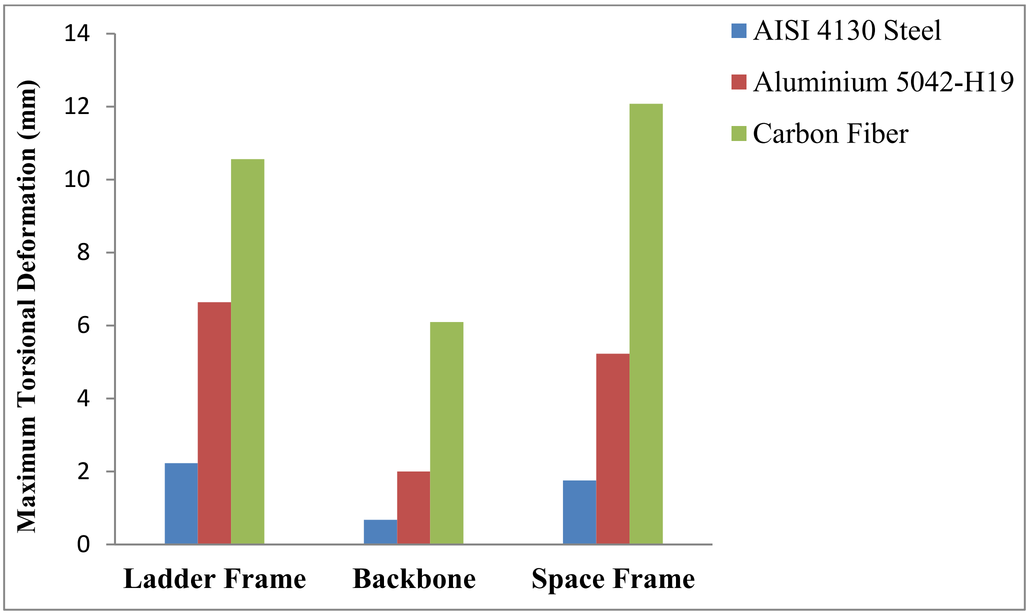

Figure 4.60. Comparative maximum torsional deformation chart of the circular hollow section profiled chassis types with assigned materials

Torsional deformation results indicate that AISI 4130 steel chassis has the lowest maximum torsional deformation value while composite chassis has the highest. Square section profiled chassis has lower maximum torsional deformation value than the circular section profiled chassis in terms of both chassis types and materials. Ladder frame chassis has the highest maximum torsional deformation values while backbone chassis has the lowest except circular tube profiled carbon fiber chassis. Circular tube profiled ladder frame is deformed less than the circular tube profiled carbon fiber chassis.

Torsional stiffness value of the chassis is calculated using the maximum torsional deformation values which is obtained from the structural analysis. Equations 3.1 and 3.2 are used for the calculation. Calculated torsional stiffness values for different chassis types are given in Tables 4.2, 4.3 and 4.4.

Table 4.2. Torsional stiffness values of the ladder frame chassis

Chassis Type	**Material**	**Section Geometry**	**Torsional Stiffness (Nm/deg)**
Ladder Frame	AISI 4130 Steel	Square	**2890.733**
Ladder Frame	Aluminium 5042-H19	Square	**968.080**
Ladder Frame	Carbon Fiber	Square	**769.761**
Ladder Frame	AISI 4130 Steel	Circular	**2048.307**
Ladder Frame	Aluminium 5042-H19	Circular	**687.197**
Ladder Frame	Carbon Fiber	Circular	**431.977**

Table 4.3. Torsional stiffness values of the backbone chassis

Chassis Type	**Material**	**Section Geometry**	**Torsional Stiffness (Nm/deg)**
Backbone	AISI 4130 Steel	Square	**9852.214**
Backbone	Aluminium 5042-H19	Square	**3336.925**
Backbone	Carbon Fiber	Square	**1797.313**
Backbone	AISI 4130 Steel	Circular	**6718.079**
Backbone	Aluminium 5042-H19	Circular	**2281.930**
Backbone	Carbon Fiber	Circular	**748.664**

Table 4.4. Torsional stiffness values of the space frame chassis

Chassis Type	Material	Section Geometry	Torsional Stiffness (Nm/deg)
Space Frame	AISI 4130 Steel	Square	**4200.346**
Space Frame	Aluminium 5042-H19	Square	**1417.962**
Space Frame	Carbon Fiber	Square	**859.058**
Space Frame	AISI 4130 Steel	Circular	**2596.231**
Space Frame	Aluminium 5042-H19	Circular	**873.033**
Space Frame	Carbon Fiber	Circular	**377.687**

Torsional stiffness value of the chassis is derived from the torsional deformation values of the chassis so comparison results of the torsional deformation values are also valid for the torsional stiffness values. Low torsional deformation value results in the high torsional stiffness value.

Torsional stiffness is the comfort characteristic of a vehicle and directly related with the chassis design and material. As a result of the equation 3.1 and 3.2, applied torque is used for the calculation and the torsional stiffness of a vehicle is not change with the variable torque magnitudes because a change in the torque will result in a change of force applied to the front wheel mountings and torsional deformation values are generated using these two forces. Torsional deformation values are generated using 198 Nm torque and dividing this torque by the 1320 mm track width of the vehicle, 150 N force is generated and used for the analysis. According to the torsional stiffness calculation, an increase in torque will not change the torsional stiffness of the chassis and in order to validate this phenomena 297 Nm and 396 Nm torque is selected and as a result of these torque magnitudes, 225 N and 300 N of forces are applied to the chassis. Square profiled aluminium space frame chassis is selected for the validation and structural analysis of the chassis is performed.

Torsional deformation values of the 150 N, 225 N and 300 N forces are obtained from the analysis results. Maximum numbers of 8 digits are used in the software to observe the variation accurately and torsional stiffness values are calculated. Detailed results are listed in Table 4.5.

Table 4.5. Torsional stiffness values of the variable forces

Force (N)	Angular Deformation (deg)	Torsional Deformation (mm)	Torsional Stiffness (Nm/deg)
150	0,1396322	3,2168879	**1418,011492**
225	0,2094477	4,8253316	**1418,015074**
300	0,2792627	6,4337758	**1418,019913**

As can be seen from the Table 4.5, torsional deformation values are increasing with the increasing number of forces while torsional stiffness values remains nearly the same. Results show that torsional stiffness value of a vehicle is directly dependent to its design and material.

4.1.4. Results of the Design Optimization

4.1.4.1. Results of the Parametric Optimization

Parametric optimization results include the signal to noise ratios of the analysis of the Taguchi design in Minitab software. Signal to noise ratios are generated using smaller is the best quality characteristics, so designs which have the smaller values of stress, deformation and weight with less variation, have the larger signal to noise ratios. Signal to noise ratios are illustrated in Figure 4.61.

↓	C1-T	C2-T	C3-T	C4	C5	C6	C7	C8	C9
	Section Geometry	Material	Chassis Type	von-Mises Stress (MPa)	Maximum Deformation (mm)	Max Torsional Deformation (mm)	Weight (kg)	SNRA1	S/N Ratio Ranking
1	Square	Steel	LadderFrame	26,344	0,697	1,578	34,810	-26,7868	8
2	Square	Steel	Backbone	17,834	0,163	0,463	56,961	-29,4974	11
3	Square	Steel	SpaceFrame	13,587	0,505	1,086	88,842	-33,0529	17
4	Square	Aluminium	LadderFrame	24,379	1,882	4,712	11,840	-22,7891	3
5	Square	Aluminium	Backbone	15,319	0,427	1,367	19,374	-21,8474	2
6	Square	Aluminium	SpaceFrame	12,706	1,356	3,217	30,218	-24,3407	5
7	Square	Composite	LadderFrame	43,251	1,844	5,926	9,467	-26,9871	9
8	Square	Composite	Backbone	17,607	0,599	2,538	14,861	-21,2844	1
9	Square	Composite	SpaceFrame	24,222	1,526	5,310	17,447	-23,6250	4
10	Circular	Steel	LadderFrame	53,220	1,599	2,227	29,406	-29,6668	12
11	Circular	Steel	Backbone	43,591	0,306	0,679	47,175	-30,1349	13
12	Circular	Steel	SpaceFrame	30,826	0,782	1,757	71,898	-31,8492	15
13	Circular	Aluminium	LadderFrame	50,408	4,443	6,638	10,002	-28,3008	10
14	Circular	Aluminium	Backbone	40,018	0,824	1,999	16,046	-26,6829	7
15	Circular	Aluminium	SpaceFrame	27,998	2,104	5,225	24,455	-25,4829	6
16	Circular	Composite	LadderFrame	99,614	4,367	10,560	7,834	-34,0290	18
17	Circular	Composite	Backbone	68,968	2,031	6,093	9,312	-30,8676	14
18	Circular	Composite	SpaceFrame	81,688	3,437	12,078	14,115	-32,4489	16

Figure 4.61. Signal to noise ratios and ranking from the largest to the smallest

Main effects plot of signal to noise ratios are illustrated in Figure 4.62.

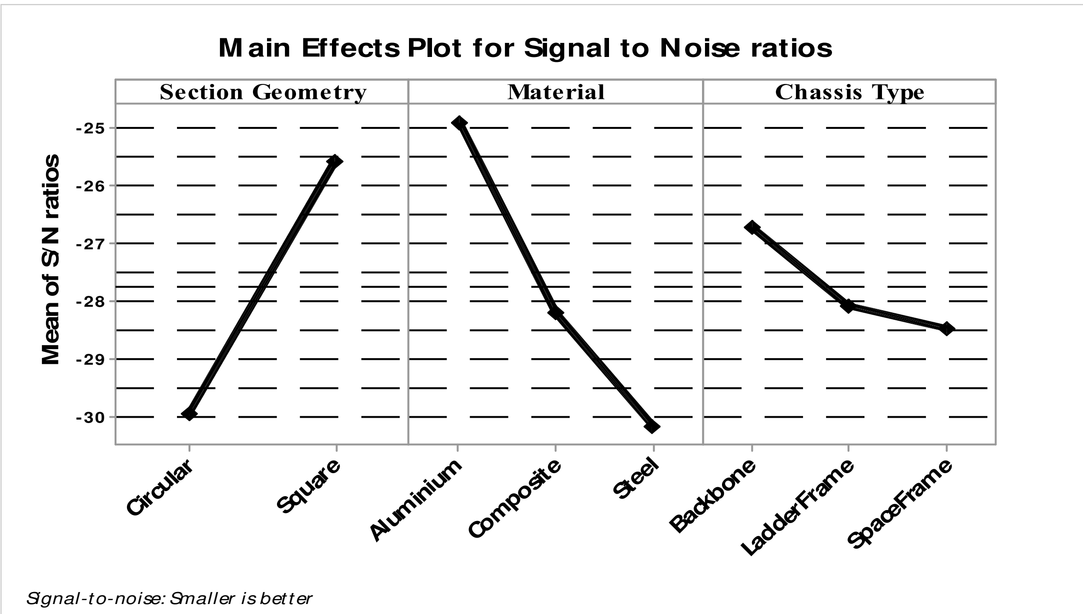

Figure 4.62. Main effects plot for signal to noise ratios

As can be seen from the Figure 4.62, effect of the material is the largest while effect of the chassis type is the smallest for the signal to noise ratios of the analysis results. Signal to ratios are negative and it means noise of the system is greater than the generated signals. In negative signal to noise ratios, the ratio that closest to zero is the largest ratio which produces the largest signal. Figure 4.61. illustrates that signal to noise ratios are ranked from the largest to smallest. Top five designs are selected and compared. The fifth design, square profiled aluminium space frame chassis is selected as the most feasible one and further optimization is applied.

4.1.4.2. Results of the Structural Optimization

Square profiled aluminium 5042-H19 space frame chassis is structurally optimized and analysed. Maximum von-Mises stress and maximum deformation values of the distributed loading are shown in Figures 4.63 and 4.64.

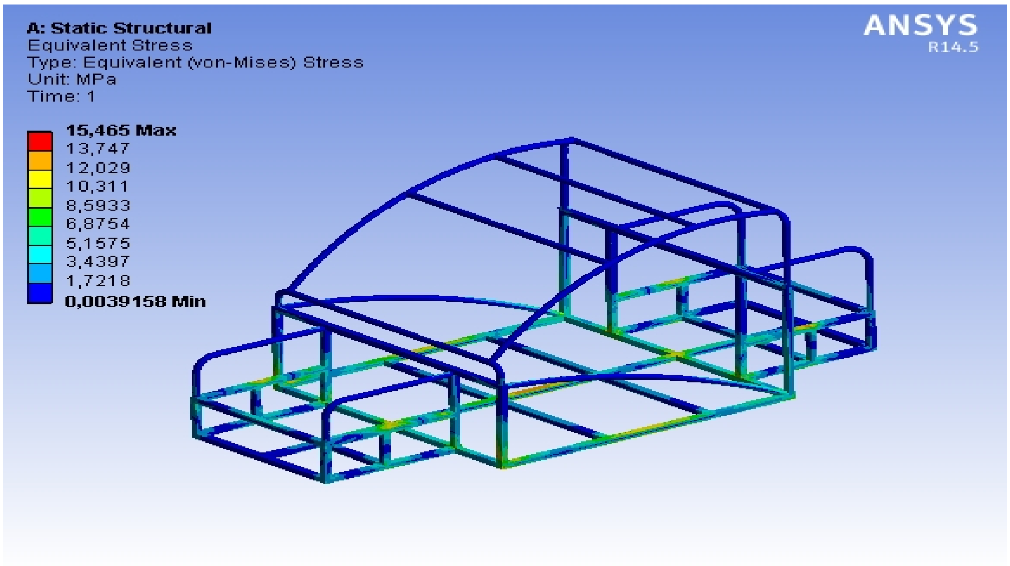

Figure 4.63. Maximum von-Mises stress of the structurally optimized chassis

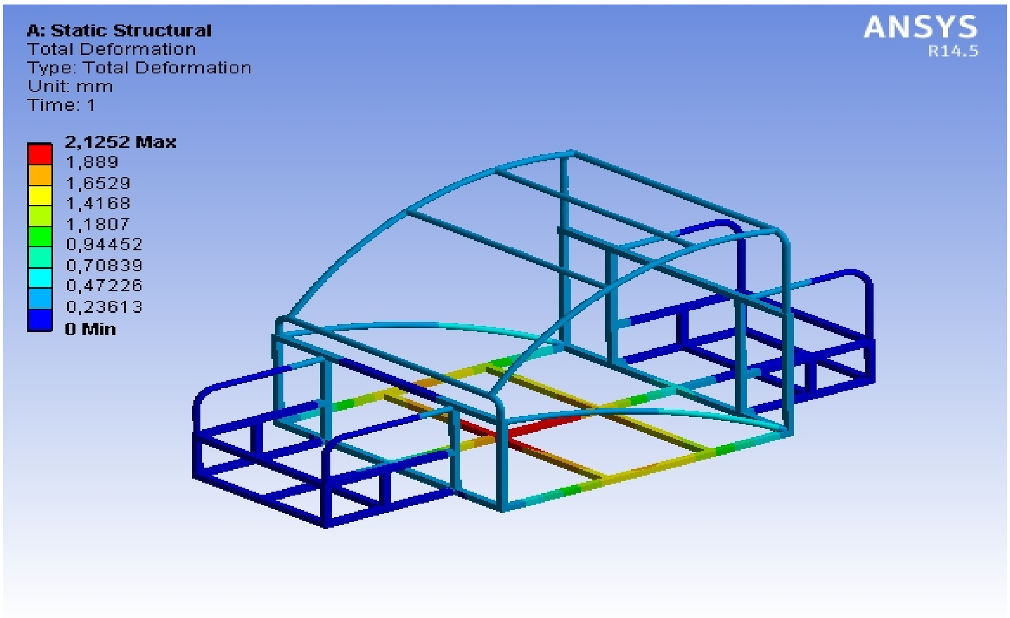

Figure 4.64. Maximum deformation of the structurally optimized chassis

Torsional deformation of the structurally optimized chassis due to torsional loading is illustrated in Figure 4.65.

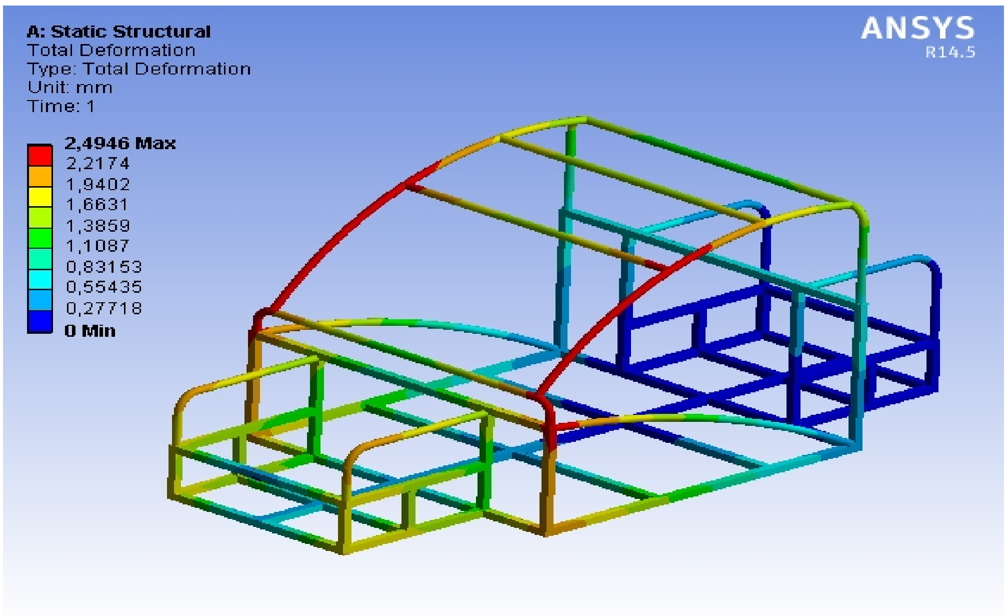

Figure 4.65. Maximum torsional deformation of the structurally optimized chassis

Weight of the optimized chassis is obtained from the ANSYS and torsional stiffness of the structurally optimized chassis is calculated using the torsional deformation values of the chassis. Analysis results for the structurally optimized square profiled aluminium space frame chassis are listed in Table 4.6.

Table 4.6. Analysis results of the structurally optimized chassis

Maximum von-Mises Stress (MPa)	Maximum Deformation (mm)	Maximum Torsional Deformation (mm)	Torsional Stiffness (Nm/deg)	Weight (kg)
15.465	2.125	2.495	1828.289	28.163

Structural optimization is aimed to increase the torsional deformation value of the chassis while decreasing the weight of the chassis. According to parametric optimization results, square profiled composite backbone chassis has the largest signal to noise ratio, but extra work needed for backbone chassis to validate the racing rules. Structural optimization is aimed to approach to the torsional stiffness value of the square profiled carbon fiber backbone chassis using square profiled aluminium 5042-H19 space frame chassis. Approaching to the 14.861 kg weight of the composite backbone chassis from 30.218 kg weight of the aluminium space frame chassis, is not possible, because of the closed box structure of the optimized aluminium space frame chassis, but any decrease in the weight; will result in the increase of the performance of the vehicle. Previous torsional stiffness value of the square profiled aluminium space frame chassis was 1417.962 Nm/deg and torsional stiffness value of the square profiled composite backbone chassis is 1797.313 Nm/deg. Structurally optimized chassis has 1828.289 Nm/deg torsional stiffness value and weighs 28.163 kg so the torsional stiffness of the chassis increased 28.94% and weight of the chassis decreased 6.8%. In addition, optimized chassis has higher torsional stiffness value than square profiled composite backbone chassis. As a result of the structural optimization maximum von-Mises stress increase, but maximum stress is still far below the yield strength of the aluminium. Rigid design is achieved as a consequence when considering the stress and deformation values although optimized design has smaller dimensions of section geometry than previous design.

5. CONCLUSION

The aim of this study was to design a chassis for an electric vehicle and main purpose of the design was to obtain a rigid and lightweight chassis. Design criteria and constraints of the chassis design are adopted from the TÜBİTAK electromobile racing rules. Various chassis designs are created using computer aided design software, considering the dimensions and locations of the other electric vehicle components like battery, electric motor, steering system, seats and rear axle by using three chassis types with two different section geometries. Structural analysis of the designs is performed using finite element method to observe performance characteristics of the different design by assigning three various materials of steel, aluminium and composite. Performance characteristics of the chassis are determined as maximum von-Mises stress, maximum deformation, maximum torsional deformation, torsional stiffness and weight. Analysis results of the chassis designs include 72 different performance data. As a result of the parametric optimization of performed Taguchi method, five of the chassis designs, which have the highest signal to noise ratios are selected. One of the most feasible designs among the five chassis designs is selected for the further optimization, which is structural optimization. As a consequence of the structural optimization of the chassis, 6.8% weight decrease and 28.94% torsional stiffness increase is achieved.

Final design consists of space frame chassis type with square section profiled main frame and circular tube section profiled support members. Material of the final design is aluminium 5042-H19. Performance characteristics of final design include,

- Maximum von-Mises stress of 15.465 MPa
- Maximum deformation of 2.125 mm
- Maximum torsional deformation of 2.495 mm
- Torsional stiffness of 1828.289 Nm/deg
- Weight of 28.163 kg

Maximum von-Mises stress value of the final design is far below the 345 MPa of yield strength of the aluminium 5042-H19. As a result of the design, analysis and optimization stages of this work, structurally rigid and lightweight electric vehicle chassis is achieved.

A Future study could include the manufacturing of the space frame chassis. Using aluminium 5042-H19 material made the chassis rigid and lightweight. Carbon fiber material use in the chassis could provide a considerable amount of weight decrease, but the major problem beyond carbon fiber materials is high cost of the raw material and application. In addition, carbon fiber space frame chassis has lower torsional stiffness value than aluminium one. In this study, 2.5 mm laminate thickness is used and a small increase of the thickness could provide higher torsional stiffness values. Moreover, torsional stiffness value is generated using numerical method and to validate the torsional stiffness of the chassis experimental method could be performed. In Çukurova University, more than one vehicle is participating for the electromobile races so manufacturing an experimental setup will be feasible. Validation of the torsional stiffness with an experimental setup could eliminate the numerical uncertainties and could increase the performance of the vehicle.

REFERENCES

ADAMS, H., 1993. Chassis Engineering. Berkley Publishing Group, USA, 133p.

BAMBACH, M. R., 2013. Fiber composite strengthening of thin-walled steel vehicle crush tubes for frontal collision energy absorption. Thin-Walled Structures, 66: 15-22.

BORIA, S., PETTINARI, S., 2014. Mathematical design of electric vehicle impact attenuators: Metallic vs. composite material. Composite Structures, 115: 51-59.

CAVAZZUTİ, M., BALDINI, A., BERTOCCHI, E., COSTI, D., TORRICELLI, E., MORUZZI, P., 2011. High performance automotive chassis design: a topology optimization based approach. Structural Multidisiplinary Optimization, 44: 45–56.

CHAPMAN, I., 2014. The end of Peak Oil? Why this topic is still relevant despite recent denials. Energy Policy, 64: 93-101.

CROLLA, D.A., 2009. Automotive Engineering Powertrain, Chassis System and Vehicle Body. Elsevier, USA, 828p.

HIRSCH, J., 2011. Aluminium in Innovative Light-Weight Car Design. Materials Transactions, 52(5): 818-824.

HIRSCH, J., AL-SAMMAN, T., 2014. Superior light metals by texture engineering: Optimized aluminium and magnesium alloys for automotive applications. Acta Materialia, 61: 818-843.

http://300sl.org/technik-300-sl-w198-technology-300-sl-w198/ (Date Accessed: 6 July 2015)

http://support.minitab.com/en-us/minitab/17/topic-library/modeling-statistics/doe/taguchi-designs/taguchi-designs (Date Accessed: 6 July 2015)

http://www.ansys.com/Products/Workflow+Technology/ANSYS+Workbench+Platform/ANSYS+Meshing (Date Accessed: 6 July 2015)

http://www.chevrolet.com/2014-silverado-3500hd-diesel-trucks.html#(Date Accessed: 6 July 2015)

http://www.peakoil.net/uhdsg/Default.htm (Date Accessed: 6 July 2015) http://www.raywills.net/rtwtechadopt.html (Date Accessed: 6 July 2015)

http://help.solidworks.com/2014/English/SolidWorks/sldworks/t_Weldments_Creating_a_Custom_Profile.htm (Date Accessed: 6 July 2015)

HUTTON, D.V., 2004. Fundamentals of Finite Element Analysis. The McGraw−Hill Companies, 494p.

KAW, A.K., 2006. MECHANICS of Composite Materials, 2nd edition. CRC ; Press, USA, 457p.

KOPP, G., BEEH, E., SCHOLL, R., KOBILKE, A., STRABBURGER, P., KRIESCHER, M., 2012. New Lightweight Structures for Advanced Automotive Vehicles - Safe and Modular. Procedia - Social and Behavioral Sciences, 48: 350-362.

LIU, Q., LIN, Y., ZONG, Z., SUN, G., LI, Q., 2013. Lightweight design of carbon twill weave fabric composite body structure for electric vehicle. Composite Structures, 97: 231–238.

MADENCI, E., GUVEN, I., 2006. The Finite Element Method and Applications in Engineering Using ANSYS. Springer Science +Business Media, USA, 686p.

MAT, M.H., GHANI, A.R.A., 2012. Design and Analysis of 'Eco' Car Chassis. Procedia Engineering, 41: 1756-1760.

NOR, M.A.M., RASHID, H., MAHYUDDIN, W.M.F.W., AZLAN, M.A.M., MAHMUD, J., 2012. Stress Analysis of a Low Loader Chassis. Procedia Engineering, 41: 995-1001.

PATEL, T.M., BHATT, M.G., PATEL, H.K., 2013. Parametric Optimization of Eicher 11.10 Chassis Frame for Weight Reduction Using FEA-DOE Hybrid Modeling. IOSR Journal of Mechanical and Civil Engineering, 6(2): 92-100.

POULLIKKAS, A., 2015. Sustainable options for electric vehicle technologies. Renewable and Sustainable Energy Reviews, 41: 1277–1287.

RILEY, W.B., GEORGE, A.R., 2002. Design, Analysis and Testing of a Formula SAE Car Chassis. SAE TECHNICAL PAPER SERIES, 2002-01-3300.

SAS Institute Inc. 2009. JMP 8 Design of Experiments Guide, Second Edition. Cary, NC: SAS Institute Inc.

SMITH, J.H., 2002. An Introduction to Modern Vehicle Design. Reed Educational and Professional Publishing, Great Britain, 585p.

TAUFIK, A.Z., RASHID, N., MAZLAN, FARUQ, M., ZAHIR, M., 2014. Electric car chassis design and analysis by using CATIA V5 R19. IOSR Journal of Mechanical and Civil Engineering, 11(4): 56-59.

WOOD, J.H., LONG, G.R., MOREHOUSE, D.F., 2004. Long-Term World Oil Supply Scenarios. Energy Information Administration Publications.

YANHONG, C., FENG, Z., 2011. The Finite Element Analysis and The Optimization Design of The Yj3128-type Dump Truck's Sub-Frames Based on ANSYS. Procedia Earth and Planetary Science, 2: 133-138.

ZIAULHAQ, M., ALAM, S., JAMALI, M. T., 2013. Study of Process Parameters Effect on Surface Finish in Al-Alloy Sand Casting by Using Taguchi Method. International Journal of Engineering Research & Technology, 2(12): 1521-1526.

CURRICULUM VITAE

Emre KOCA was born in Adana in 1988. He earned his Bachelor of Science degree from Mechanical Engineering Department of İzmir Institute of Technology in 2013. He is currently studying for his Master of Science degree in Automotive Engineering department of Çukurova University.